IN THE UNITED STATES PATENT AND TRADEMARK OFFICE
(MBHB 09-333-US)

In re Application of: William J. Carroll	)	Group Art Unit: 3762
Serial No.: 10/761,424	)	Examiner: Stoklosa, Joseph A.
Filed: January 22, 2004	)	Confirmation No. 1421
For: Spinal Cord Stimulation with Interferential Current	)	

Mail Stop Amendment
Commissioner for Patents
P.O. Box 1450
Alexandria, VA 22313-1450

DECLARATION OF WILLIAM CARROLL UNDER 37 CFR § 1.132

Dear Sir:

I, William Carroll, declare as follows:

1. I am the sole inventor of the present application. I am qualified to make this declaration based on my knowledge of the medical device sector, my experience with spinal pain control devices, and my familiarity with prior art devices and the history of spinal cord pain management.

2. I have 33 years of experience in this industry.

McDONNELL BOEHNEN
HULBERT & BERGHOFF LLP
300 SOUTH WACKER DRIVE
CHICAGO, IL 60606
(312)913-0001

3. I am currently the Chief Scientific Officer and Executive VP of Meagan Medical, Inc., a company that is involved in Research and Development of Electrical Stimulation devices in the Medical Device area.

4. I obtained a bachelor degree from Lafayette College in Biology with a Minor in Chemistry in 1973.

5. I have authored or co-authored the following publications:

Research Articles / Publications:

Burch FX, Tarro JN, Greenberg JJ, Carroll WJ. Evaluating the benefits of patterned stimulation in the treatment of osteoarthritis of the knee. Osteoarthritis and Cartilage 2008; 16: 865-872.

Nawrock MA, Martinez SA, Hughes J, Lincoln JD, Shih M, Zheng H, Carroll WJ. Augmentation of intertransverse process lumbar fusion. Vet Comp Orthop Traumatol 2006; 19: 72-80.

Porter J, Yeung AT, Carroll WJ. Electrical stimulation as adjunct therapy for low back and neck pain. J Minim Invasive Spinal Tech 2004; 4: 43-45.

Briggs KK, Martinez SA, Smith LV, Carroll WJ, Zimmermann JA, Shih M, Feldman R, Lincoln JD. Comparison of the osteogenic effects between two surface interferential stimulation devices to enhance surgically based spinal fusion. Vet Comp Orthop Traumatol 2004; 17: 41-47.

Carroll B, Lamm K, Rennie S. *Suggested Stimulation Techniques for TENS.* High Sierra Medical, 1991.

Yu J, Carroll W. *Electrode Placement Manual for TENS.* Medtronic Neuro Division, 1982.

Abstracts:

Shih M-S, Carroll WJ. Effective interferential stimulation on osteogenesis. Proceedings of 28th American Bone and Mineral Research Society Annual Meeting, 2006.

McDONNELL BOEHNEN
HULBERT & BERGHOFF LLP
300 SOUTH WACKER DRIVE
CHICAGO, IL 60606
(312)913-0001

Nawrocki MA, Martinez SA, Hughes J, Lincoln JD, Shih M-S, Carroll WJ. Interferential stimulation for augmentation of intertransverse process lumbar fusion in a rabbit spinal fusion model. Proceedings of 32nd Veterinary Orthopedic Society Annual Meeting, 2004.

Shih M-S, Feldman RS, Leininger RJ, Martinez SA, Lincoln JD, Briggs KK, Carroll WJ. Promotion of Spinal Fusion by Surface Interferential Stimulation Device. Proceedings of 50th Annual Meeting of the Orthopaedic Research Society, 2004.

Shih M-S, Feldman RS, Leininger RJ, Martinez AS, Lincoln JD, Briggs KK, Carroll WJ. Promotion of Spinal Fusion by Surface Interferential Stimulation Device. International Bone and Mineral Society Annual Meeting Proceedings, 2003.

Shih M-S, Negron A, Bell EC, Carroll WJ. Improved Lumbar BMD and Biomechanical Strength by Surface Interferential Stimulation Devices in Established OVX Osteopenia of Rats. A Pilot Study. International Bone and Mineral Society Annual Meeting Proceedings, 2003.

Briggs KK, Martinez SA, Zimmermann JA, Carroll WJ, Shih M-S, Feldman R. A comparison of the osteogenic effects between two different surface interferntial stimulation devices to enhance surgically based spinal fusion. American College of Veterinary Surgeon Annual Meeting Proceedings, 2002.

6. In spinal cord stimulation (SCS), it is necessary to provide deep stimulation for effective pain relief. (*See*, e.g., Exhibit A, "Effectiveness of Spinal Cord Stimulation in the Management of Chronic Pain: Analysis of Technical Drawbacks and Solutions", Holsheimer, Jan, Neurosurgery: Volume 40(5), May 1997, pp 990-999).

7. Effective pain relief can be achieved by activation of the Gracile nucleus and Pyramid tract in the spinal cord. (*See*, e.g., USP 6,871,099 and USP 7,349,743). The Gracile nucleus and Pyramid tract are acending and decending tracts in the dorsal column of the spinal cord. (*See, e.g.,* Figure 1, Exhibit B).

McDONNELL BOEHNEN
HULBERT & BERGHOFF LLP
300 SOUTH WACKER DRIVE
CHICAGO, IL 60606
(312)913-0001

8. The spinal cord is encased in a thick membrane called the dura mater, and inside a layer of the dura mater is cerebrospinal fluid. (*See*, e.g., Exhibit A).

9. The cerebrospinal fluid is conductive, and stimulation that spreads through the fluid can cause pain if the current density becomes too high near the dorsal root ganglia that lie along a vertebral column by the spine. (*See,* e.g., Exhibit A).

10. It is desired to provide deep stimulation through the dura mater of the spinal cord for activating the Gracile nucleus and Pyramid and other portions of the Dorsal Column using low levels of stimulation so as to avoid spreading of stimulation through the cerebrospinal fluid.

11. Using an interferential current SCS method of the present application, stimulation may be provided deep through the dura mater with low current levels, thus lowering the threshold of activation of the Gracile nucleus and Pyramid. (*See,* e.g., Exhibit B).

12. With spinal cord stimulation, if current is simply increased, the effect may be to spread stimulation through the cerebrospinal fluid, resulting in stimulation of the dorsal root ganglia, which causes chest and thoracic pain. (*See*, e.g., Exhibit A).

13. Using an interferential current SCS method of the present application, low levels of stimulation can be provided, and deep penetration through the dura mater can be achieved without spreading of the stimulation and resulting side effects.

McDONNELL BOEHNEN
HULBERT & BERGHOFF LLP
300 SOUTH WACKER DRIVE
CHICAGO, IL 60606
(312)913-0001

14. A study was performed in the Neuronano Lund Research Center University in Sweden by Marcus Granmo and Jens Schouenborg with the electrical stimulator of the present application. A copy of the study and results is included as Exhibit B. The study demonstrates that using the interferential electrical stimulator of the present application, a beat frequency is obtained that provides deep and localized stimulation.

15. The study in Exhibit B included an experimental setup as follows:

(a) Adult rats (Sprague-Dawley, 200-230 grams) were used and were anesthetized with isoflurane gas (1.8% in a mixture of 60/40 % NO_2 and oxygen), as described, for example, in Kalliomäki, J., Granmo, M., Schouenborg, J. *Pain.* 2003 Jul;104(1-2):195-200, enclosed as Exhibit C.

(b) Two pairs of stimulation electrodes (bipolar stimulation, 4 electrodes in total) were placed epidurally (to a dura mater in an epidural space) on the spinal cord in two configurations; (i) a crossed and (ii) a parallel configuration (*See*, e.g., Figure 2 of Exhibit B).

(c) Recording microelectrodes were inserted in the Gracile nucleus and the Pyramid in the brainstem (*See*, e.g., Figure 1 of Exhibit B). The Gracile nucleus receives ascending sensory information from dorsal column tracts that run relatively superficial in the dorsal part of the spinal cord. The pyramid, as part of the corticospinal tract, conveys descending motor commands from the brain to the spinal cord.

(d) In the rat spinal cord, the pyramidal tract is located deep in the dorsal column, i.e. deeper than the dorsal column of the spinal cord activating the Gracile nucleus (*See*, e.g., Figure 1 of Exhibit B).

(e) By spinal cord stimulation, activating the pyramid tract fibers antidromically, evoked volleys in this relatively deep tract were recorded, thus giving information about depth of

McDONNELL BOEHNEN
HULBERT & BERGHOFF LLP
300 SOUTH WACKER DRIVE
CHICAGO, IL 60606
(312)913-0001

penetration of the stimulation. After each experiment, the animals were perfused with formalin and the caudal brain stem was sectioned to verify the electrode position in the brainstem. (*See*, e.g., Exhibit B, p. 1).

16. Experiments were performed using two types of stimulation paradigms, each of which was applied to both electrode pairs that were placed epidurally in the two configurations shown in Figure 2 of Exhibit B:

(i) Sinus waves of about 500 μs width (corresponding to 2000 Hz waves) applied at a frequency of about 100 Hz (e.g., pulsed sine waves of 500 μs width applied at a rate of 100 pulses per second corresponding to 2000 Hz waves). (*See*, e.g., Exhibit B, p. 2 and Figure 3).

(ii) Sinus waves of about 500 μs (corresponding to 2000 Hz) were applied to one set of electrode pairs, and sinus waves of about 476 μs (corresponding to 2100 Hz) were applied to the other set of electrode pairs to create an interference pattern. The sinus waves applied at about 100 and about 105 Hz, respectively (e.g., pulsed sine waves of 500 μs width applied at a rate of 100 pulses per second corresponding to 2000 Hz waves, and pulsed sine waves of 476 μs width applied at a rate of 105 pulses per second corresponding to 2100 Hz waves). A resulting beat frequency signal of 100 Hz was produced proximate to the subject's spinal cord. (*See*, e.g., Exhibit B, p. 2 and Figure 3).

17. During the experiments of the study in Exhibit B, measurements were performed of SCS evoked activity in the Gracilis nucleus and for antidromic evoked volleys in the Pyramid using the recording microelectrodes. Stimulation intensity was increased or decreased in increments as shown in the table below.

McDONNELL BOEHNEN
HULBERT & BERGHOFF LLP
300 SOUTH WACKER DRIVE
CHICAGO, IL 60606
(312)913-0001

Intensity Range	Increments
10-50 mV	10 mV
50-400 mV	25 mV
400-900 mV	50 mV
900-1200 mV	100 mV
≥ 1200 mV	250 mV

A lowest stimulation intensity eliciting a clear response was considered a threshold for evoking activity in the Gacilis nucleus and the Pyramid. (*See*, e.g., Exhibit B, p. 2).

18. During the experiments of the study in Exhibit B, each sampled data file is an average of about 400 single recording experiments. Latency of the Pyramid tract responses which were used in the analysis (16-19 m/s) were consistent with those observed in the literature (*See, e.g.*, Exhibit D, Mediratta and Nicoll J *Physiol.* 1983 Mar; 336:545-6 1; Exhibit E, Stewart et al. *Brain Res.* 1990 Feb 5; 508(2):34 1-4; and Exhibit F, Chapman and Yeomans *Neuroscience* 1994, 59(3):699-711).

19. The Experiments showed that thresholds for activation of both the Gracile nucleus and the Pyramid were significantly lower when using 100 + 105 Hz interferential current stimulation than using conventional 100 + 100 Hz stimulation in either the parallel or crossed configuration (*See*, e.g., Figures 6 and 7 in Exhibit B and reproduced below).

McDONNELL BOEHNEN
HULBERT & BERGHOFF LLP
300 SOUTH WACKER DRIVE
CHICAGO, IL 60606
(312)913-0001

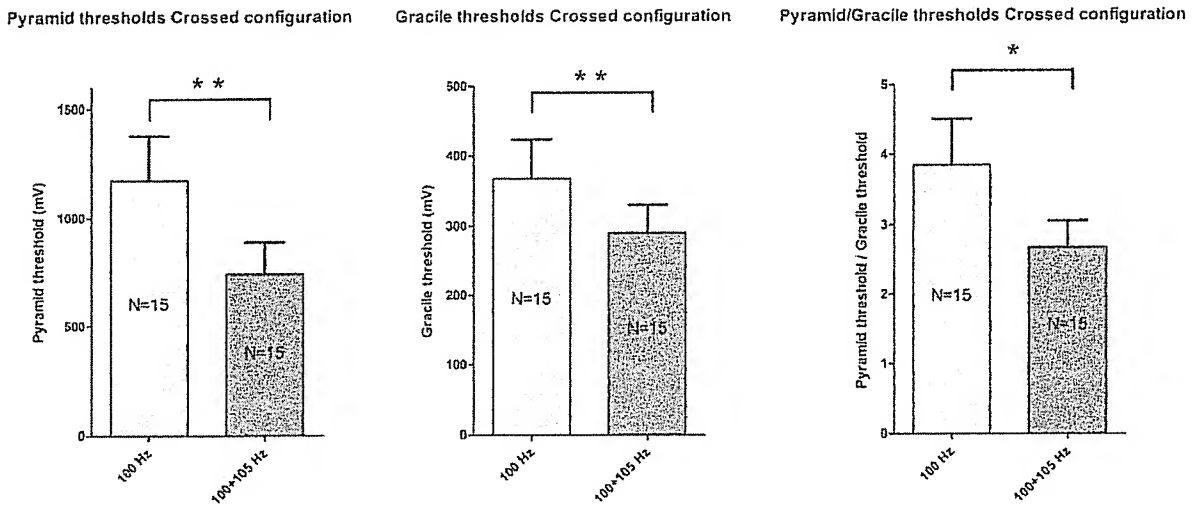

Figure 6. Comparisons of threshold data after 100+100 Hz versus 100+105 Hz stimulation using a crossed electrode configuration. Results after Wilcoxon signed rank significance test is shown. N equals the number of animals used, e.g., 15.

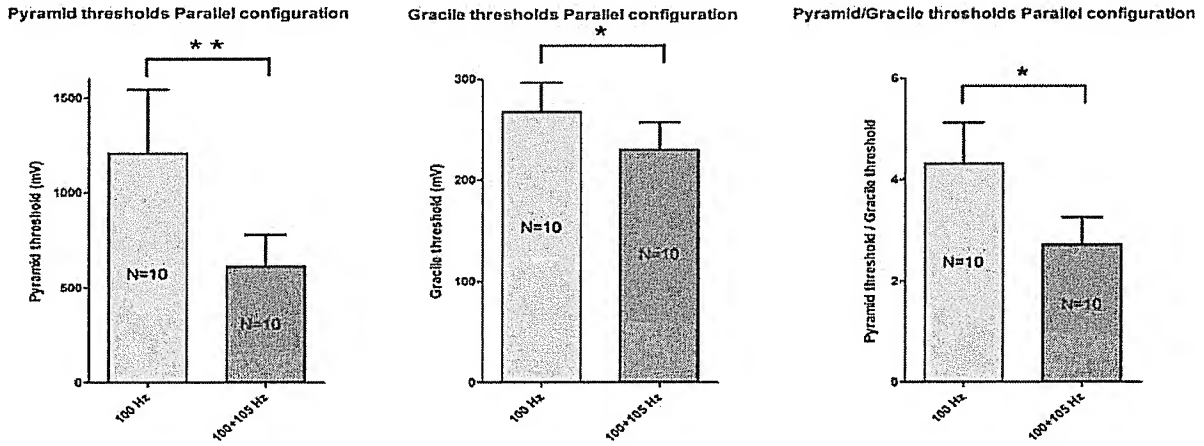

Figure 7. Comparisons of threshold data after 100+100 Hz versus 100+105 Hz stimulation using a parallel electrode configuration. Results after Wilcoxon signed rank significance test is shown. N equals the number of animals used, e.g., 10.

20. As seen in Figures 6-7 of Exhibit B reproduced above, for Pyramid activation, conventional stimulation required about 1200 mV (in the parallel and cross configuration); by

McDONNELL BOEHNEN
HULBERT & BERGHOFF LLP
300 SOUTH WACKER DRIVE
CHICAGO, IL 60606
(312)913-0001

comparison, interferential stimulation required only about 700 mV in the cross configuration or about 600 mV in the parallel configuration. For Gracile activation, conventional stimulation required about 375 mV in the cross configuration or about 275 mV in the parallel configuration; by comparison, interferential stimulation required only about 290 mV in the cross configuration or about 225 mV in the parallel configuration.

21. To yield a better understanding of the efficacy of the stimulation, a ratio of the threshold for Pyramid tract activation versus the threshold for Gracile nucleus activation was graphed in Figures 6-7 of Exhibit B (reproduced above). The lower the ratio, the more efficient stimulation to the deep Pyramidal tract in relation to the Gracile nucleus tract (which is more superficial). The graphs illustrate ratios of about 4 using the conventional stimulation as compared to only about 2 using the interferential stimulation. Thus, interferential stimulation achieves better penetration to the deeper Pyramidal tract than conventional stimulation.

22. The experimental results of the study in Exhibit B demonstrate that interference stimulation with 100 + 105 Hz (2000 Hz + 2100 Hz) is more effective than 100 + 100 Hz conventional stimulation in activating the pathways studied, both from a threshold and depth-penetration perspective. This indicates that the formation of an interference pattern or beat frequency provided a lower threshold and better penetration.

23. Applying stimulation using conventional surface electrodes does not enable deep penetration of the pyramid tract. Electricity follows a path of least resistance, and applying stimulation on the surface of the skin using surface electrodes does not allow for stimulation

McDONNELL BOEHNEN
HULBERT & BERGHOFF LLP
300 SOUTH WACKER DRIVE
CHICAGO, IL 60606
(312)913-0001

through the vertebrae. Bone is an insulator (*See*, e.g., Exhibit G, p. 8, Table 1 of conductivities of tissues). Bone has a conductivity of 0.06 s/m, while skin has a conductivity of 0.436 s/m. To achieve stimulation levels of the pyramid tract as seen in the study of Exhibit B using surface stimulation, stimulation would need to be applied at a voltage level so high that it would result in tissue damage and pain.

24. The table below summarizes the results of the study described in Exhibit B. It shows the approximate voltage levels required to activate the Gracile nucleus and the Pyramid tract in the spinal cord using an interferential implantable electrode configuration and a conventional implantable electrode configuration. The table also includes estimates for approximate voltages levels that would be required using an interferential surface electrode configuration. For example, using the study shown in Exhibit G, it can be calculated that to achieve stimulation of the Gracile nucleus and the Pyramid in the spinal cord using an interferential surface electrode configuration, voltage levels would be required that are much greater than 1200 mV, and are more on the order of 100's of volts, for example. In any event, the voltage levels are so high that they are physiologically unsafe.

	Results using Interferential Implantable Electrode Configuration		Results using Conventional Implantable Electrode Configuration		Results using Interferential Surface Electrode Configuration
	Parallel Configuration	Crossed Configuration	Parallel Configuration	Crossed Configuration	
Pyramid Activation Threshold	600 mV	700 mV	1200 mV	1200 mV	>> 1200 mV
Gracile Activation Threshold	225 mV	290 mV	275 mV	375 mV	>> 1200 mV

McDONNELL BOEHNEN
HULBERT & BERGHOFF LLP
300 SOUTH WACKER DRIVE
CHICAGO, IL 60606
(312)913-0001

25. As shown in the table, the interferential implantable electrode configuration of the present application achieves activation of the Gracile nucleus and Pyramid in the spinal cord at much lower voltage levels than are required with a conventional implantable electrode configuration, thereby providing effective pain relief while minimizing the risk of stimulation of the dorsal root ganglia, which leads to chest and thoracic pain. (*See*, e.g., Exhibit B).

I further declare that all statements made herein of my own knowledge are true and that all statements made herein on information and belief are believed to be true, and that all statements are made with the knowledge that willful false statements are punishable by fine or imprisonment or both (18 U.S.C. § 1001) and may jeopardize the validity of the application or any patent issuing thereon.

Respectfully Submitted,

Date: March 10, 2010

By: /William Carroll/
William Carroll

McDONNELL BOEHNEN
HULBERT & BERGHOFF LLP
300 SOUTH WACKER DRIVE
CHICAGO, IL 60606
(312)913-0001

Exhibit A

ADVERTISEMENT

High quality article reprints.
Order Today!

ADVERTISEMENT

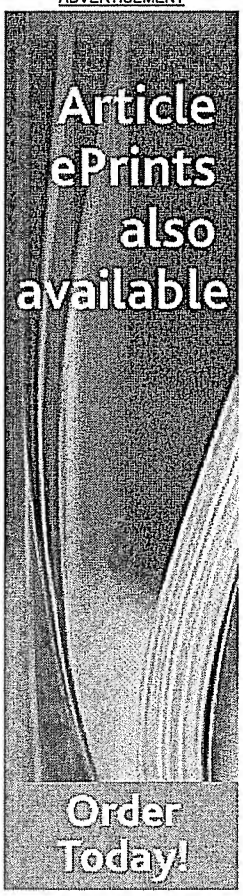

Neurosurgery:Volume 40(5)May 1997pp 990-999

Effectiveness of Spinal Cord Stimulation in the Management of Chronic Pain: Analysis of Technical Drawbacks and Solutions [Technique Assessment]

Holsheimer, Jan PhD

Department of Electrical Engineering, Institute for Biomedical Technology, University of Twente, Enschede, The Netherlands

Received, September 5, 1996. Accepted, November 25, 1996.

Reprint requests: Dr. Jan Holsheimer, Division of Biomedical Engineering, Department of Electrical Engineering, University of Twente, P.O. Box 217, NL-7500 AE Enschede, The Netherlands.

Abstract TOP

OBJECTIVE: A major drawback of currently available spinal cord stimulation (SCS) systems for the management of chronic intractable pain, especially of widespread pain patterns as in reflex sympathetic dystrophy, is the generally limited paresthesia coverage. The aim of this study is to analyze the origin of this problem and to provide solutions.

METHODS: Results from theoretical studies, in which a computer model was used to mimic the effects of SCS on spinal nerve fibers, were used to analyze which factors may limit paresthesia coverage. Model predictions were verified by empirical data from clinical literature.

RESULTS: When using common SCS electrodes, both perception threshold and motor/discomfort threshold are generally related to dorsal root stimulation. Because these thresholds have a small ratio (~1:1.4), stimulation of dorsal column fibers and paresthesia coverage is limited by this small range of stimulation. When the distance between the epidural electrode and spinal cord is large (midthoracically), the threshold for dorsal column stimulation exceeds discomfort threshold, resulting only in segmental paresthesia. The range of dorsal column stimulation and paresthesia coverage can be improved when using either an optimally dimensioned rostrocaudal bi-/tripole or a transverse tripole ("guarded cathode"). When applying the latter in combination with a dual channel pulse generator providing simultaneous pulses, paresthesias can simply be changed to optimally cover the painful area.

CONCLUSION: Paresthesia coverage and pain management by SCS can be improved when using electrodes as proposed.

Since the introduction of spinal cord stimulation (SCS) by Shealy et al. (25), this technique has been used increasingly in the treatment of chronic, intractable pain. Previous reports demonstrate that successful pain relief is only obtained when the painful area is completely covered by the topography of the stimulation paresthesias (2, 18, 20, 21).

Although the SCS technique has evolved in various aspects, several major drawbacks of its application have not yet been solved. One problem is the difficulty of obtaining a permanent optimal position of the lead(s) to cover the painful dermatomes with paresthesia. Another related problem is the usually small range of stimulation amplitudes between the perception threshold (PT) and the discomfort threshold (DT), often preventing a complete coverage of the painful area by paresthesia needed for a maximum therapeutic effect (18, 20). This latter problem is usually "solved" by avoiding adverse electrode positions, resulting in excessive radicular stimulation, mainly occurring at midthoracic levels(T4-T7) (1, 20). The strategy to solve the problem of optimal electrode positioning has been to increase the number of electrode contacts, thereby increasing the rostrocaudal area in which contacts may be selected as a cathode or an anode. This strategy is based on the expectation that the probability to obtain an appropriate position and combination of cathodes and anodes for any patient will increase as the number of available contact positions is increased. This principle led to the development and application of rostrocaudal arrays consisting of four or eight contacts, usually spaced by 6 to 7 mm, and the implantation of more leads in parallel (16, 17, 26). Whereas a four-contact array enables 65 anode-cathode combinations (including monopolar combinations in which the metal case of an implanted pulse generator is the anode), more than 6000 combinations may be selected when using an eight-contact array (22). Although testing large numbers of combinations in a patient can be automated (17, 22), it is still very time consuming.

This empirical method is the only one that can be used, as long as a knowledge-based method is not available. To our knowledge, Law and Miller(18) were the first to stress the importance of documenting stimulation parameters to develop a systematic approach in the application of SCS. Since then, these parameters and the clinical effects have been documented by several physicians (1, 2, 16, 17, 20-22). Their data analysis led to relevant conclusions regarding the best electrode position to cover a specified body area with paresthesia (1), the most appropriate cathode-anode combinations (16, 17, 21, 22), and, therefore, a preselection of the potentially best positions and combinations to be tested in a patient.

Article Outline
- Abstract
- VERIFICATION OF MODEL PREDICTIONS
  - Neural structures activated in SCS
  - PT generally related to DR stimulation
    - Model prediction
    - Empirical evidence
    - Summary
  - DT related to DR stimulation
    - Model prediction
    - Empirical evidence
    - Summary
  - Segmentary paresthesia most probable in midthoracic stimula...
    - Model prediction
    - Empirical evidence
    - Summary
  - Paresthesia coverage effected by the anode-cathode combinat...
    - Model prediction
    - Empirical evidence
  - Verification of model predictions: Conclusions
- METHODS TO IMPROVE PARESTHESIA COVERAGE
  - Rostrocaudal contact array
  - Transverse tripolar lead (TTL) (U.S. Patent No. 5,501,703)
- DISCUSSION
- ACKNOWLEDGMENT
- APPENDIX: THE SCS COMPUTER MODEL
- REFERENCES
  - COMMENTS

Figures/Tables
- Figure 1
- Figure 2
- Figure 3
- Figure 5
- Table 1
- Figure 4

Apart from these empirical studies, theoretical analyses by computer modeling have been performed to obtain a better understanding of the effects of the electrical pulses on spinal cord nerve fibers. Such an approach was initiated by Coburn (3, 4) and continued at the University of Twente (7, 10, 29-31). These investigations led primarily to the determination of relations between geometrical parameters, i.e., spinal anatomy and electrode geometry, and spinal nerve fiber responses underlying paresthesia and the modulation of pain pathways (7, 8, 10, 11). The model has been validated by empirical data(28).

The question addressed in this study is which physical factors prevent a sufficient paresthesia coverage by SCS in a portion of the patients with chronic pain. Therefore, predictions from computer modeling are presented and verified by empirical data from the literature. Based on the conclusions, methods to improve the technical performance of SCS systems are presented as well. A short description of the SCS computer model is presented in the Appendix.

VERIFICATION OF MODEL PREDICTIONS TOP

Neural structures activated in SCS TOP

According to the "gate-control" theory of Melzack and Wall (19), the suppression of pain sensations, accompanied by paresthesia, results from the activation of large cutaneous afferents(Aαβ fibers). Because these nerve fibers consist of a dorsal root(DR) fiber that bifurcates in an a scending and a descending dorsal column(DC) fiber, paresthetic sensations can be evoked by both DC and DR stimulation. However, the potential paresthesia coverage will strongly differ when either DCs or DRs are stimulated. When stimulating the DCs, fibers corresponding to all dermatomes from the sacral ones up t o the electrode level may be activated, thus resulting in a broad paresthesia coverage.(Because DC fiber diameters and positions in the DCs vary, stimulu s amplitudes for their excitation will vary as well.) When stimulating DRs, fibers will be activated in a limited number of rootlets close to the cathodal con tact(s), resulting in paresthesia confined to one or two dermatomes at each body side.

The stimulus strengths needed for DC and DR fiber activation increase when the (epidural) electrode-to-spinal cord distance is increased. Computer modeling predicts that thresholds of the largest DC and DR fibers are almost identical when this distance is small (≤2 mm). However, because of the configuration of the electrical field, DC fiber thresholds rise much more than DR fiber thresholds when this distance is increased (11) (see Fig. 1). This distance, and thus the threshold ratio for DC and DR fiber stimulation, varies both along the vertebral column (lowest in the cervical area, higher in the low thoracic area, and highest in the midthoracic area) and among patients (9).

FIGURE 1. Calculated threshold stimuli of a 15-µm DC fiber and a 15-µm DR fiber as a function of the electrode-to-spinal cord distance.

SCS not only activates large cutaneous fibers, but proprioceptive fibers as well (13). The latter are most likely to cause the painful sensations related to DT and presumably originate from spinal motor reflexes. Dimitrijevic et al. (5) concluded that motor responses to SCS are related to DR fiber stimulation. Direct stimulation of neurons in the ventral spinal cord and ventral roots is not likely to occur, because of their large distance from the dorsal electrode. Computer simulations predict that stimulation of motor fibers in a ventral root will require an approximately 14-fold stimulus amplit ude as compared with large DR fibers.

PT generally related to DR stimulation TOP

Model prediction TOP

Computer simulations predict that at all electrode-to-spinal cord distances, except for very small values, the stimulus to e xcite a DR fiber is smaller than the threshold stimulus of a DC fiber having a similar caliber (4, 11, 29) (see Fig. 1). This indicates that PT is usually related to stimulation of DR fibers. Moreover, PTs as a function of the vertebral level of stimulation fit well to the corresponding calculated DR fiber thresholds (8), whereas DC fiber thresholds vary much more (see Fig. 1).

Empirical evidence TOP

Law (16) and Hunter and Ashby (13) reported that the initial paresthesia usually corresponds to the spinal segment near the cathodal contact (most rostral dermatomes), indicating that DR fibers have lower thresholds than DC fibers. In their mapping study of sensory responses to SCS, Barolat et al. (1) demonstrated that most body areas have the highest probability of paresthesia when the stimulating cathode is at the level o f the corresponding DR entry zone, suggesting that DR fibers demonstrate a higher probability to be activated than DC fibers. Barolat et al. (2) reported that the average PT value progressively decreases as the electrode is further away from the radiological midline. The average values at (low) thoracic levels dropped to 70% (3-5 mm from midline) and 47% (>5 mm from midline) as compared with a position within 3 mm from midline. This observation also indic ates that PT is related to the activation of DR fibers, because at more than 5 mm from midline, the electrode is still close to a DR, but distant from the DCs. At midcervical and low thoracic levels, PT was reduced even more, as demonstrated both empirically (6) and theoretically (8).

Summary TOP

It is likely that PT for stimulation paresthesias is generally related to the activation of DR fibers, whereas DC fibers usu ally need higher stimuli for their activation. Part of the DC fibers may be recruited first when the electrode-to-spinal cord distance is less than approximate ly 2 mm, which may occur when the electrode is at a cervical level. The placement of two or three (stiff) electrodes in parallel at a low thoracic level, pres umably causing a significantly reduced electrode-to-spinal cord distance, may also lead to the primary stimulation of some dermatomes corresponding to DC fibers(JD Law, personal communication). A strict condition is that the center of the cathode corresponds to the spinal cord midline. Only a slightly asymmetrical po sition will result in a reduction of the ipsilateral DR fiber threshold exceeding the reduction of the lowest DC fiber threshold, thus favoring the primary activatio n of DR fibers.

DT related to DR stimulation TOP

Model prediction TOP

The computer model predicts that two DR fibers in the same root, having a different caliber, have a constant ratio of their threshold stimuli, as is true for neighboring DC fibers of different sizes. The threshold ratio of a DC fiber and a DR fiber, however, varies strongly with th e electrode-to-spinal cord distance, both among vertebral levels and among patients (as described under Neural Structures Activated in SCS) (see Fig. 1). If the ratio of PT and DT does vary strongly with electrode position and among patients, these thresholds, therefore, might not be related to the same fiber typ e. However, either DC or DR fibers might be involved if the ratio of PT and DT is constant. In the latter case, DT might be related to DR stimulation, because it was demonstrated that PT is related to DR stimulation as well (as described under PT Generally Related to DR Stimulation).

Empirical evidence TOP

Jobling et al. (14) calculated that the mean ratio DT:PT from 15 patients with upper and midthoracic bipolar stimulation was approximately 1.38 . Barolat et al. (G. Barolat, J He, B Ketcik, manuscript in preparation) also calculated this ratio from their clinical database, which inclu ded almost 4000 bipolar and monopolar combinations from 106 patients. Except for the levels C5-T1, mean values for stimulation at vertebral levels C1-L1 were 1.33 -1.46 (mean, 1.38). For the levels C5-T1, mean values were 1.51-1.57 (mean, 1.53) (see below).

Law (16) reported that segmental motor activity usually occurs in the most rostral area regarding the electrode level, whereas Hunte r and Ashby (13) observed that, at 3 pulses per second stimulation, the initial motor response corresponds to the level of the stimulating cathode. Bo th reports indicate that motor threshold is related to DR stimulation. Dimitrijevic et al. (5) also concluded that motor responses to SCS are related to DR fiber stimulation.

Summary TOP

From the constant ratio DT:PT (~1.38) and other empirical evidence, we can conclude that DT is probably related to stimulation of DR fibers. The slightly higher ratio (~1.53) when stimulating at the levels C5-T1 is presumably a result of the small electrode-to-spinal cord dista nce at the cervical enlargement in some of the patients, resulting in DC fiber thresholds lower than those of DR fibers (Fig. 1). Under these conditions, the ratio DT:PT will be increased, because PT is related to the stimulation of DC fibers, whereas DT is related to DR fiber stimulation. Law (17) also reported a higher mean ratio (1.58) in 46 patients with low thoracic bi- and tripolar stimulation, presumably resulting from an electrode-to-spinal cord distance near the lumbar en largement, reduced by the implantation of two or three percutaneous electrodes in parallel (as described under PT Generally Related to DR Stimulation). From the level at which the stimulation was given, Law concluded that body areas first covered with paresthesia are related to DC fiber stimulation (JD Law, personal communication), which is in accordance with the higher ratio DT:PT he found.

Segmentary paresthesia most probable in midthoracic stimulation TOP

Model prediction TOP

Because the mean electrode-to-spinal cord distance is largest in the midthoracic area (9), DC fiber thresholds are most likely to exceed DT (~1.4 PT) when the SCS electrode is at the levels T4-T7 (see Fig. 1). Therefore, DC fibers are least likely to be activated below DT when stimulating midthoracically, and an exclusive segmental response to DR stimulation will generally occur.

Empirical evidence TOP

It is well known that, in midthoracic stimulation (T4-T7), a painful band around the chest often dominates and restricts the spread of paresthesia (1, 2, 20). A rostral segmentary band of motor stimulation occurs before other dermatomes can be covered with paresthesia, indicating that the threshold for the activation of DC fibers exceeds both the threshold of cutaneous DR fibers and (large) proprioceptive DR fibers.

Summary TOP

Some patients may not demonstrate only a segmentary response but a broader paresthesia coverage when stimulated midthoracically. This is presumably because of the large anatomical variation among patients, resulting in a small electrode-to-spinal cord distance in some patients.

Paresthesia coverage effected by the anode-cathode combination TOP

Model prediction TOP

The computer model predicts that, in comparison to monopolar stimulation, bipolar and tripolar stimulation result in a reduced DC fiber threshold as compared with the DR fiber threshold, and that a reduction of the contact distance in bi-/tripolar stimulation has the same effect (11). These data indicate that the difference between the DC fiber threshold and the (usually lower) DR fiber threshold is least when using a narrow bi-/tripole instead of a monopole or a wide bi-/tripole. Consequently, (narrow) bi-/tripolar stimulation enables the largest number of DC fibers to be activated in the range of stimulation between PT and DT, and is thus likely to result in the broadest paresthesia coverage.

Empirical evidence TOP

Krainick et al. (15), who implanted bipolar electrodes endodurally, reported that in monopolar stimulation paresthesias were always confined to a limited body area, whereas in bipolar stimulation paresthesias were strongly extended in a caudal direction. Barolat et al. (2) observed that stimulation with a narrow bipole results in a broader paresthesia coverage than a bipole with a large contact separation. Law (16, 17) and North et al. (21, 22) reported that patients preferred stimulation with a narrow bipole or tripole (central cathode), in contrast to combinations with a larger contact spacing or a monopole (presumably because of a broader paresthesia coverage). North et al. (21, 22) also reported that, in midthoracic stimulation, radicular effects may be avoided best when using a "guarded tripole," whereas Krainick et al. (15) observed that, in contrast to monopolar stimulation, no painful radicular side effects were experienced with bipolar stimulation.

Verification of model predictions: Conclusions TOP

Both empirical and computer modeling data indicate that, in SCS, stimulation of large cutaneous afferents in the DCs is limited by the simultaneous activation of DR fibers. Because of the electric field imposed by stimulation with commonly applied SCS electrodes, large DR fibers are likely to have a lower threshold for their activation than large DC fibers. Moreover, smaller size (proprioceptive) DR fibers set the threshold DT by inducing painful motor responses. As a consequence, paresthesia generally starts at the spinal level corresponding to the electrode position and may spread caudally. When, because of a patient's anatomy, threshold stimuli of DC fibers are high as compared with DR fibers, only a small proportion of the DC fibers can be activated below DT and paresthesia coverage will be limited. The most extreme situation exists midthoracically, where the mean electrode-to-spinal cord distance is largest and DC fiber thresholds exceed DT. Therefore, the exclusive DR fiber activation results in radicular band paresthesia and pain on the chest or the abdominal wall. When stimulating at the cervical or low-thoracic portions of the spine, where the electrode-to-spinal cord distance is generally smaller, a mixed activation of DR and DC fibers occurs and results in a broader paresthesia coverage. In Figure 2, two situations are presented. The left one (Fig. 2a) demonstrates a mixed activation of DR and DC fibers, whereas the right one (Fig. 2b) demonstrates an almost exclusive DR fiber recruitment between PT and DT.

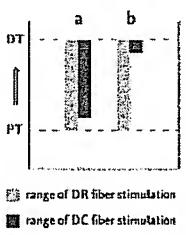

FIGURE 2. Mixed activation of DR and DC fibers(*a*) and almost exclusive DR fiber activation (*b*) in the range of stimulation between PT and DT (=1.4 PT).

Because the coverage of a large body area with paresthesia increases the likelihood of completely covering the painful area, the efficacy of SCS in the treatment of chronic pain (especially complex pain patterns) will generally be improved when using an anode-cathode combination and geometry that enhances DC stimulation or reduces DR stimulation. In the next section, two approaches to broaden paresthesia coverage are presented.

METHODS TO IMPROVE PARESTHESIA COVERAGE TOP

DC stimulation can be enhanced by changing the imposed electric field in such a way that the threshold for stimulation of DC fibers is reduced in comparison with the threshold for DR fiber stimulation. This effect can be realized either by optimization of the geometry of a rostrocaudal epidural array or by the use of a transverse tripolar epidural array.

Rostrocaudal contact array TOP

A systematic analysis of the effects of the size, spacing, and combination of anodes and cathodes on the thresholds of DC and DR fiber stimulation in a midcervical and a midthoracic spinal cord model led to the following conclusions (11). Low threshold DC stimulation, resulting in a broad paresthesia coverage, is favored by tripolar (central cathode) and bipolar stimulation, with contacts having small lengths and spacings ("narrow bi-/tripole"). Low threshold DR stimulation, giving paresthesias in only few (rostral) dermatomes, is obtained by monopolar stimulation with a long contact, or bi-/tripolarly with long contacts and large spacings ("wide bi-/tripole").

These effects are shown in Figure 3, A-F, representing part of the transverse section of the midcervical model (see Fig. 5). Recruitment lines in the DCs, indicating the maximum depth at which the largest DC fibers (12-μm diameter) are activated at a determined stimulation voltage, are drawn in these figures. The selected voltages were related to the threshold voltage (T) of the largest DR fibers (15-μm diameter) and recruitment lines were calculated at 1.0 T and 1.5 T (=DT). When only one line is shown in a figure, the 1.0 T recruitment line is missing and the threshold of any DC fiber exceeds T. The presence of two lines indicates that DC fibers between these lines have thresholds between 1.0 T and 1.5 T, whereas fibers between the dorsal line and the DC border have thresholds lower than those of the largest DR fibers.

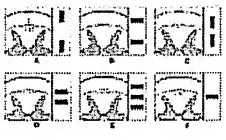

FIGURE 3. DC fiber activation by various rostrocaudal anode-cathode configurations, represented by recruitment lines in the DCs at stimulation amplitudes 1.0 T and 1.5 T (T = DR fiber threshold); midcervical spinal cord model (2.0 mm electrode-to-spinal cord distance); electrode geometry shown at right side. Wide bipole with long contacts (*A*); wide bipole with short contacts (*B*); narrow bipole with long contacts (*C*); narrow bipole (*D*); narrow tripole (central cathode) (*E*); monopole (*F*).

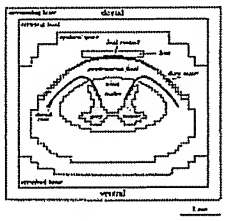

FIGURE 5. Transverse section of the midcervical model.

At the right side of each model section, the corresponding (longitudinal) contact configuration is shown. A "wide bipole," having 3.0 mm long and 1.0 mm wide contacts separated by 4.0 mm (edge-to-edge), is modeled at a symmetrical position regarding the spinal cord and shown in Figure 3A. In the model of Figure 3B, the contacts are turned by 90 degrees, still having a 4.0 mm separation. The contacts in Figure 3C have the same orientation as in Figure 3A, but their separation is reduced to 1.0 mm, whereas, in Figure 3D, their orientation is changed as well ("narrow bipole"). The "wide bipole"(Fig. 3A) only recruits a small (median) area at voltages of 1.0 T or less. This area, as well as the DC area enclosed by the 1.5 T recruitment line, is increasingly larger in the models of Fig. 3, B, C, and D, respectively. A "narrow tripole"(Fig. 3E) with the same dimensions as the "narrow bipole" produces the largest recruited area, covering the complete lateral extent of the DCs at 1.5 T. In contrast, a monopole (cathode) having the same contact size (Fig. 3F) only produces a small recruited area at 1.5 T and no DC fiber recruitment at voltages below 1.2 T. The lowest value (PT) of the DR fiber and DC fiber thresholds (the latter at the dorsomedial border of the DCs), as well as their ratio (DC:DR) and the range of stimulation defined as the ratio DT:PT (DT = 1.4 × DR fiber threshold) are presented in Table 1 for each model (Fig. 3, A-F).

TABLE 1. Lowest Fiber Threshold (Perception Threshold), Dorsal Column-Dorsal Root Fiber Threshold Ratio (Dorsal Column: Dorsal Root), and Range of Stimulation (Discomfort Threshold:Perception Threshold) for Each Electrode Configuration Presented in Figure 3[a]

We demonstrate that the DT:PT ratio of 1.4 may rise far beyond the mean value for currently available SCS electrodes and that an increasing DT:PT ratio is accompanied by an increasing DC fiber recruitment. Under optimal stimulation conditions ("narrow tripole"), a wide area of the DCs can be activated, resulting in a broad paresthesia coverage. It needs to be considered, however, that less fibers than shown in the figures will be recruited in the median part of the DCs, because these DC fibers have a smaller diameter than those in the lateral DCs (12, 23). Taking into account the stimulation voltage and current needed, we calculated the following optimal geometry for the narrow bi-/tripole: contact length approximately 1.5 mm and spacing 2 to 2.5 mm (for any SCS electrode type), contact width approximately 4 mm (for laminectomy electrodes) (J Holsheimer, WA Wesselink, manuscript submitted for publication).

Transverse tripolar lead (TTL) (U.S. Patent No. 5,501,703) TOP

When using a TTL as shown in Figure 4A, the central cathode, inducing nerve fiber depolarization and excitation (24), is closest to the DCs, whereas the lateral anodes, inducing hyperpolarization, are near the DRs. Stimulation with a TTL will, therefore, result in an increased threshold to stimulate DR fibers as compared with DC fibers and will thus favor a broad paresthesia coverage (27).

FIGURE 4. TTL powered by two pulse generators giving simultaneous pulses of variable amplitudes V1 and V2 (*A*). Recruitment lines in the DCs at amplitudes 1.0 T and 1.5 T (T = DR fiber threshold) and V1 = V2 (*B*). Recruitment lines with V1 = 3V2(*C*); midcervical model.

The central cathode is 1.0 mm long and 2.0 mm wide (to take advantage of the geometrical aspects described in the previous section), whereas the anodes are 2.0 mm long and 1.0 mm wide, with an edge-to-edge separation of 2.0 mm to the cathode (Fig. 4A). Modeling results are shown in Figure 4, B and C (similar to Fig. 3). In Figure 4B, the electrode is placed symmetrically to the spinal cord, and the two anodes have the same voltage. The shapes of the recruitment lines are different from those in Figure 3; medially, they penetrate deeper in the DCs, which may result in an improved caudal paresthesia coverage.

Another advantage of the TTL is that the recruited DC area can be moved to either side when powered by a dual channel pulse generator producing simultaneous pulses of different amplitudes, thus thereby shifting the area of paresthesias. In Figure 4C, the voltage between the cathode and the left anode is three times the voltage between the cathode and the right anode, resulting in a shift of the recruited area to the right side of the DCs. A corresponding shift of the body area covered with paresthesia will result. The significance of this option becomes clear from the data of Barolat et al. (2), who demonstrate that even when leads are positioned perfectly at the radiological midline, only 27% of the patients experienced bilateral and symmetrical paresthesias. These results are in accordance with a magnetic resonance imaging study demonstrating that the anteroposterior midlines of the spinal cord and the vertebra are 1 to 2 mm apart in 40% of the patients (9), resulting in a significant asymmetry of paresthesias (8).

Preliminary clinical data from low-thoracic stimulation with a TTL system in several patients (J Holsheimer, B Nuttin, GW King, WA Wesselink, J Gybels, P de Sutter, manuscript in preparation) are in accordance with computer model predictions. Paresthesia can be moved to either side of the body, the DT:PT ratio has high values (2-4), and a broad paresthesia coverage is obtained.

DISCUSSION TOP

Modeling the immediate effects of electrical stimulation on spinal cord nerve fibers is an appropriate method for the quantitative analysis of these effects. Moreover, it is a useful tool in the design of SCS electrodes. However, a model is a simplification of reality, and the analysis of SCS presented here does not cover all phenomena. Improvements are still necessary to cover all relevant empirical data.

The electric field imposed by the current generation of SCS electrodes favors DR fiber stimulation and, therefore, limits paresthesia coverage and the efficacy of this therapy, especially in complex pain. Technical predictors of a successful relief include stimulation by a rostrocaudal narrow bi-/tripole in a symmetrical position to the spinal cord and a small electrode-to-spinal cord distance, resulting in a low PT and a high ratio DT:PT. A single optimal electrode is applicable at all levels from C1 to L1.

When using the TTL and a dual channel pulse generator with independent voltage control of each channel, positioning of the electrode will be less critical, whereas changes in paresthesia coverage resulting from electrode migration or histological changes may simply be corrected by changing the amplitude of one or both stimulation channels, thereby avoiding electrode repositioning by surgical intervention.

ACKNOWLEDGMENT TOP

I am grateful to Wilbert Wesselink, M.Sc. for modeling the cases described in this article.

APPENDIX: THE SCS COMPUTER MODEL TOP

The SCS computer model consists of two parts. Three-dimensional models, as the midcervical one shown in Figure 5, represent the white and gray matter of the spinal cord and surrounding anatomical structures (intradural cerebrospinal fluid, dura mater, epidural fat, vertebral bone). Each model compartment is characterized by its specific electrical conductivity. The geometry of each model is based on transverse magnetic resonance images (9). The dimensions of the modeled spinal segments are 60 mm (rostrocaudal), 20 to 25 mm (lateral), and approximately 25 mm (anteroposterior). Each model consists of 175,616 cubic volume elements of variable dimensions. Electrode contacts (anodes, cathodes) are placed in the dorsal epidural space next to the dura mater and are set at different voltages. Subsequently, the voltages at the 185,193 grid points of the three-dimensional model are calculated.

The second part of the SCS model consists of electrical cable models of myelinated DC and DR fibers. These models demonstrate a voltage and time-dependent nodal membrane resistance, enabling the simulation of excitation. The rostrocaudal DC fibers have transverse collaterals entering the dorsal horns. Each DR fiber is connected to an ascending and a descending DC fiber, whereas its orientation may be varied. The potentials in the three-dimensional model corresponding to the nodal positions of DC and DR fibers are used to calculate the threshold voltages for the excitation of these fibers when applying a rectangular pulse (usually 210 μs). The SCS model has been described in detail in previous reports (28-31).

REFERENCES TOP

1. Barolat G, Massaro F, He J, Zeme S, Ketcik B: Mapping of sensory responses to epidural stimulation of the intraspinal neural structures in man. **J Neurosurg** 78:233-239, 1993.
[Context Link]

2. Barolat G, Zeme S, Ketcik B: Multifactorial analysis of epidural spinal cord stimulation. **Stereotact Funct Neurosurg** 56:77-103, 1991.
[CrossRef] [Context Link]

3. Coburn B: Electrical stimulation of the spinal cord: Two-dimensional finite element analysis with particular reference to epidural electrodes. **Med Biol Eng Comput** 18:573-584, 1980.
[Medline Link] [CrossRef] [Context Link]

4. Coburn B: A theoretical study of epidural electrical stimulation of the spinal cord: Part II-Effects on long myelinated fibers. **IEEE Trans Biomed Eng** 32:978-986, 1985.
[Medline Link] [Context Link]

5. Dimitrijevic MR, Faganel J, Sharkey PC, Sherwood AM: Study of sensation and muscle twitch responses to spinal cord stimulation. **Int Rehabil Med** 2:76-81, 1980.
[Medline Link] [Context Link]

6. He J, Barolat G, Holsheimer J, Struijk JJ: Perception threshold and electrode position for spinal cord stimulation. **Pain** 59:55-63, 1994.
[CrossRef] [Context Link]

7. Holsheimer J, Struijk JJ: How do geometric factors influence epidural spinal cord stimulation? A quantitative analysis by computer modeling. **Stereotact Funct Neurosurg** 56:234-249, 1991.
[CrossRef] [Context Link]

8. Holsheimer J, Barolat G, Struijk JJ, He J: Significance of the spinal cord position in spinal cord stimulation. **Acta Neurochir Suppl (Wien)** 64:119-124, 1995.
[Context Link]

9. Holsheimer J, den Boer JA, Struijk JJ, Rozeboom AR: MR assessment of the normal position of the spinal cord in the spinal canal. **AJNR Am J Neuroradiol** 15:951-959, 1994.
[Context Link]

10. Holsheimer J, Struijk JJ, Rijkhoff NJM: Contact combinations in epidural spinal cord stimulation: A comparison by computer modeling. **Stereotact Funct Neurosurg** 56:220-233, 1991.
[CrossRef] [Context Link]

11. Holsheimer J, Struijk JJ, Tas NR: Effects of electrode geometry and combination on nerve fibre selectivity in spinal cord stimulation. **Med Biol Eng Comput** 33:676-682, 1995.
[CrossRef] [Context Link]

12. Horch KW, Burgess PR, Whitehorn D: Ascending collaterals of cutaneous neurons in the fasciculus gracilis of the cat. **Brain Res** 117:1-17, 1976.
[CrossRef] [Context Link]

13. Hunter JP, Ashby P: Segmental effects of epidural spinal cord stimulation in humans. **J Physiol** 474:407-419, 1994.
[CrossRef] [Context Link]

14. Jobling DT, Tallis RC, Sedgwick EM, Illis LS: Electronic aspects of spinal-cord stimulation in multiple sclerosis. **Med Biol Eng Comput** 18:48-56, 1980.
[Context Link]

15. Krainick J-U, Thoden U, Riechert T: Spinal cord stimulation in post-amputation pain. **Surg Neurol** 4:167-170, 1975.
[Context Link]

16. Law JD: Spinal stimulation: Statistical superiority of monophasic stimulation of narrowly separated, longitudinal bipoles having rostral cathodes. **Appl Neurophysiol** 46:129-137, 1983.
[Context Link]

17. Law JD: Targeting a spinal stimulator to treat the"failed back surgery syndrome." **Appl Neurophysiol** 50:437-438, 1987.
[Context Link]

18. Law JD, Miller LV: Importance and documentation of an epidural stimulating position. **Appl Neurophysiol** 45:461-464, 1982.
[Context Link]

19. Melzack R, Wall PD: Pain mechanisms: A new theory. **Science** 150:971-978, 1965.
[Medline Link] [CrossRef] [Context Link]

20. North RB: Spinal cord stimulation for chronic, intractable pain, in Devinsky O, Beric A, Dogali M (eds): *Electrical and Magnetic Stimulation of the Brain and Spinal Cord.* New York, Raven Press, 1993, pp 289-301.
[Context Link]

21. North RB, Ewend MG, Lawton MT, Piantadosi S: Spinal cord stimulation for chronic, intractable pain: Superiority of "multi-channel" devices. **Pain** 44:119-130, 1991.
[CrossRef] [Context Link]

22. North RB, Nigrin DJ, Fowler KR, Szymanski RE, Piantadosi S: Automated "pain drawing" analysis by computer-controlled, patient-interactive neurological stimulation system. **Pain** 50:51-57, 1992.
[CrossRef] [Context Link]

23. Petit D, Burgess PR: Dorsal column projection of receptors in cat hairy skin supplied by myelinated fibers. **J Neurophysiol** 31:849-855, 1968.
[Context Link]

24. Ranck JB Jr: Which elements are excited in electrical stimulation of mammalian central nervous system: A review. **Brain Res** 98:417-440, 1975.
[CrossRef] [Context Link]

25. Shealy CN, Mortimer JT, Reswick JB: Electrical inhibition of pain by stimulation of the dorsal columns: Preliminary clinical report. **Anesth Analg** 46:489-491, 1967.
[Fulltext Link] [Medline Link] [CrossRef] [Context Link]

26. Simpson BA: A new dual bipolar electrode system for spinal cord stimulation, in Galley D, Illis LS, Krainick JU, Meglio M, SierJC, Staal MJ (eds): *Proceedings of the 1st International Congress of the International Neuromodulation Society.* Bologna, Monduzzi Editore, 1992, pp 13-17.
[Context Link]

27. Struijk JJ, Holsheimer J: Transverse tripolar spinal cord stimulation: Theoretical performance of a dual channel system. **Med Biol Eng Comput** 34:273-279, 1996.
[CrossRef] [Context Link]

28. Struijk JJ, Holsheimer J, Barolat G, He J, Boom HBK: Paresthesia thresholds in spinal cord stimulation: A comparison of theoretical results with clinical data. **IEEE Trans Rehabil Eng** 1:101-108, 1993.
[Context Link]

29. Struijk JJ, Holsheimer J, Boom HBK: Excitation of dorsal root fibers in spinal cord stimulation: A theoretical study. **IEEE Trans Biomed Eng** 40:632-639, 1993.
[CrossRef] [Context Link]

30. Struijk JJ, Holsheimer J, van der Heide GG, Boom HBK: Recruitment of dorsal column fibers in spinal cord stimulation: Influence of collateral branching. **IEEE Trans Biomed Eng** 39:903-912, 1992.
[Medline Link] [CrossRef] [Context Link]

31. Struijk JJ, Holsheimer J, van Veen BK, Boom HBK: Epidural spinal cord stimulation: Calculation of field potentials with special reference to dorsal column nerve fibers. **IEEE Trans Biomed Eng** 38:104-110, 1991.
[Medline Link] [CrossRef] [Context Link]

COMMENTS TOP

This study by Holsheimer is a good example of how cooperation between clinical neurosurgery and biomedical engineering can foster a better understanding of physiological phenomena and provide remedies for the technical drawbacks of surgical methods.

It is well known that an adequate placement of the electrode (i.e., the cathode located between the dorsal median sulcus and the dorsal root [DR] entry zone area, at the [upper] level of the spinal cord segments corresponding to the pain) may not produce enough well-tolerated paresthesias to sufficiently cover the pain territory and thus be effective.

In the first part of the article, the author recalls several neuroelectrological facts, verified from model predictions and clinical observations. "Beneficial" paresthesias produced by spinal cord stimulation(SCS) result predominantly from stimulation of the lemniscal fibers in their dorsal column (DC) part because of their topographical regroupment there, rather than from stimulation at their DR level. The stimulation threshold for DR is significantly lower than for DC. The range between perception threshold and discomfort threshold is narrow. Discomfort is caused by segmental paresthesias and also painful motor contractions originating from spinal motor reflexes. Discomfort prevents increasing stimulation intensity and limits involvement of the DC fibers.

Because the potential paresthesia coverage is much more important with DC than with DR stimulation, Holsheimer tried to design new electrodes that preferentially were able to stimulate the DC fibers and performed tests on an ingenious SCS computer model. The principles of the model, which was described in detail by the author and his colleagues in previous reports, are clearly summarized in the Appendix in the article. The newly designed electrodes were capable of providing a better involvement of DC fibers for this model and were of two types, including optimally dimensioned rostrocaudal bi-/tripole electrodes and a transverse tripolar lead (TTL). According to the laboratory testing, these new electrodes seem to be a real advance in the technology of SCS.

In the Discussion in the article, the author states, "When using the TTL and a dual channel pulse generator with independent voltage control of each channel, positioning of the electrode will be less critical, whereas changes in paresthesia coverage caused by electrode migration or histological changes may simply be corrected by changing the amplitude of one or both stimulation channels, thereby avoiding electrode repositioning by surgical intervention." The author might be right for the positioning of the electrode and also for electrode migration (although this is not frequent in well-trained surgical hands). For histological changes caused by chronic stimulation, which explain, at least partly, some secondary failures, the problem seems far from being solved by only technical adjustments.

In this article, which does not deal with clinical features and, consequently, does not have to mention pathological data, the author probably underestimates some important anatomical impossibilities to stimulate the adequate fibers. In a significant number of patients affected with persistent neuropathic pain, the lemniscal fibers corresponding to the painful territory that the electrodes must stimulate simply do not exist anymore.

This is the case in which the lesion has totally interrupted the primary afferent neurons in their radicular part, i.e., between the spinal ganglion and the cord, and also in which the ganglion cells have been destroyed (as, for instance, by the herpes zoster virus). In such cases, the fibers are degenerated from the lesion up to their synapse, with the secondary neuron at the brain stem level. The same applies in patients with totally interrupted lemniscal pathways at the level of the spinal cord. This lack of "valid" fibers to stimulate in the DCs clearly explains failures in a number of so-called "malpositioned" electrode cases (3, 4, 6).

Before indicating SCS, and even before preimplantation percutaneous trials, it seems important to consider the anatomicophysiological status of the primary afferent (lemniscal) fibers because of the cost of SCS technology. That is the reason why, in the process of the selection of patients, we have instituted as a general rule an exploration of the integrity of the lemniscal fibers by a careful clinical examination and, if necessary, somesthetic evoked potential recording (5) and also an exploration of the dorsal horn circuitry by measurements of the nociceptive (RIII) flexion reflexes (1, 2).

This may help in making a logical choice of treatment, either SCS, if the primary afferent neurons are still functional in their central part (i.e., from the ganglion up to the brain stem), or implantation of the electrode at the level of the somesthetic relay nucleus of the thalamus or in front of the precentral motor cortex, if the axons of the primary afferent neurons have totally degenerated up to the brain stem.

Despite ignoring the complexity of the problem from an anatomicopathological point of view, the author should be acknowledged for having explored the biophysiological mechanisms of SCS, and for bringing to clinicians' attention an interesting electrical model of the spinal cord. The newly designed electrodes might solve a part, if not all, of the technical problems and thereby improve the efficiency of the SCS method.

Marc Sindou

Lyon, France

1. Garcia-Larrea L, Sindou M, Mauguiere F: Clinical use of nociceptive flexion reflex recording in the evaluation of functional neurosurgical procedures. **Acta Neurochir Suppl (Wien)** 46:53-57, 1989.
[Context Link]

2. Garcia-Larrea L, Sindou M, Mauguiere F: Nociceptive flexor reflexes during analgesic neurostimulation in man. **Pain** 39:145-146, 1989.
[Context Link]

3. Keravel Y, Sindou M, Athayde A: Indication of analgesic neurostimulation in chronic neurological pain, in Scherpereel P, Maynadier J, Blond S (eds): *The Pain Clinic II.* Amsterdam, VNU Science Press, 1987, pp 167-185.
[Context Link]

4. Keravel Y, Sindou M, Blond S: Stimulation and ablative neurosurgical procedures in the peripheral nerves and the spinal cord fordeafferentation and neuropathic pain, in Besson J-MR, Guilbaud G (eds):*Lesions of Primary Afferent Fibers as a Tool for the Study of Clinical Pain.* Amsterdam, Elsevier, 1991, pp 315-334.
[Context Link]

5. Mertens P, Sindou M, Gharios B, Garcia-Larrea L, Mauguiere F: Spinal cord stimulation for pain treatment: Prognostic value of somesthetic evoked potentials. **Acta Neurochir (Wien)** 117:90-91, 1992.
[Context Link]

6. Sindou M, Mertens P, Keravel Y: Neurochirurgie de la douleur. **EMC Neurol** 17:700B-715B, 1996.

SCS remains one of the few treatments available for the suffering in patients caused by intractable pain after multiple unsuccessful operations. It is particularly useful for patients with arachnoiditis. The use of long-acting oral narcotics in these patients is currently under study, and there is some literature on the use of intrathecal narcotics administered through implanted pumps. However, neither technique has the background of information that is available for SCS.

Currently, it seems that patient selection is the first key ingredient of the successful use of SCS. Comorbidities that influence the pain complaint need to be investigated and treated. It is important to be certain that pain is what is being treated.

The second important feature of successful stimulation is in the delivery of stimulation. Variables that are important include electrode position, electrode design, and the parameters of stimulation. The author explores a number of issues. The first is the question of which neural structures are activated by stimulation. Our early research suggested that all were activated. However, it does seem from the author's model that large DR fibers are most susceptible to stimulation. He also concludes that the perception threshold is related to DR stimulation. A major factor is discomfort brought about by stimulation. The author concludes that unpleasant paresthesias are most likely to occur with the stimulation of DR fibers.

The key feature of successful stimulation is paresthesias that occur throughout the entire area of perceived pain. Only when this occurs is pain relief likely to be sufficient. The author concludes that a narrow stimulation field that is either bipolar or tripolar allows the largest number of DC fibers to be activated and thus produces the broadest paresthesia coverage.

The most important aspect of the article is that which deals with methods to improve the broad occurrence of paresthesias. The author discusses appropriate electrode array and, specifically, describes a transverse tripolar electrode system that maximizes paresthesias. Proof of effectiveness will be required, but the theoretical considerations are important. Anything that maximizes coverage of the painful area with paresthesias will improve the results of spinal stimulation. The most common cause of failure, in my experience, is the inability to get stimulation in the painful areas, thus leaving some of the pain uncovered and, therefore, unrelieved.

Donlin M. Long

Baltimore, Maryland

The implantation of SCS systems for pain control is arguably the most common operation currently performed in North America and Europe for the treatment of chronic pain. The technology has evolved from the original gate control theory proposed by Melzak and Wall and expanded by Shealy in the late 1960s with the application of so-called "DC stimulation." The original devices were extensions of the cardiac pacemaker technology of the time. What has occurred during the ensuing three decades has been a refinement of generator technology, including the development of totally implantible systems, battery technology with an advanced lifetime of the implanted units, programming technology with the use of radiofrequency-coupled programming, microchip technology with smaller and "more intelligent" systems, and electrode technology with multicontact systems and a wide variety of geometries. Change in this field has been incremental rather than revolutionary.

SCS is now the treatment of choice for a wide variety of chronic pain problems, most of those related to damage in some form to either the peripheral or central nervous system, so-called neuropathic pain. In my opinion, it is the surgical treatment of choice for failed back surgery syndrome, but may also be considered for patients with peripheral neuropathic pain caused by metabolic or traumatic neuropathy, nerve root injury from a wide variety of causes, postherpetic neuralgia, so-called "end-zone" pains in paraplegics, "reflex sympathetic dystrophy," post-thoracotomy and postmastectomy pain, and other

disorders. A trial of SCS is easily implemented by placement of a percutaneous electrode, which facilitates the possibility of treating a large variety of conditions with this method. The technique does not produce irreversible damage to the nervous system, is testable, and is one of very few surgical procedures that have demonstrated efficacy for conditions such as failed back surgery syndrome.

Holsheimer's work adds significantly to our understanding of SCS and will promote the future improvement in and application of this technology. He has concluded that SCS of the DCs, and by coverage of the painful region by nonpainful paresthesias, is limited mostly by simultaneous activation of DR fibers. This DR activation produces both segmental paresthesia, and at times, painful reflex motor responses. He has tested the theoretical performance of two electrode designs that may limit the spread of stimulation to the DR. This design incorporates a "transverse tripole" array of electrodes that incorporates a "guarded cathode," i.e., a cathode flanked on either side by anodes. The central cathode (inducing proximate fiber depolarization and excitation) is, in this arrangement, closest to the DCs, whereas lateral anodes (inducing hyperpolarization and inhibition) are closest to the DRs. Stimulation with a TTL will therefore result in an increased threshold to stimulate DR fibers compared with DC fibers. Additionally, in a two-channel system, the voltage applied to each cathode/anode pair (common cathode) can be varied independently. The laterality of the stimulation can be then easily controlled.

If successfully applied, what this might mean is that SCS electrodes may become much more effective to use and that positioning the electrode will be to some extent much less critical. Electrodes could then, for example, be placed under general anesthesia in a region that was predicted a priori to produce the optimal stimulation.

I expect that the application of TTL technology and further innovations in SCS will make this technology an even more popular alternative for pain control. Future challenges in this field will continue to involve the education of health care providers and insurance companies on the safety and efficacy of the procedure, as well as improving the cost effectiveness of the technique.

Kim J. Burchiel

Portland, Oregon

This is the latest in an important series of articles from Holsheimer and colleagues, describing finite element modeling of SCS. The predictions of the model may be and, in some cases, have been verified by current probe measurements, psychophysical studies, and evoked potential studies. The model has important implications for electrode placement, electrode design, and pulse generator design.

This work has culminated in a novel design, the "TTL." For many years, the design of stimulating electrode arrays has been in accordance with the principle that, for maximum efficiency, the stimulating dipole needs to be oriented parallel to the nerve fiber to be stimulated. Although this aspect, like other elements of conventional wisdom, remains true, it seems that it has constrained electrode design. Orienting a tripole transversely is a clever notion, which is predicted by Holsheimer's model to have distinct potential advantages. Common clinical problems (i.e., recruiting the low back), however, may or may not be addressed by this method.

As with any basic advance in the laboratory, this modeling and design work requires clinical corroboration. This will be of importance to researchers and clinicians with interest in the management of chronic pain, and SCS in particular. In addition, this technology may have broader applications in functional neurostimulation.

Richard B. North

Baltimore, Maryland

Everyone with experience of SCS knows that the prerequisite for obtaining pain relief is that the stimulation-induced paresthesias cover the painful region. However, the placement of the electrode to achieve this goal may sometimes be difficult. Therefore, the article by Holsheimer provides useful information and helps to understand how an electrode, whether uni- or multipolar, placed epidurally may activate adjacent neuronal elements and produce not only paresthesias but also uncomfortable sensations, as well as muscle contractions. The author has, over the years, published a series of articles in which he has demonstrated that the generation of these phenomena as a result of epidural stimulation may be better understood by the use of a computerized model of the spinal canal and the compartments surrounding the spinal cord and roots.

In the present study, Holsheimer discusses, from a theoretical point of view, how SCS performed with different electrode configurations and locations may activate preferentially DC or DR fibers. He confronts these findings and conclusions, based on data derived from his model, with clinical observations reported in the literature. This approach may, however, be subject to bias in the selection of available clinical data, and one may get the impression that the author himself has a relatively limited experience of performing SCS-electrode implantations. For example, it is a rare phenomenon that stimulation produces uncomfortable sensations. It may happen that when stimulation is applied at a midthoracic level, the patient may report a local painful sensation in the back, but when increasing the stimulus strength, this unpleasant sensation is replaced by paresthesias that may be segmental or invade more caudal portions of the trunk or the leg.

The author further argues that SCS often tends to activate DR fibers rather than fibers contained in the DCs because of the orientation of the electric field and the lower thresholds of the former. If that were the case, SCS might be equivalent to transcutaneous electrical nerve stimulation, apart from stimulating the roots on the preganglionic portion of the neuron instead of the postganglionic portion. This conclusion is contradictory to the common observation that patients who fail to respond to transcutaneous electrical nerve stimulation may nevertheless enjoy excellent pain relief with SCS. One needs to also consider the possibility that SCS may activate neuronal elements also in the DR entry zone and thus in the upper part of the dorsal horn.

I am surprised that the author does not discuss the importance of pulse width of the stimuli for the distribution of the paresthesias. In my experience with SCS for more than two decades, I have often observed that the segmental or "long tract" distribution may be markedly influenced by varying the pulse width. A short width, 50 to 100 microseconds, tends to be associated with segmental spreading of the paresthesias, whereas long widths, 300 to 500 microseconds, often produce sensations that spread more caudally. This is particularly the case when the electrode is located at midthoracic levels, but the same applies to locations in the cervical spine.

The author describes a new tripolar electrode design, in which the anodal poles are individually controlled by a two-channel stimulator. This electrode configuration seems most promising because it may be optimal for the selective activation of the DC on either side. Perhaps such an electrode array can be designed to permit implantation via the percutaneous route, and that it can be produced to be cost-effective. Unfortunately, the cost of SCS devices is still too high to permit a further dissemination of this effective mode of pain treatment.

Clearly, more experimental work is needed to elucidate the important issue of understanding how and why SCS functions, both regarding which neuronal elements are activated by the stimulating current and regarding the underlying physiological mechanisms by which pain relief is achieved. Without such knowledge, we may not be able to improve the efficacy of the method.

Björn A. Meyerson

Stockholm, Sweden

Keywords:
Chronic pain; Dorsal column stimulation; Dorsal root stimulation; Epidural electrodes; Paresthesia; Spinal cord stimulation

Copyright © by the Congress of Neurological Surgeons

Copyright © 2008, Congress of Neurological Surgeons. All rights reserved.
Published by Lippincott Williams & Wilkins.
Copyright/Disclaimer Notice • Privacy Policy
Subscribe to our RSS feed

Close

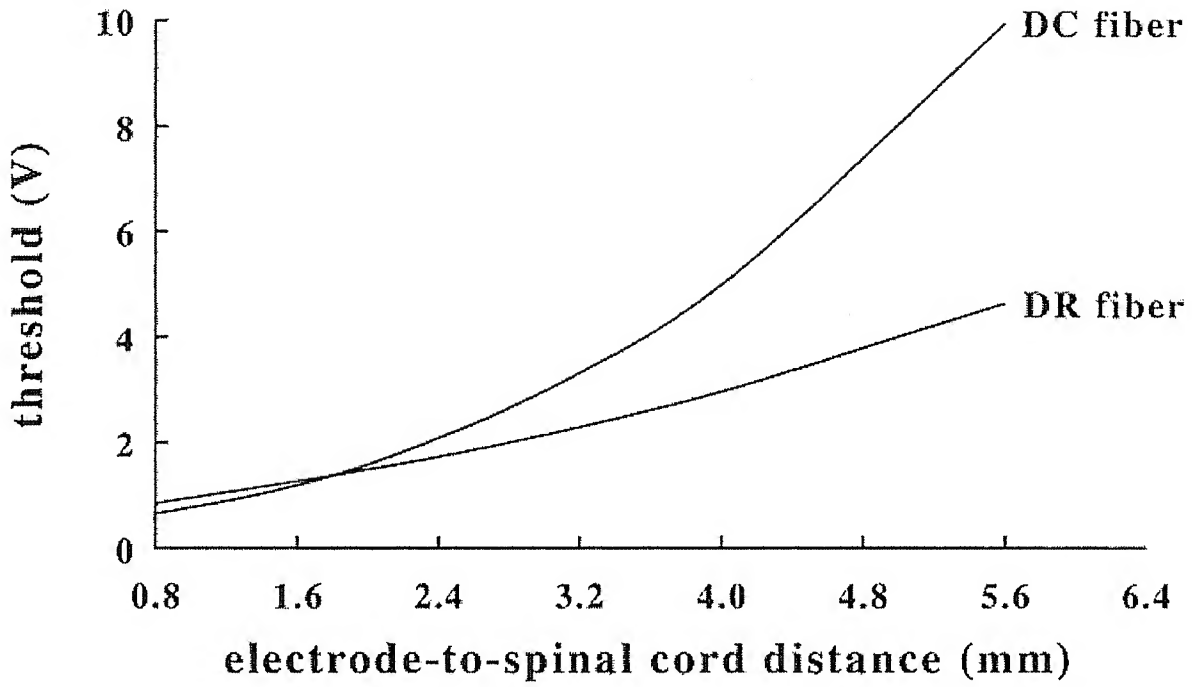

FIGURE 1. Calculated threshold stimuli of a 15-μm DC fiber and a 15-μm DR fiber as a function of the electrode-to-spinal cord distance.

Close

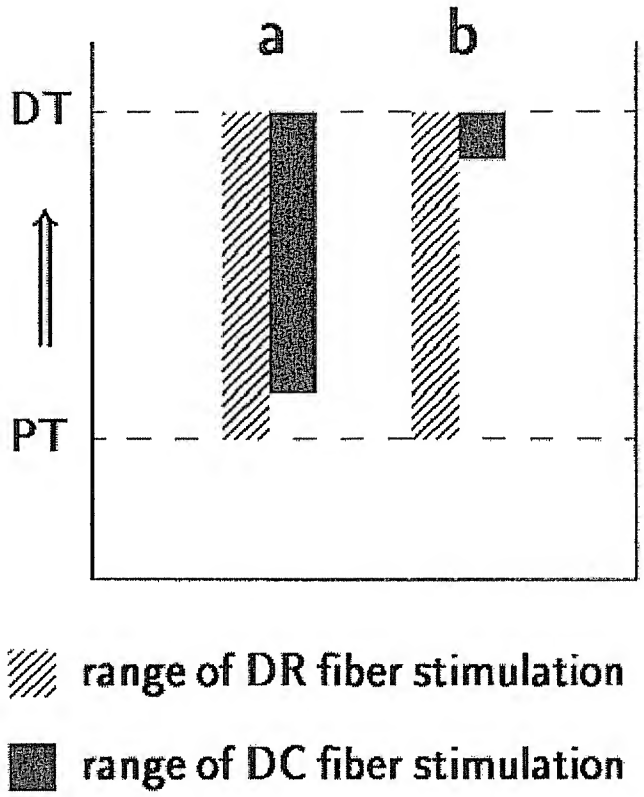

FIGURE 2. Mixed activation of DR and DC fibers(*a*) and almost exclusive DR fiber activation (*b*) in the range of stimulation between PT and DT (=1.4 PT).

Close

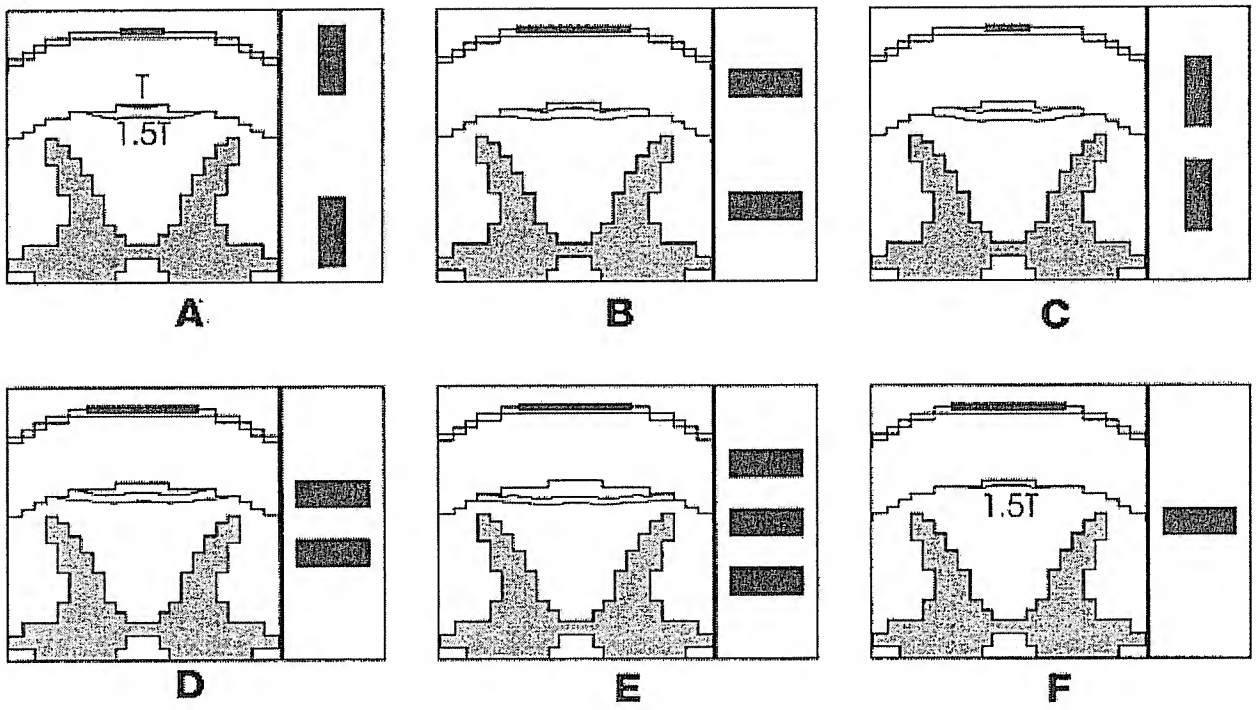

FIGURE 3. DC fiber activation by various rostrocaudal anode-cathode configurations, represented by recruitment lines in the DCs at stimulation amplitudes 1.0 T and 1.5 T (T = DR fiber threshold); midcervical spinal cord model (2.0 mm electrode-to-spinal cord distance); electrode geometry shown at right side. Wide bipole with long contacts (*A*); wide bipole with short contacts (*B*); narrow bipole with long contacts (*C*); narrow bipole (*D*); narrow tripole (central cathode) (*E*); monople (*F*).

Close

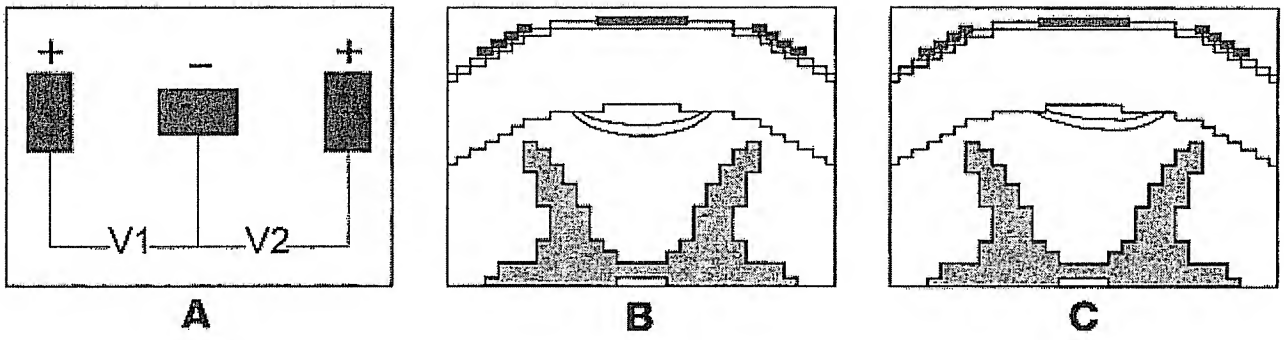

FIGURE 4. TTL powered by two pulse generators giving simultaneous pulses of variable amplitudes V1 and V2 (*A*). Recruitment lines in the DCs at amplitudes 1.0 T and 1.5 T (T = DR fiber threshold) and V1 = V2 (*B*). Recruitment lines with V1 = 3V2(*C*); midcervical model.

Close

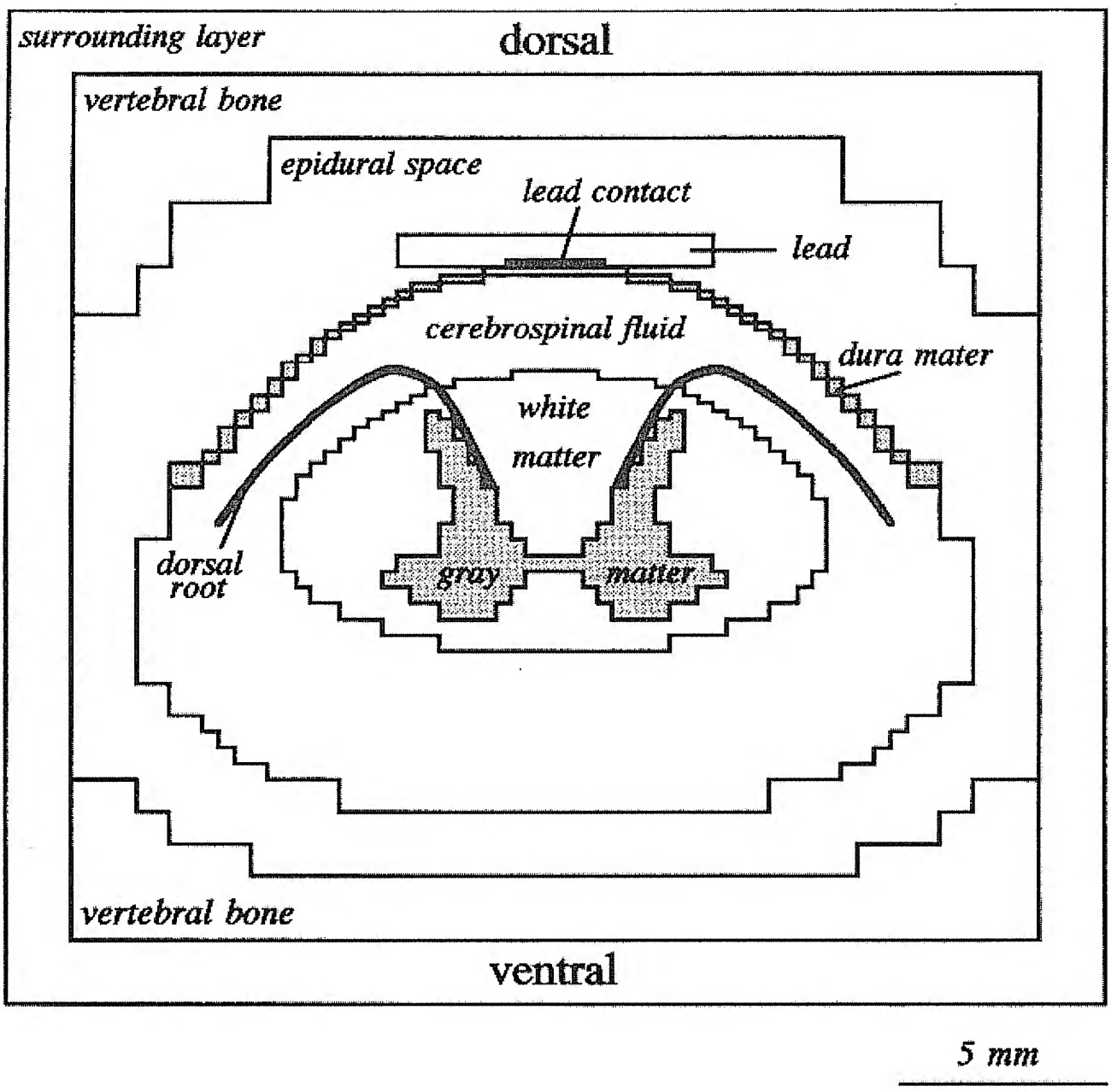

FIGURE 5. Transverse section of the midcervical model.

Close

Model	*Fig. 3A*	*Fig. 3B*	*Fig. 3C*	*Fig. 3D*	*Fig. 3E*	*Fig. 3F*
PT (volts)	2.80	2.36	2.85	3.47	2.90	1.18
DC:DR	0.94	0.77	0.69	0.57	0.34	1.23
DT:PT	1.49	1.82	2.04	2.45	4.08	1.40

[a] **PT, perception threshold; DC, dorsal column; DR, dorsal root; DT, discomfort threshold.**

TABLE 1. Lowest Fiber Threshold (Perception Threshold), Dorsal Column-Dorsal Root Fiber Threshold Ratio (Dorsal Column: Dorsal Root), and Range of Stimulation (Discomfort Threshold:Perception Threshold) for Each Electrode Configuration Presented in[a]

Exhibit B

RS Medical final project report

Evaluation of a new method for spinal cord stimulation (SCS)

Marcus Granmo & Jens Schouenborg
Neuronano Research Center, Lund University, Sweden

Aim

To test a new method for stimulation of the dorsal column based on interference between different stimulators. The hypothesis is that deeper pathways in the spinal cord can be more effectively stimulated than conventional SCS if an interference pattern with a beat frequency is achieved.

Project outlines

- Test a new method for spinal cord stimulation based on interference between two stimulation frequencies.
- Compare this with conventional stimulation.
- Simultaneous recordings from the Gracile nucleus and the Pyramid in the brainstem render easy comparison of the effect of stimulation (Fig. 1).
- Multiple analysis parameters are presented.

Experimental setup

Adult rats (Sprague-Dawley, 200-230 grams) anesthetized with isoflurane gas (1.8 % in a mixture of 60/40 % NO_2 and oxygen) were used (A detailed description of the preparation can be found in Kalliomäki, J., Granmo, M., Schouenborg, J. *Pain.* 2003 Jul;104(1-2):195-200). Two pairs of stimulation electrodes (bipolar stimulation, 4 electrodes in total) were placed epidurally on the spinal cord in either a crossed or parallel configuration (Fig. 2). Recording microelectrodes were inserted in the Gracile nucleus and the Pyramid in the brainstem. The Gracile nucleus receives ascending sensory information from dorsal column tracts which run relatively superficial in the dorsal part of the spinal cord. The pyramid, as part of the corticospinal tract, conveys descending motor commands from the brain to the spinal cord. In the rat spinal cord a major tract is located deep in the dorsal column, i.e. deeper than the dorsal column of the spinal cord activating the gracile nucleus (Fig. 1). By spinal cord stimulation, activating the pyramid tract fibers antidromically, we could record evoked volleys in this relatively deep tract, thus giving information about depth penetration of the stimulation. After each experiment, the animals were perfused with paraformaldehyde (10%) and the caudal brain stem was sectioned to verify the electrode position in the brainstem. Only experiments in which a location of the electrode in the pyramide tract was verified are included in this report (Fig. 4).

Stimulation and recording
Measurements were performed of SCS evoked activity in the Gracilis nucleus and for antidromic evoked volleys in the Pyramid. The stimulation electrodes were placed epidurally in two different configurations, crossed and parallel (Fig. 2). Two types of stimulation paradigms were used: 1. Sinus waves of 500 μs width (corresponding to 2000 Hz waves) applied at a frequency of 100 Hz to both electrode pairs. 2. An interference pattern of 500 μs + 476 μs (corresponding to 2000 and 2100 Hz respectively) sinus waves applied at 100 and 105 Hz respectively. Beat frequency 5 Hz (Fig. 3).

Data analysis
Thresholds of SCS evoked responses were collected. Stimulation intensity was increased or decreased in specific steps. For intensities in the range of 10-50 mV, steps of 10 mV were used, in the range 50-400 mV steps of 25 mV, in the range 400-900 mV steps of 50 mV, in the range 900-1200 mV steps of 100 mV and intensities over 1200 mV steps of 250 mV were used. The lowest stimulation intensity eliciting a clear response was considered the threshold. Each sampled data file is an average of 400 single recording sweeps (Fig. 4 and 5). The latency of the Pyramid responses which were used in the analysis (16-19 m/s) were consistent with those observed in the literature (Mediratta and Nicoll *J Physiol.* 1983 Mar;336:545-61, Stewart et al. *Brain Res.* 1990 Feb 5;508(2):341-4, Chapman and Yeomans *Neuroscience* 1994, 59(3):699-711). Pair-wise comparison of the two different stimulation paradigms (100 + 100 Hz versus 100+105 Hz) was performed in each animal. The collected data was analyzed for statistical significance using non-parametric tests (Paired comparisons - Wilcoxon signed rank test, non-paired - Mann-Whitney, where applicable). All data used for analysis is found in the attached file "RS analysis" (GraphPad document).

Results
In general, the thresholds for activation of both the Gracile nucleus and the Pyramid were significantly lower when using 100 + 105 Hz interference than conventional 100 + 100 Hz stimulation (figure 6 and 7). To yield a better understanding of the efficacy of the stimulation, the ratio between Pyramid and Gracile thresholds was used. Also here, 100 + 105 Hz stimulation showed a lower relative threshold than 100 Hz (figure 6 and 7). Furthermore, the difference between crossed and parallel electrode configuration was tested (figure 8 and 9). No significant difference was observed between these two parameters.

Conclusions
We conclude that interference stimulation with 100 + 105 Hz (2000 Hz + 2100 Hz) is more effective than 100 + 100 Hz stimulation in activating the pathways studied, both from a threshold and depth penetration perspective. This implies that the formation of an interference pattern or beat frequency provided a lower threshold and better penetration. However, there was no significant difference in result between the two stimulation electrode configurations. Since only two configurations was tested we cannot rule out the possibility that configuration of the electrodes may play a role. Further studies, for example involving larger animals and a greater number of spatial configurations are needed to clarify this issue.

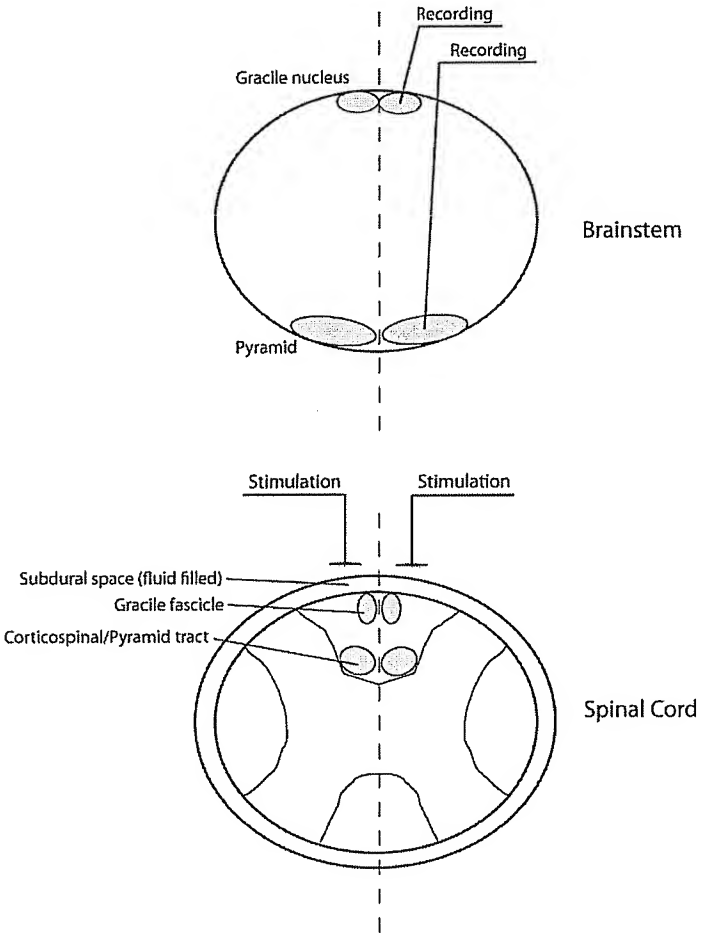

Figure 1. Schematic drawing of spinal cord and brainstem illustrating the targeted neural pathways as well as stimulation and recording electrodes.

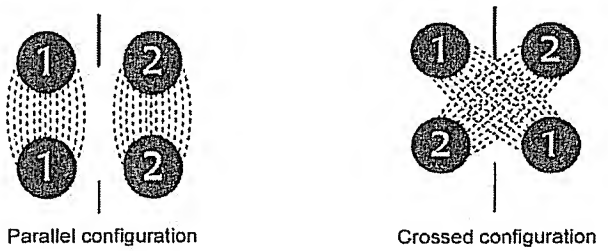

Figure 2. Stimulation electrode configurations. Bipolar stimulation with two pairs of electrodes was used in either a parallel (to the spinal cord) or a crossed pattern.

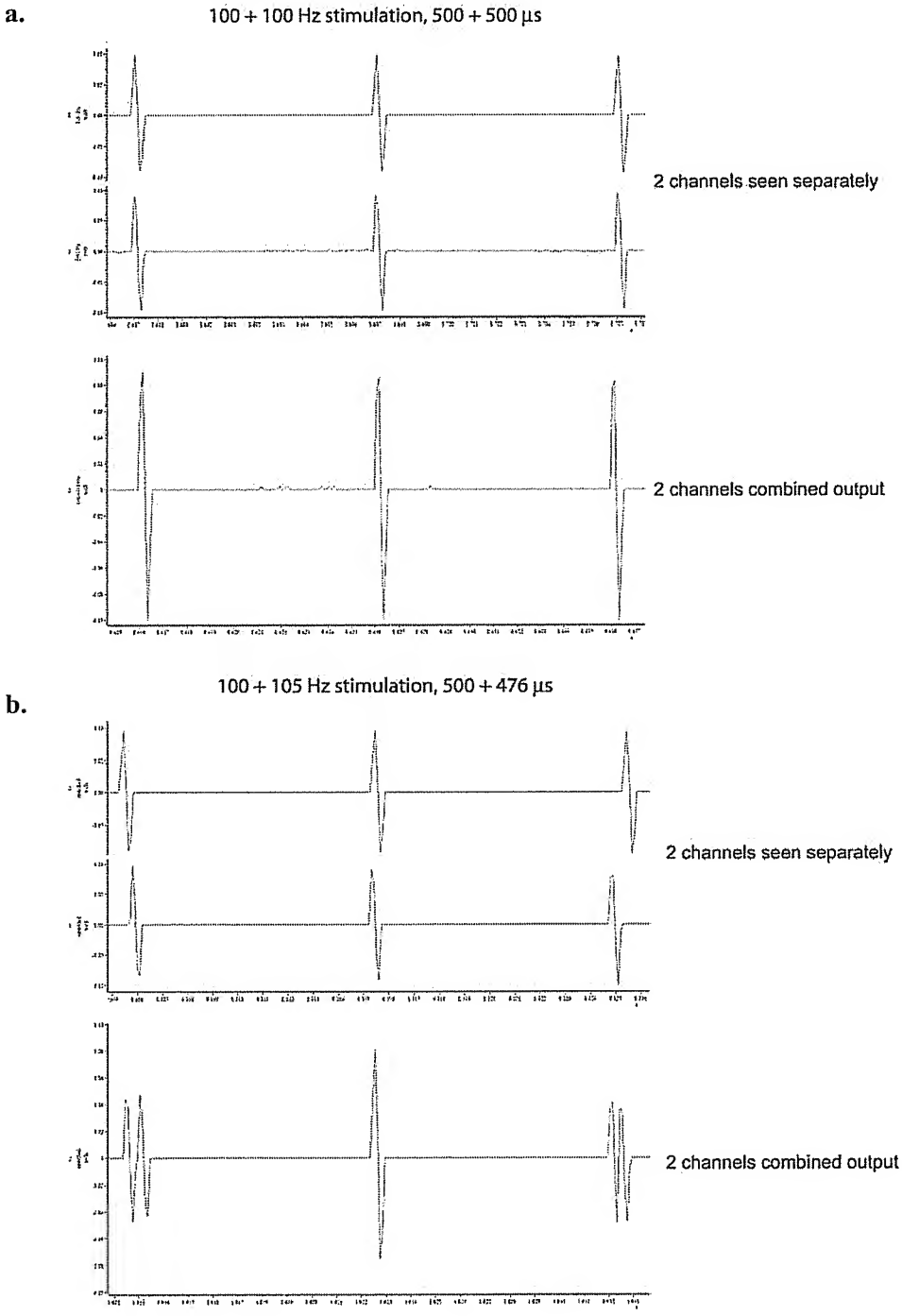

Figure 3. Output pulses from SCS stimulators. Upper part of each picture shows output from each stimulator, lower part shows the combined output from both stimulators. **a.** 100 + 100 Hz stimulation. Sine waves of 500 µs width corresponding to 2000 Hz stimulation were used. **b.** Stimulation output pulses during 100 + 105 Hz stimulation. Sine waves width of 500 µs and 476 µs (corresponding to 2000 and 2100 Hz respectively) were used.

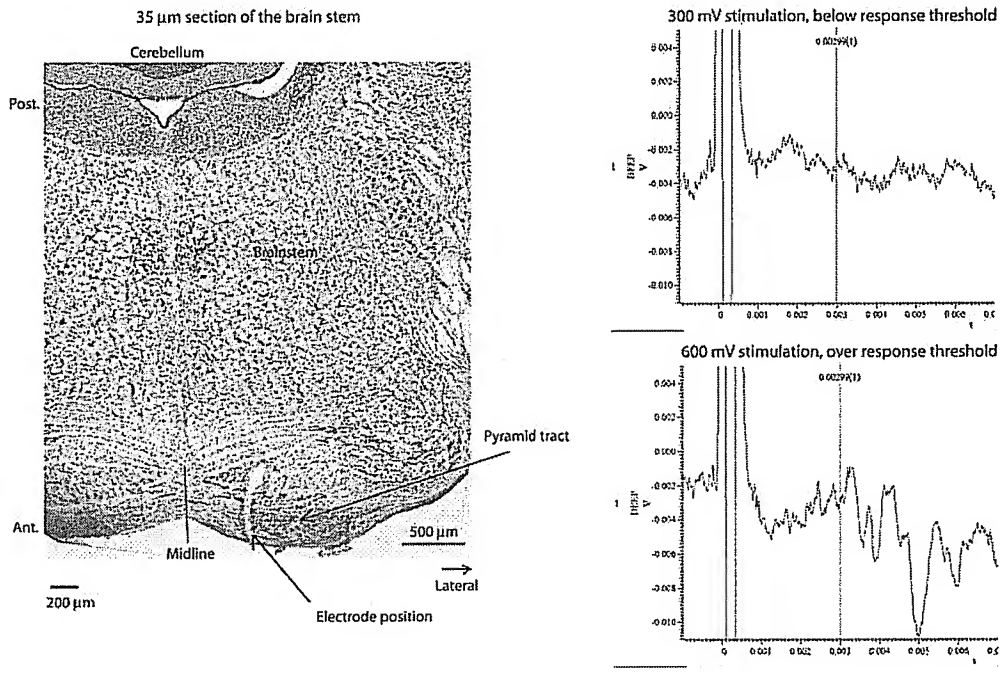

Figure 4. Example of matched histological verification and sampled electrophysiological data from one experiment. Pyramid responses after 100 + 105 Hz stimulation is seen.

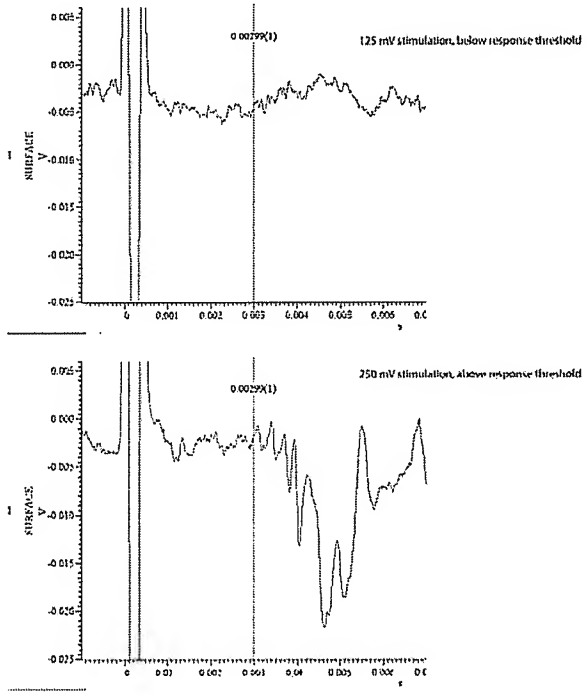

Figure 5. Examples of Gracile responses after 100+105 Hz stimulation. From the same experiment as Fig. 4.

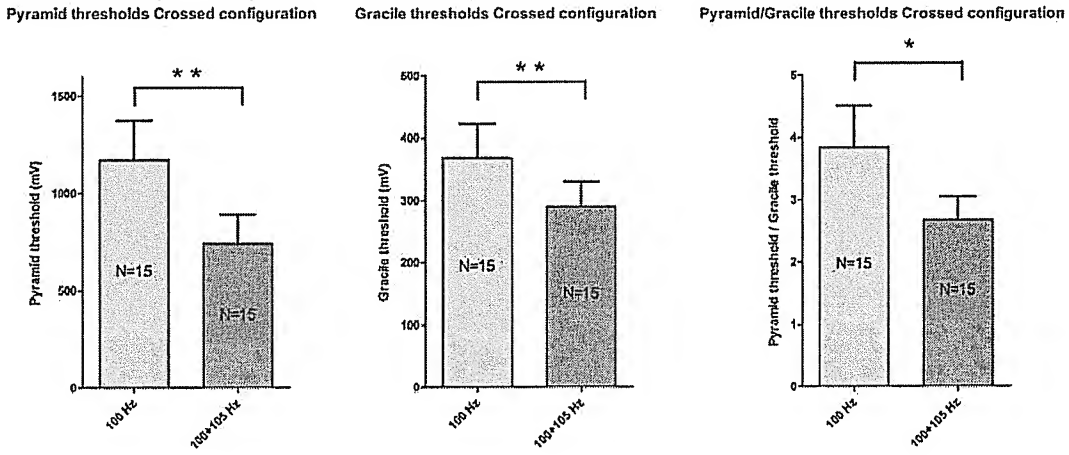

Figure 6. Comparisons of threshold data after 100+100 Hz versus 100+105 Hz stimulation using a crossed electrode configuration. Results after Wilcoxon signed rank significance test is shown. N equals the number of animals used.

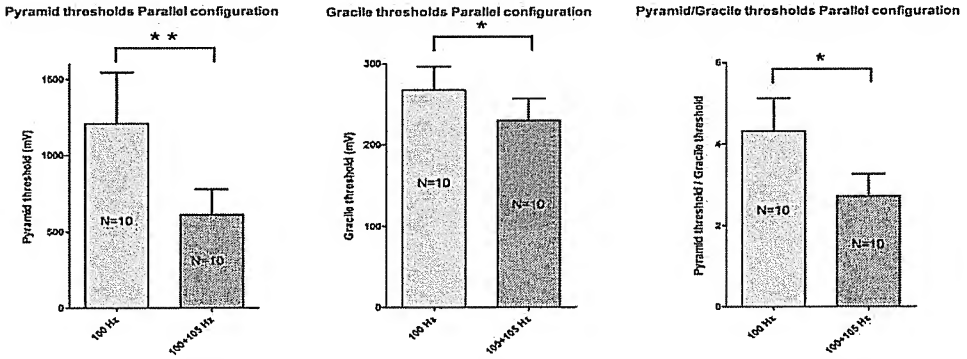

Figure 7. Comparisons of threshold data after 100+100 Hz versus 100+105 Hz stimulation using a parallel electrode configuration. Results after Wilcoxon signed rank significance test is shown. N equals the number of animals used.

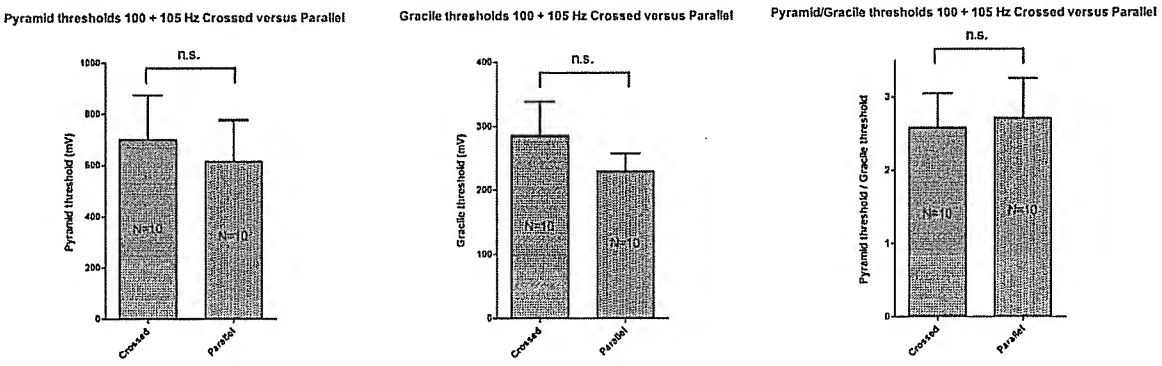

Figure 8. Comparisons of threshold data after crossed versus parallel electrode configuration using 100+105 Hz stimulation. Results after Mann-Whitney significance test is shown (n.s.= no significance). N equals the number of animals used.

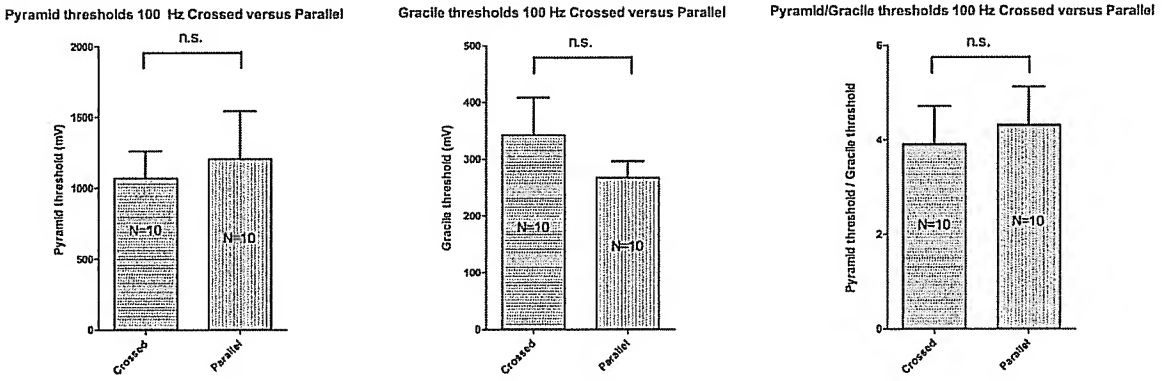

Figure 9. Comparisons of threshold data after crossed versus parallel electrode configuration using 100+100 Hz stimulation. Results after Mann-Whitney significance test is shown (n.s.= no significance). N equals the number of animals used.

Figure 3a

100 + 100 Hz stimulation, 500 + 500 µs

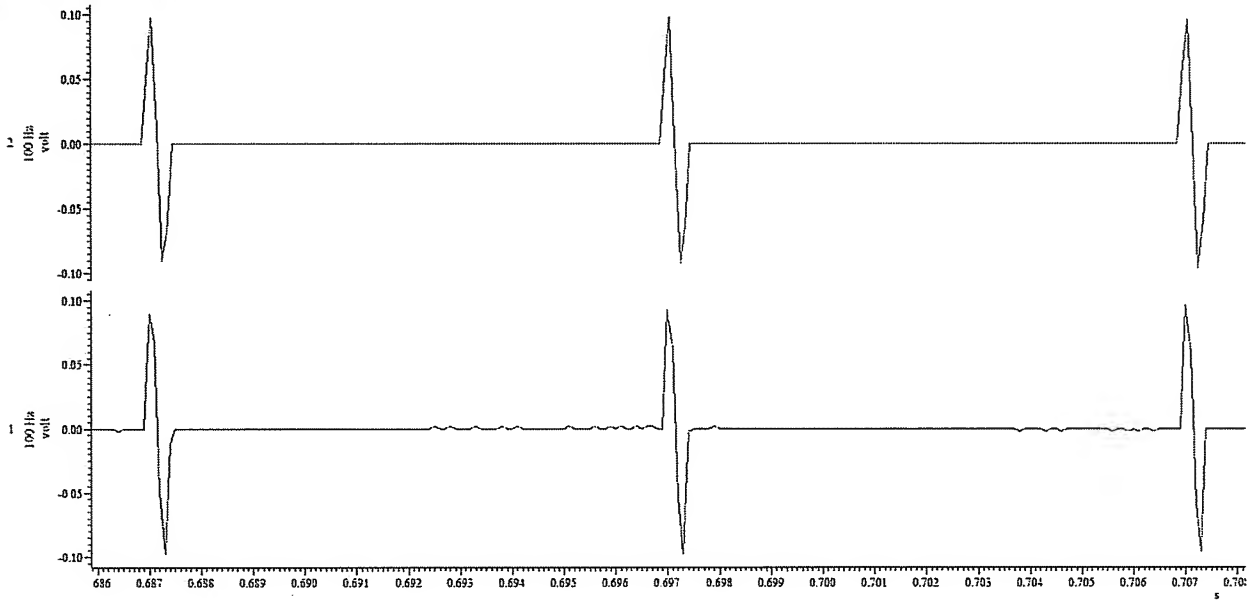

2 channels seen separately

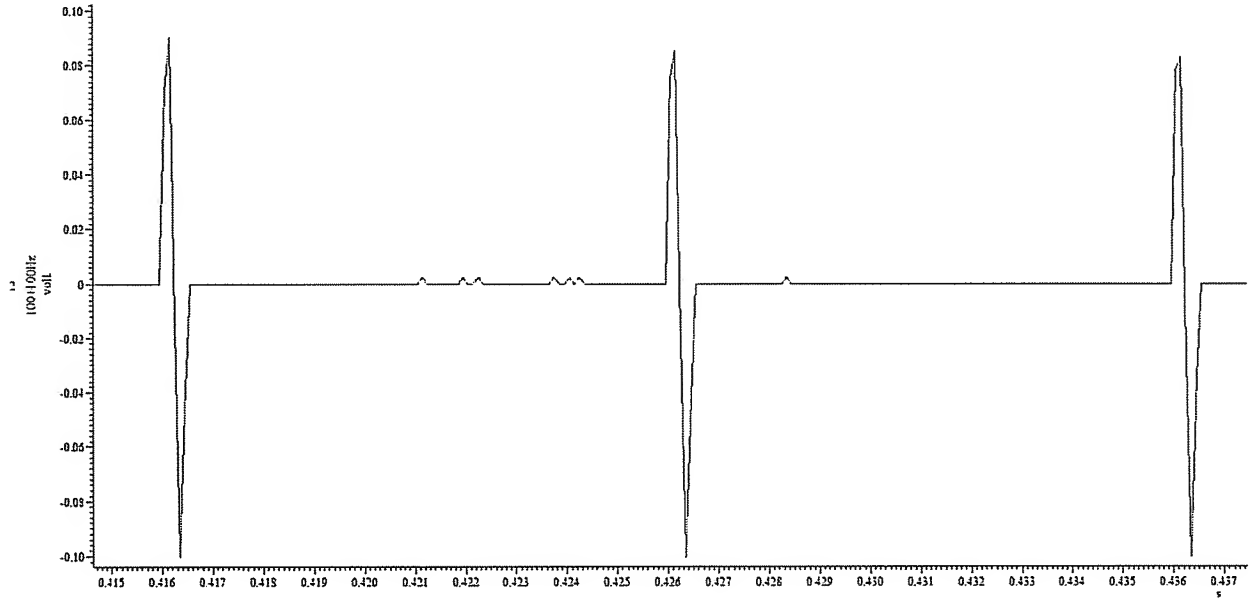

2 channels combined output

Figure 3b

100 + 105 Hz stimulation, 500 + 476 µs

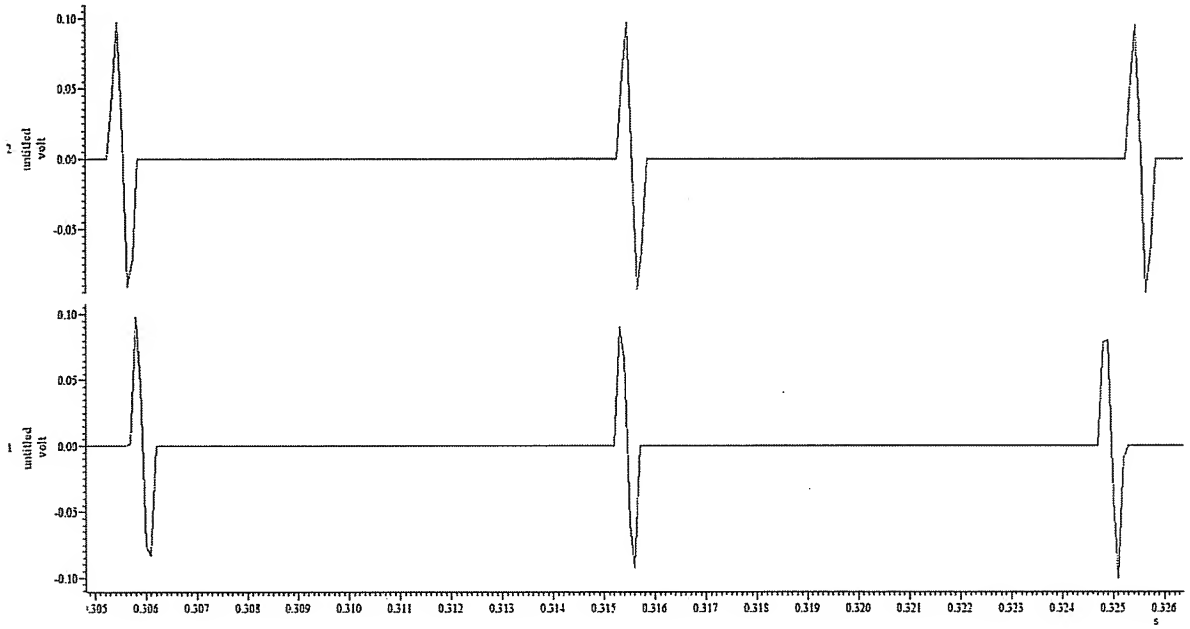

2 channels seen separately

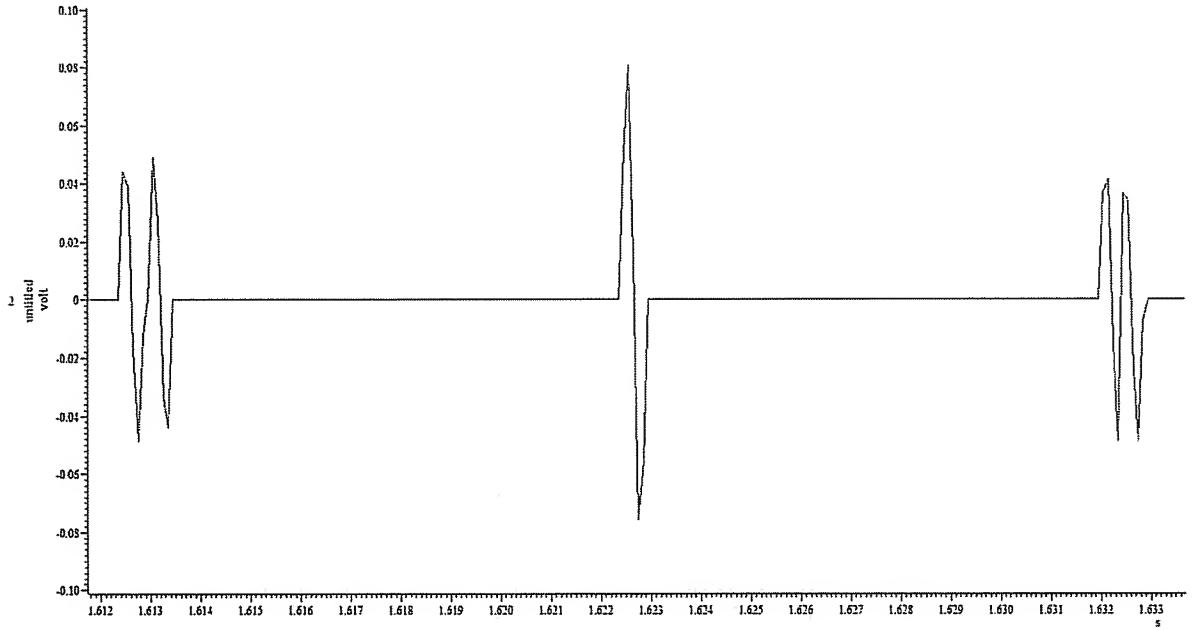

2 channels combined output

Figure 4

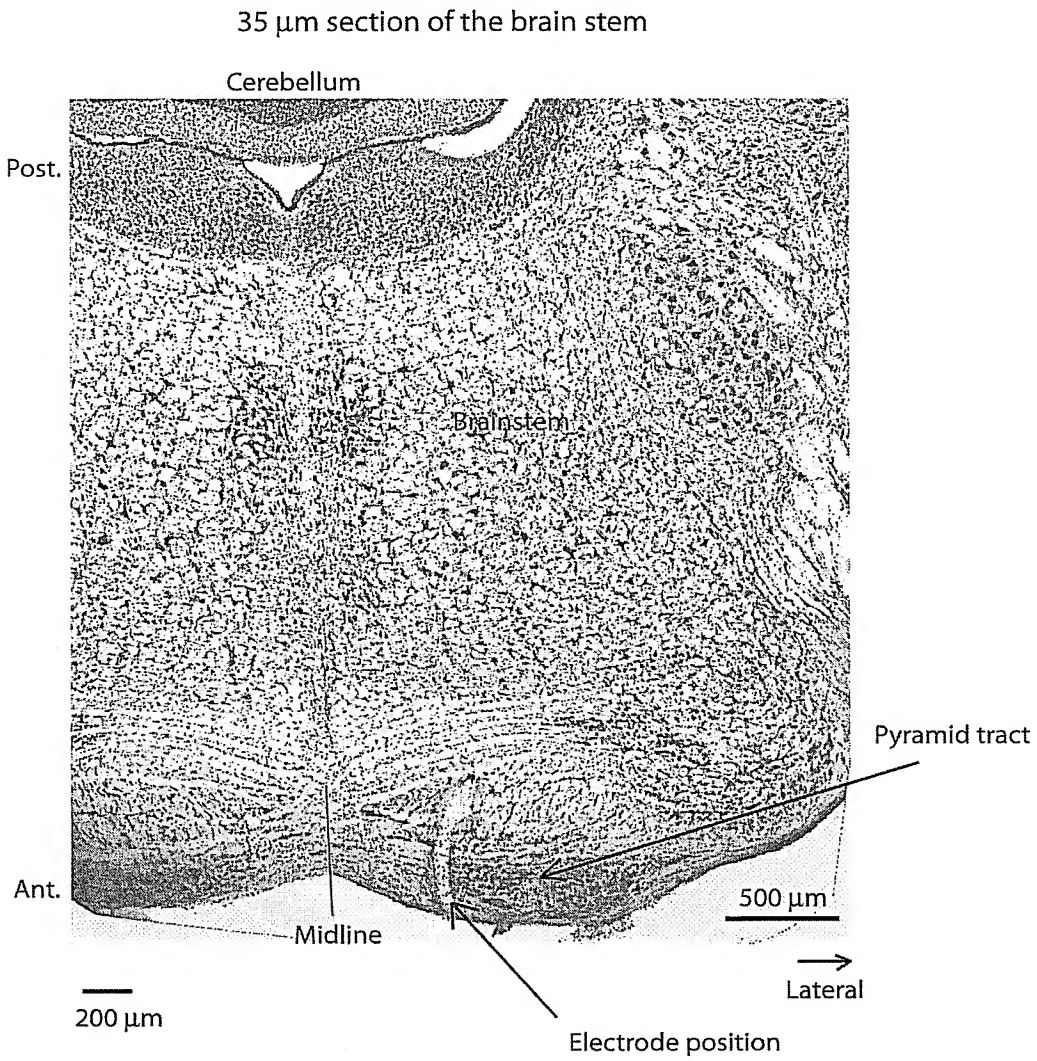
35 µm section of the brain stem
Cerebellum
Post.
Brainstem
Pyramid tract
Ant.
500 µm
Midline
Lateral
200 µm
Electrode position

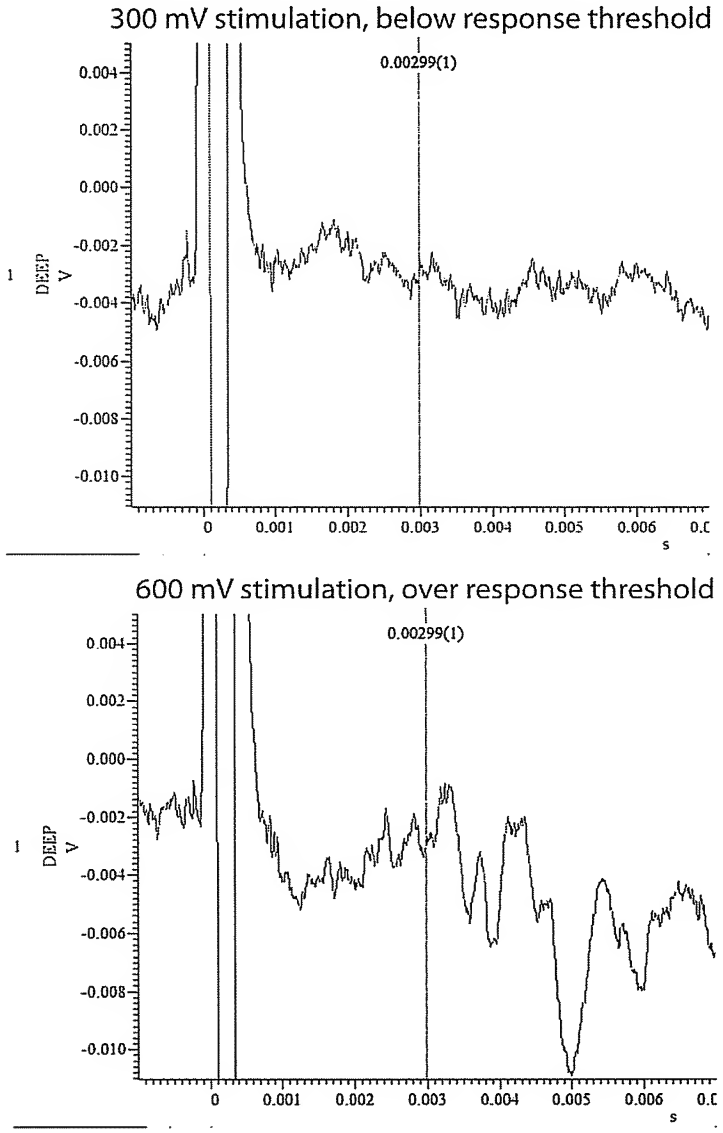
300 mV stimulation, below response threshold
0.00299(1)
DEEP
V
s
600 mV stimulation, over response threshold
0.00299(1)
DEEP
V
s

Figure 5

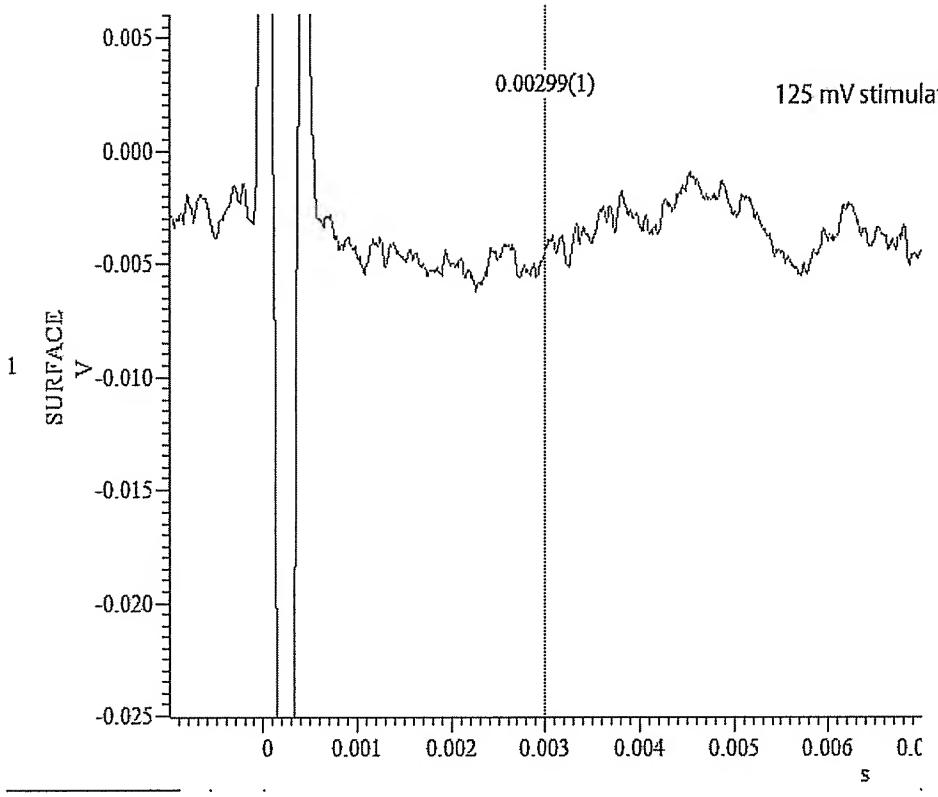
0.00299(1)
125 mV stimulation, below response threshold
SURFACE
V
1
0.005
0.000
-0.005
-0.010
-0.015
-0.020
-0.025
0
0.001
0.002
0.003
0.004
0.005
0.006
s

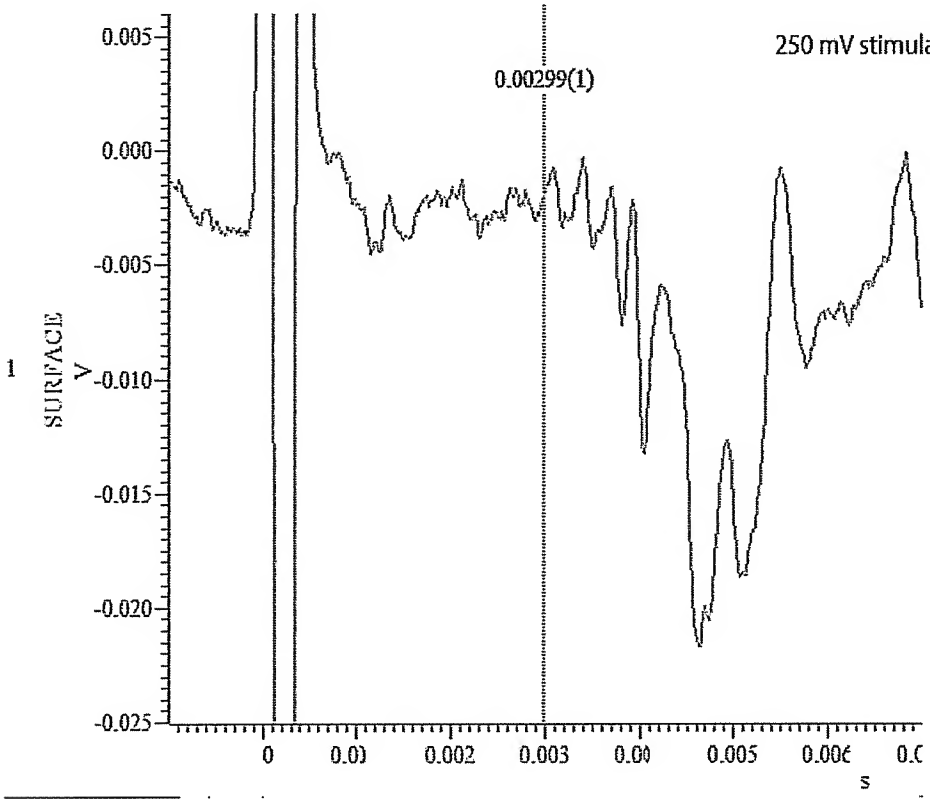
0.00299(1)
250 mV stimulation, above response threshold
SURFACE
V
1
0.005
0.000
-0.005
-0.010
-0.015
-0.020
-0.025
0
0.002
0.003
0.005
s

Exhibit C

Pain 104 (2003) 195–200

PAIN

www.elsevier.com/locate/pain

Spinal NMDA-receptor dependent amplification of nociceptive transmission to rat primary somatosensory cortex (SI)

Jarkko Kalliomäki, Marcus Granmo*, Jens Schouenborg

Section for Neurophysiology, Department of Physiological Sciences, Lund University, BMC F10, S-221 84 Lund, Sweden

Received 6 February 2002; accepted 2 January 2003

Abstract

The role of NMDA mechanisms in spinal pathways mediating acute nociceptive input to the somatosensory cortex is not clear. In this study, the effect of NMDA-antagonists on nociceptive C fibre transmission to the primary somatosensory cortex (SI) was investigated. Cortical field potentials evoked by CO_2-laser stimulation of the skin were recorded in the halothane/nitrous oxide anaesthetized rat.

The SI nociceptive evoked potential (EP) amplitudes were dependent on the frequency of noxious heat stimulation. The amplitudes of SI potentials evoked by CO_2-laser pulses (duration 15–20 ms, stimulation energy 21–28 mJ/mm^2) delivered at a frequency of 0.1 Hz were approximately 40% of the amplitudes of potentials evoked by 1.0 Hz stimulation.

After intrathecal lumbar application of either of the NMDA-antagonists CPP or MK-801, the amplitudes of nociceptive SI potentials, evoked by 1.0 Hz stimulation of the contralateral hindpaw, were reduced to approximately 40% of controls. By contrast, field potentials evoked by 0.1 Hz stimulation of the hindpaw were unaffected by MK-801.

SI potentials evoked by 1.0 Hz stimulation of the contralateral forepaw did not change after lumbar application of CPP or MK-801, indicating that the depression of hindpaw EPs was due to a segmental effect in the spinal cord.

It is concluded that spinal NMDA-receptor mechanisms amplify the acute transmission of nociceptive C fiber input to SI in a frequency-dependent way.

© 2003 International Association for the Study of Pain. Published by Elsevier Science B.V. All rights reserved.

Keywords: Nociception; Pain; C fibre; Somatosensory cortex; NMDA-receptor; Wind-up

1. Introduction

The primary somatosensory cortex (SI) has an important role in nociceptive sensory-discriminative processing, as has been demonstrated by several animal and human studies (Kenshalo and Isensee, 1983; Lamour et al., 1983; reviews by Kenshalo and Willis, 1991; Bushnell et al., 1999). A major input to SI originates from nociceptive C fibers (Schouenborg et al., 1986; Kalliomäki et al., 1993a). This input is mediated by multiple ascending pathways, located in the lateral and dorsal funiculi of the spinal cord (Kalliomäki et al., 1993b).

Nociceptive C fibre transmission to SI in the rat is dose-dependently inhibited by intrathecal application of morphine (Kalliomäki et al., 1998), indicating an opioid sensitive synaptic relay in the spinal cord. Recording of SI nociceptive C fibre evoked potentials (EPs) may therefore be a useful method to monitor ascending pain-related information to the cerebral cortex.

Nociceptive spinal cord dorsal horn neurones exhibit activity-dependent plasticity that can be elicited by certain types of noxious influences. One example is the *wind-up* phenomenon (Mendell, 1966; Schouenborg and Sjölund, 1983; Schouenborg, 1984; review by Herrero et al., 2000), that is a frequency-dependent increase of the C fibre responses that may last several minutes. Wind-up has been demonstrated both after electrical nerve stimulation and noxious heat stimulation (Price et al., 1978). Psychophysical studies suggest that wind-up may also be of relevance for human pain perception (Price et al., 1977; Lundberg et al., 1992). Furthermore, 'wind-up-like pain', dependent on *N*-methyl-D-aspartate (NMDA)-receptor activity, has been described in various clinical pain conditions (Kristensen et al., 1992; Eide et al., 1994, 1995; Nikolajsen et al., 1996; Stubhaug et al., 1997; review by Eide, 2000).

* Corresponding author. Tel: +46-46-2224651; fax: +46-46-2224546.
E-mail address: marcus.granmo@mphy.lu.se (M. Granmo).

0304-3959/03/$30.00 © 2003 International Association for the Study of Pain. Published by Elsevier Science B.V. All rights reserved.
doi:10.1016/S0304-3959(03)00002-2

The initial reports on the pharmacology of wind-up showed that it is inhibited by antagonists of the NMDA-receptor, as was demonstrated by using topical application of AP-5 onto the spinal cord surface (Dickenson and Sullivan, 1987) and by iontophoresis of ketamine on nociceptive dorsal horn neurons (Davies and Lodge, 1987). Later it was reported that wind-up is inhibited in neurons of the deep dorsal horn, while it is *increased* in neurons of the intermediate dorsal horn, after AP-5 (Dickenson and Sullivan, 1990). Another investigator described increased wind-up in both intermediate and deep nociceptive neurons after AP-5 (Svendsen et al., 1999). Thus, the effects of NMDA-antagonists on wind-up of nociceptive spinal cord neurons seem to be heterogeneous. It would therefore be of interest to clarify whether ascending nociceptive transmission to the cerebral cortex is dependent on spinal NMDA mechanisms.

The aim of this study was to investigate whether cortical C fibre EPs are dependent on the stimulation frequency and on spinal cord NMDA-receptor activity. Short pulses of noxious radiant heat emitted by a CO_2-laser were used to activate cutaneous C nociceptors (Devor et al., 1982; Bromm et al., 1984; Kalliomäki et al., 1993a). The highly potent and selective NMDA-antagonists CPP (competitive; Davies et al., 1986; Lehmann et al., 1987) and MK-801 (non-competitive; Wong et al., 1986) were used for topical spinal application. Both antagonists have been widely used in the study of nociception and seem to specifically suppress facilitated states of nociceptive transmission (Coderre and Melzack, 1992; Yamamoto and Yaksh, 1992a,b; Kristensen et al., 1994).

2. Methods

2.1. Animals used

Eleven male Wistar rats weighing 250–450 g were used. All rats received food and water ad libitum and were kept in a 12-h day–night cycle and at a constant environmental temperature of 21°C (humidity 65%). Approval for the experiments was obtained in advance from the regional ethical committee in Lund/Malmö. Principles for laboratory animal care (NIH publication No. 86-23, revised 1985) were followed in every respect.

2.2. Surgery and preparation

The rats were anesthetized with halothane (1.0–2.0% during surgery) in a mixture of 1/3 oxygen and 2/3 nitrous oxide. The trachea was cannulated and the end-expiratory pCO_2 (3.0–4.5%) was continuously monitored. An infusion of 30–50 μl/min of 5% glucose in Ringer's acetate was given in the right jugular vein. Mean arterial blood pressure (90–140 mmHg) was monitored continuously in the right brachial artery. The rectal temperature was kept between 36.5 and 38.5°C using a feed-back regulated heating system.

The lumbar (L3–L6) segments of the spinal cord were exposed by a laminectomy. The spinous processes of Th 11 and the first sacral vertebrae were clamped and the chest lifted to facilitate ventilation. The pelvis was supported from underneath to reduce stress on the vertebrae. The head of the rat was fixed by ear bars and a nose ring. Pancuronium bromide (0.5 mg) was given and the animal was artificially ventilated. Cerebrospinal fluid was drained between the base of the skull and the first cervical vertebra, to avoid cortical oedema. A craniotomy exposing the right parietal cortex was made. The dura of the parietal cortex and the exposed lumbar spinal cord was cut and covered with saline.

Local infiltration of 2.0 mg/ml lignocaine (Xylocaine) with 1.2 μg/ml adrenaline was made during all surgery to reduce nociceptive input during surgery and to minimize possible postoperative excitability changes (Clarke and Matthews, 1990).

After completion of surgery, the halothane level was lowered to 0.5–0.6% in the same gas mixture as before. This anesthetic level was characterized by an electrocorticogram dominated by 4–6 Hz theta waves, with no signs of desynchronization during noxious stimulation. The blood pressure was stable also during noxious stimulation. Spinal administration of CPP or MK-801 did not affect the electrocorticogram or the blood pressure. Experiments were terminated after signs of deterioration, i.e. precipitous drops in blood pressure or expiratory pCO_2 levels.

2.3. Stimulation and recordings

A mechanical stimulator with a blunt metal probe (0.8 mm diameter) attached to a coil, was used for tactile stimulation. The probe was displaced by a current pulse (10 ms) generated by a Grass stimulator. The stimulation was adjusted to cause a light touch of the skin, without any visible joint movement. Tactile stimulation of the left hindpaw/forepaw was used to delineate the SI hindlimb and forelimb areas in all rats (Kalliomäki et al., 1993a).

The glabrous skin of the left hindpaw/forepaw was stimulated with radiant heat pulses emitted by a CO_2-laser (Irradia, Sweden; wavelength 10.6 μm, output power 10 W, beam diameter 3.0 mm, pulse duration 15 or 20 ms). These stimulation energies (21–28 mJ/mm^2) have previously been shown to evoke cortical field potentials in rat SI, due to the activation of cutaneous nociceptive C fibres (Kalliomäki et al., 1993a,b). No visible damage to the skin was observed using this stimulation. The local skin temperature was monitored throughout the experiments, being 32 ± 2°C.

Each skin site was stimulated with four pulses, at frequencies of either 0.1 or 1.0 Hz. Thereafter a non-overlapping, nearby skin site was stimulated with four pulses (to avoid desensitization of C-nociceptors), and so forth, until an averaged recording of 16 sweeps had been obtained. A pause of at least 10 min was made before the

same skin site was stimulated again. In most experiments, two different regions of the glabrous skin (distal pads and digits) were stimulated.

Recordings of EPs were made from the cortical surface with a fine silver ball-tipped electrode. In the beginning of each experiment, a baseline was obtained from at least four averaged ($n = 16$) SI potentials evoked by CO_2-laser stimulation of each skin region. After control recordings either CPP (5–50 μg in 100 μl saline) or MK-801 (5–25 μg in 100 μl saline) was applied onto the exposed lumbar spinal cord, and the recordings were continued. In some rats, a ten times higher subsequent dose (50 μg) was given within 1–3 h. The doses of NMDA-antagonists used were within the range of effective doses found previously in various models of spinal nociceptive hyperexcitability (Dickenson and Sullivan, 1987; Haley et al., 1990; Coderre and Melzack, 1992; Mao et al., 1992; Ren et al., 1992; Yamamoto and Yaksh, 1992a,b; Hoheisel et al., 1997).

2.4. Data analysis

The onset and peak latencies of CO_2-laser EPs were determined from the control recordings in each rat. The amplitudes of all CO_2-laser EPs were measured between the onset and peak latencies determined from the control recordings, whereafter they were transformed into percent of the mean control EP amplitude. Transformed EP amplitude data were then pooled from several rats and used for statistical analysis. The Mann–Whitney U test was used for all statistical analysis, $P < 0.05$ being considered as a statistically significant difference.

3. Results

Nociceptive C fibre transmission to the right SI was assessed by recording cortical field potentials evoked by CO_2-laser stimulation (1.0 Hz; 21–28 mJ/mm^2) of the contralateral hindpaw (Kalliomäki et al., 1993a, 1998). These potentials consisted of a late surface positive wave having an approximately constant latency in each rat (mean peak latency = 332 ms, SEM = 6.5 ms, 11 rats, on stimulation of the digits of the hindpaw). Since the potentials vary in amplitude, due to the background electrocorticogram, an average of 16 sweeps was regularly used. The control recordings had a standard deviation of approximately 30% of the mean amplitude.

3.1. Partial depression of nociceptive C fibre transmission to SI by intrathecally applied NMDA-antagonists (MK-801, CPP)

Pooled data from five rats showed that the EP mean amplitude (1.0 Hz stimulation) after application of MK-801 (5 μg) was reduced to 74% of controls ($P < 0.05$). After a subsequent dose of 50 μg of MK-801 the EP mean amplitude tended to be further reduced (41% of controls; $P < 0.01$; five rats) but it did not differ significantly from the EP at the 5 μg dose (Fig. 1).

In four rats where CPP (5 μg) was applied onto the lumbar spinal cord, the EP mean amplitude (1.0 Hz stimulation) was also reduced (37% of controls; $P < 0.001$). A higher dose (50 μg) did not result in any further reduction of the EP mean amplitude (43% of controls; $P < 0.001$; three rats) (Fig. 1).

No systematic change of the latencies of EPs were found after the administration of either MK-801 or CPP.

3.2. Frequency dependence of the effect of NMDA-antagonists on nociceptive C fibre transmission to SI

In four rats, CO_2-laser stimulation was alternately given with frequencies of 0.1 and 1.0 Hz. With stimulation at a frequency of 0.1 Hz, the EP mean amplitude was 36% ($P < 0.001$) of the amplitude obtained with 1.0 Hz stimulation (Fig. 2). In the same rats, the EPs due to 1.0 Hz stimulation were reduced to 38% of controls ($P < 0.01$) after application of MK-801 (50 μg), while the 0.1 Hz EPs did not change significantly (Fig. 2).

3.3. Segmental versus non-segmental effects of NMDA antagonists

In order to clarify if the effect of NMDA-antagonists on the nociceptive input to SI was due to a segmental spinal mechanism, potentials evoked by noxious CO_2-laser stimulation (1.0 Hz) of the forepaw and the hindpaw, were recorded from the forepaw and hindpaw areas of contralateral SI, respectively (Fig. 3). After lumbar application of an NMDA-antagonist (5 μg CPP in three rats or 50 μg MK-

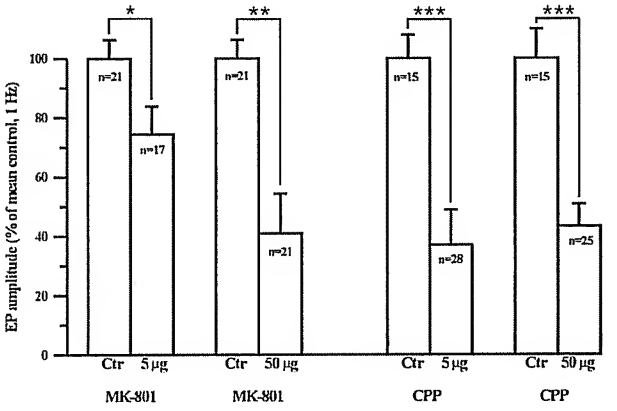

Fig. 1. Diagram of the effects of two different doses of MK-801 and CPP on SI potentials evoked by 1.0 Hz CO_2-laser stimulation. The grand mean amplitudes of CO_2-laser evoked SI potentials are shown in percent of the mean control amplitude. Each grand mean is based on recordings pooled from three to five rats and sampled during a period of up to 150 min before/after the intrathecal lumbar application of different doses of CPP or MK-801, as indicated. The number of averaged recordings (each based on 16 sweeps) is indicated with n. Error bars indicate SEM. The results of significance tests are also shown.

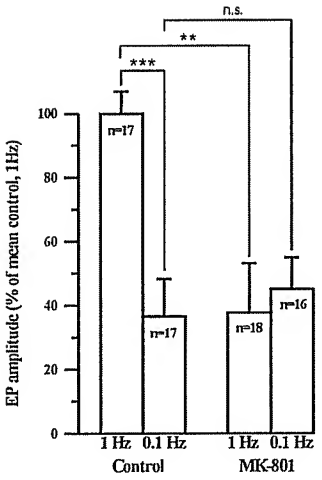

Fig. 2. Diagram of the effect of MK-801 on SI potentials evoked by different frequencies of CO_2-laser stimulation (0.1 or 1.0 Hz). The grand mean amplitudes of CO_2-laser evoked SI potentials are shown in percent of the mean control amplitude obtained with 1.0 Hz stimulation. Each grand mean is based on recordings pooled from four rats and sampled during a period of up to 150 min before/after the intrathecal lumbar application of MK-801 (50 μg). The number of averaged recordings (of 16 sweeps) is indicated with *n*. Error bars indicate SEM. The results of significance tests are also shown.

801 in two rats), the hindpaw EP mean amplitudes were reduced to 28% of controls ($n = 5$ rats), while there was no effect on potentials evoked from the forepaw (105% of controls, $n = 5$ rats). These findings indicate that the depression of hindpaw EPs was due to a segmental spinal mechanism.

4. Discussion

This study demonstrates that intrathecal application of NMDA-receptor antagonists (CPP or MK-801) partially depresses nociceptive C fibre transmission to SI. This effect is selectively exerted on the larger potentials evoked by 1.0 Hz noxious thermal CO_2-laser stimulation, while the smaller potentials evoked by 0.1 Hz stimulation are unaffected. Thus, nociceptive C fibre transmission to SI can be amplified by spinal NMDA mechanisms in a frequency-dependent way.

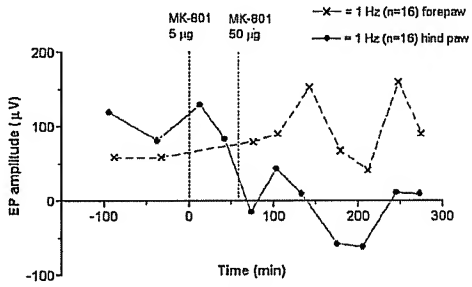

Fig. 3. Diagram of the effect of MK-801 on SI potentials evoked by CO_2-laser stimulation of the hindpaw or the forepaw, in one rat. Each dot or cross indicates the amplitude of one averaged recording (of 16 sweeps) of SI potentials, evoked by CO_2-laser stimulation (1.0 Hz) of the hindpaw or the forepaw. The times for intrathecal lumbar application of different doses of MK-801 are indicated with hatched lines.

NMDA-receptor antagonists may affect nociception both at the level of the spinal cord dorsal horn and also at higher levels in the somatosensory pathways (Eaton and Salt, 1990; Chizh et al., 2001). The present finding that the lumbar application of NMDA-antagonists depresses nociceptive SI potentials evoked from the lumbar level, while not affecting transmission from the cervical level, indicates that the effect of topical application is segmentally exerted. Furthermore, in other studies using comparable techniques for intrathecal application of NMDA antagonists (Dickenson and Sullivan, 1987, 1990; Haley et al., 1990; Hoheisel et al., 1997), the effective concentrations for inhibition of different types of C fibre dependent spinal hyperexcitability were of the same order of magnitude as in the present study (taking into account the higher potency of CPP compared to AP-5; Davies et al., 1986).

The responses of dorsal horn neurones and spinothalamic neurones to single mechanical or thermal noxious stimuli are relatively little affected by NMDA-receptor antagonists (Headley et al., 1987; Dougherty et al., 1992; Chizh et al., 1997). The wind-up of C fibre responses in spinal cord neurons was initially reported to be inhibited by NMDA-antagonists (Dickenson and Sullivan, 1987; Davies and Lodge, 1987). However, very heterogeneous effects of NMDA-antagonists on wind-up have been reported later on (Dickenson and Sullivan, 1990; Svendsen et al., 1999). The present study shows that nociceptive C fibre input to SI is dependent on both stimulation frequency and NMDA-receptor activity, which may suggest that NMDA-antagonists inhibit wind-up in those spinal cord neurons that are involved in ascending nociceptive transmission to SI.

In normal human volunteers, a selective reduction of temporal summation of second pain was seen after administration of the NMDA-antagonist dextromethorphan (Price et al., 1994), which is possibly a correlate to the present findings.

In conclusion, it was demonstrated that nociceptive C fibre transmission to SI is amplified by an increased frequency of noxious heat stimulation. This amplification mechanism is dependent on activation of spinal cord NMDA-receptors. A possible physiological role for such a mechanism may be temporal summation of C fibre evoked pain compensating for the decline in C fibre input over time (Schouenborg and Dickenson, 1988).

Acknowledgements

Supported by the Swedish Medical Research Council Projects No. 10569 and 1013, the Medical Faculty of Lund University, Astra Hässle Inc., Knut and Alice Wallenberg's Foundation, Elsa and Thorsten Segerfalk's Foundation, Greta and Johan Kock's Foundation, Magnus Bergvall's

Foundation, Åke Wiberg's Foundation, the Crafoord Foundation and The Royal Physiographic Society in Lund.

References

Bromm B, Jahnke MT, Treede RD. Responses of human cutaneous afferents to CO_2-laser stimuli causing pain. Exp Brain Res 1984;55: 158–66.

Bushnell MC, Duncan GH, Hofbauer RK, Ha B, Chen JI, Carrier B. Pain perception: is there a role for primary somatosensory cortex? Proc Natl Acad Sci USA 1999;96:7705–9.

Clarke RW, Matthews B. The thresholds of the jaw opening reflex and trigeminal brain stem neurons to tooth-pulp stimulation in acutely and chronically prepared cats. Neuroscience 1990;36:105–14.

Chizh BA, Cumberbatch MJ, Herrero JF, Stirk GC, Headley PM. Stimulus intensity, cell excitation and the *N*-methyl-D-aspartate receptor component of sensory responses in the rat spinal cord in vivo. Neuroscience 1997;80:251–65.

Chizh BA, Reissmuller E, Schlutz H, Scheede M, Haase G, Englberger W. Supraspinal vs spinal sites of the antinociceptive action of the subtype-selective NMDA antagonist ifenprodil. Neuropharmacology 2001;40: 212–20.

Coderre TJ, Melzack R. The role of NMDA-receptor operated calcium channels in persistent nociception after formalin-induced tissue injury. J Neurosci 1992;12:3671–5.

Davies J, Evans RH, Herrling PL, Jones AW, Olverman HJ, Pook P, Watkins JC. CPP, a new potent and selective NMDA antagonist. Depression of central neuron responses, affinity for (3H)D-AP5 binding sites on brain membranes and anticonvulsant activity. Brain Res 1986; 382:169–73.

Davies SN, Lodge D. Evidence for involvement of *N*-methylaspartate receptors in 'wind-up' of class 2 neurones in the dorsal horn of the rat. Brain Res 1987;424:402–6.

Devor M, Carmon A, Frostig R. Primary afferent and spinal sensory neurons that respond to brief pulses of intense infrared laser radiation: a preliminary survey in rats. Exp Neurol 1982;76:483–94.

Dickenson AH, Sullivan AF. Evidence for a role of the NMDA receptor in the frequency dependent potentiation of deep rat dorsal horn nociceptive neurones following C fibre stimulation. Neuropharmacology 1987;26:1235–8.

Dickenson AH, Sullivan AF. Differential effects of excitatory amino acid antagonists on dorsal horn nociceptive neurones in the rat. Brain Res 1990;506:31–9.

Dougherty PM, Palecek J, Paleckova V, Sorkin LS, Willis WD. The role of NMDA and non-NMDA excitatory amino acid receptors in the excitation of primate spinothalamic tract neurons to mechanical, chemical, thermal and electrical stimuli. J Neurosci 1992;12(8): 3025–41.

Eaton SA, Salt TE. Thalamic NMDA receptors and nociceptive sensory synaptic transmission. Neurosci Lett 1990;110:297–302.

Eide PK. Clinical trials of NMDA-receptor antagonists as analgesics. In: Devor M, Rowbotham MC, Wiesenfeld-Hallin Z, editors. Proceedings of the ninth World Congress on pain. Progress in pain research and management, vol. 16. Seattle, WA: IASP Press, 2000. p. 817–32.

Eide PK, Jorum E, Stubhaug A, Bremnes J, Breivik H. Relief of post-herpetic neuralgia with the *N*-methyl-D-aspartic acid receptor antagonist ketamine: a double-blind, cross-over comparison with morphine and placebo. Pain 1994;58:347–54.

Eide PK, Stubhaug A, Stenehjem AE. Central dysesthesia pain after traumatic spinal cord injury is dependent on *N*-methyl-D-aspartate receptor activation. Neurosurgery 1995;37:1080–7.

Haley JE, Sullivan AF, Dickenson AH. Evidence for spinal *N*-methyl-D-aspartate receptor involvement in prolonged chemical nociception in the rat. Brain Res 1990;518:218–26.

Headley PM, Parsons CG, West DC. The role of *N*-methylaspartate receptors in mediating responses of rat and cat spinal neurones to defined sensory stimuli. J Physiol 1987;385:169–88.

Herrero JF, Laird JMA, Lopez-Garcia JA. Wind-up of spinal cord neurones and pain sensation: much ado about something? Prog Neurobiol 2000; 61:169–203.

Hoheisel U, Sander B, Mense S. Myositis-induced functional reorganisation of the rat dorsal horn: effects of spinal perfusion with antagonists to neurokinin and glutamate receptors. Pain 1997;69:219–30.

Kalliomäki J, Weng HR, Nilsson HJ, Schouenborg J. Nociceptive C fibre input to the primary somatosensory cortex (SI). A field potential study in the rat. Brain Res 1993a;622:262–70.

Kalliomäki J, Weng HR, Nilsson HJ, Yu YB, Schouenborg J. Multiple spinal pathways mediate cutaneous nociceptive C fibre input to the primary somatosensory cortex (SI) in the rat. Brain Res 1993b;622: 271–9.

Kalliomäki J, Luo XL, Yu YB, Schouenborg J. Intrathecally applied morphine inhibits nociceptive C fiber input to the primary somatosensory cortex (SI) of the rat. Pain 1998;77:323–9.

Kenshalo DR, Isensee O. Responses of primate SI cortical neurons to noxious stimuli. J Neurophysiol 1983;50:1479–96.

Kenshalo DR, Willis WD. The role of the cerebral cortex in pain sensation. In: Peters A, Jones EG, editors. The cerebral cortex. New York, NY: Plenum Press, 1991. p. 153–212.

Kristensen JD, Svensson B, Gordh T. The NMDA-receptor antagonist CPP abolishes neurogenic 'wind-up pain' after intrathecal administration in humans. Pain 1992;51:249–53.

Kristensen JD, Karlsten R, Gordh T, Berge OG. The NMDA antagonist 3-(carboxypiperazin-4-yl)propyl-1-phosphonic acid (CPP) has antinociceptive effect after intrathecal injection in the rat. Pain 1994;56:59–67.

Lamour Y, Willer JC, Guilbaud G. Rat somatosensory (SmI) cortex: I. Characteristics of neuronal responses to noxious stimulation and comparison with responses to non-noxious stimulation. Exp Brain Res 1983;49:35–45.

Lehmann J, Schneider S, McPherson S, Murphy DE, Bernard P, Tsai C, Bennett DA, Pastor G, Steel DJ, Boehm C, Cheney DL, Liebman JM, Williams M, Wood PL. CPP, a selective *N*-methyl-D-aspartate (NMDA)-type receptor antagonist: characterization in vitro and in vivo. J Pharmacol Exp Ther 1987;240:737–46.

Lundberg LER, Jorum E, Holm E, Torebjörk HE. Intra-neural electrical stimulation of cutaneous nociceptive fibres in humans: effects of different pulse patterns on magnitude of pain. Acta Physiol Scand 1992; 146:41–8.

Mao J, Price DD, Mayer DJ, Lu J, Hayes RL. Intrathecal MK-801 and local nerve anesthesia synergistically reduce nociceptive behaviors in rats with experimental peripheral mononeuropathy. Brain Res 1992;576: 254–62.

Mendell LM. Physiological properties of unmyelinated fiber projections to the spinal cord. Exp Neurol 1966;16:316–32.

Nikolajsen L, Hansen CL, Nielsen J, Keller J, Arendt-Nielsen L, Jensen TS. The effect of ketamine on phantom pain: a central neuropathic disorder maintained by peripheral input. Pain 1996;67:69–77.

Price DD, Hu JW, Dubner R, Gracely RH. Peripheral suppression of first pain and central summation of second pain evoked by noxious heat pulses. Pain 1977;3:57–68.

Price DD, Hayes RL, Ruda MA, Dubner R. Spatial and temporal transformations of input to spinothalamic tract neurons and their relation to somatic sensation. J Neurophysiol 1978;41:933–47.

Price DD, Mao J, Frenk H, Mayer DJ. The *N*-methyl-D-aspartate receptor antagonist dextromethorphan selectively reduces temporal summation of second pain in man. Pain 1994;59:165–74.

Ren K, Hylden JLK, Williams GM, Ruda MA, Dubner R. The effects of a non-competitive NMDA receptor antagonist, MK-801, on behavioral hyperalgesia and dorsal horn neuronal activity in rats with unilateral inflammation. Pain 1992;50:331–44.

Schouenborg J. Functional and topographical properties of field potentials

evoked in rat dorsal horn by cutaneous C-fibre stimulation. J Physiol 1984;356:169–92.

Schouenborg J, Dickenson AH. Long-lasting neuronal activity in rat dorsal horn evoked by impulses in cutaneous C fibres during noxious mechanical stimulation. Brain Res 1988;439:56–63.

Schouenborg J, Sjölund BH. Activity evoked by A- and C-afferent fibers in rat dorsal horn and its relation to a flexion reflex. J Neurophysiol 1983; 50:1108–21.

Schouenborg J, Kalliomäki J, Gustafsson P, Rosén I. Field potentials evoked in rat primary somatosensory cortex (SI) by impulses in cutaneous Aβ- and C-fibres. Brain Res 1986;397:86–92.

Stubhaug A, Breivik H, Eide PK, Kreunen M, Foss A. Mapping of punctuate hyperalgesia around a surgical incision demonstrates that ketamine is a powerful suppressor of central sensitization to pain following surgery. Acta Anaesthesiol Scand 1997;41:1124–32.

Svendsen F, Rygh LJ, Hole K, Tjoelsen A. Dorsal horn NMDA receptor function is changed after peripheral inflammation. Pain 1999;83: 517–23.

Wong EHF, Kemp JA, Priestley T, Knight AR, Woodruff GN, Iversen LL. The anticonvulsant MK-801 is a potent *N*-methyl-D-aspartate antagonist. Proc Natl Acad Sci USA 1986;83:7104–8.

Yamamoto T, Yaksh TL. Comparison of the antinociceptive effects of pre- and posttreatment with intrathecal morphine and MK801, an NMDA antagonist, on the formalin test in the rat. Anesthesiology 1992a;77: 757–63.

Yamamoto T, Yaksh TL. Spinal pharmacology of thermal hyperesthesia induced by constriction injury of sciatic nerve. Excitatory amino acid antagonists. Pain 1992b;49:121–8.

Exhibit D

J. Physiol. (1983), **336**, *pp.* 545–561
With 8 text-figures
Printed in Great Britain

CONDUCTION VELOCITIES OF CORTICOSPINAL AXONS IN THE RAT STUDIED BY RECORDING CORTICAL ANTIDROMIC RESPONSES

BY N. K. MEDIRATTA AND J. A. R. NICOLL

From the Department of Physiology, The Medical School, University of Bristol, University Walk, Bristol BS8 1TD

(*Received 10 August 1982*)

SUMMARY

1. The rat corticospinal tract was stimulated at the medullary pyramid and at different levels in the spinal cord (segments C2/3, T2, T12) and responses were recorded from the surface of the cerebral cortex and extracellularly from individual cortical neurones.

2. Irrespective of the site stimulated, the earliest surface and single unit responses had frequency-following and other characteristics which indicated they resulted from antidromic invasion of corticospinal neurones.

3. Synaptically mediated discharges with longer latency were also evoked in cortical neurones other than corticospinal neurones. At least in part these discharges probably resulted from stimulus spread to the dorsal column–medial lemniscus pathway.

4. Corticospinal neurones were almost all between 1·0 and 1·5 mm beneath the cortical surface while synaptically excited units were at all depths greater than 0·4 mm.

5. By stimulating at two sites, estimates of conduction velocity were obtained for single corticospinal axons. For those reaching at least as far as T12, velocities caudal to the pyramid ranged from 5 to 19 m/s (mean $11{\cdot}4 \pm 2{\cdot}9$ m/s; S.D.). Slow axons in the pyramid (antidromic latency $> 2{\cdot}5$ ms) could rarely be excited from T12.

6. By stimulating at three sites (pyramid, T2, T12) most axons reaching T12 were found to have similar conduction velocities in the 'cervical' (pyramid–T2) and 'thoracic' (T2–T12) cord. However, in 15% of the axons the 'thoracic' velocity was at least 25% less than the cervical.

7. The results are discussed and related to those from previous investigations.

INTRODUCTION

The corticospinal tract in the rat is a substantial pathway which passes through the medullary pyramid and subsequently travels via the contralateral dorsal column for the whole length of the spinal cord (e.g. Dunkerley & Duncan, 1969; Brown, 1971; Ullan & Artieda, 1981).

It is clearly desirable that the conduction velocity of this important pathway should be established. However, although Porter & Sanderson (1964) and others

Downloaded from J Physiol (jp.physoc.org) at unknown institution on March 9, 2010

(Ohta, 1968; Stone, 1972) have investigated the latency and other characteristics (i.e. form and spatial distribution) of antidromic responses evoked in the cerebral cortex by electrical stimulation of the medullary pyramid, there have been no comparably detailed studies of responses evoked by stimulation of the corticospinal tract at spinal levels.

Porter & Sanderson (1964) found that the earliest cortical surface response to pyramidal stimulation had a latency to peak of 2 ms (approximately 1·2 ms to onset) and showed that it resulted from antidromic invasion of neurones contributing axons to the pyramid. However, it is not certain to what extent this and later responses were attributable to stimulation of corticospinal axons because the medullary pyramid also contains numerous corticobulbar axons. Indeed, the latter may outnumber the former by as much as two to one (McComas & Wilson, 1968).

McComas & Wilson (1968) recorded from six cortical neurones which were antidromically invaded both from pyramid and cervical cord and by measurement of the distance between the sites of stimulation the conduction velocity in the spinal portion of the axons was calculated to range between 7·6 and 10·8 m/s. More recently, however, Elger, Speckmann, Caspers & Janzen (1977) have concluded that the corticospinal tract in the rat contains numerous axons which conduct at approximately 60 m/s.

The large discrepancy between this result and that of McComas & Wilson prompted the present investigation. The approach used was to characterize the responses elicited in the cortex by stimulation at the pyramid and at different levels of the spinal cord. Measurements of antidromic latencies and of conduction distances then allowed the calculation of conduction velocities between the sites of stimulation (cf. McComas & Wilson, 1968). Stimulation was sometimes applied at the pyramid and at two spinal levels in order to determine the conduction velocity for two different portions of a single axon. Most of the results relate to axons descending at least to segment T12.

METHODS

Twenty-five albino rats (average weight 380 g) were used. Anaesthesia was induced with halothane vapour (Fluothane; I.C.I.), followed by intraperitoneal injection of 50 mg/kg sodium pentobarbitone (Sagatal; BDH). Subsequent maintenance doses (10 mg/kg) were given intravenously via a cannula in the femoral vein. Rectal temperature was maintained at 36–38 °C with a thermostatically controlled electric blanket and an infra-red lamp. The trachea was cannulated.

The animal was placed in a head holder (Kopf Instruments) in the orientation required for the stereotaxic system of Fifkova & Marsala (1967). The spinal column was extended and immobilized by clamps on the spinous processes of appropriate vertebrae. To allow stimulation of the corticospinal tract at spinal levels short laminectomies were carried out to expose the dura overlying the dorsal surface of the cord at one or two of segmental levels C2/3, T2 and T12. The dura was reflected and the cord surface was protected by a layer of paraffin oil at 37 °C.

A wide craniotomy was subsequently made to expose the left cerebral hemisphere and a burr hole was made in the occipital bone near the mid line to allow access for a pyramidal-stimulating electrode. The scalp edges were sutured to a metal ring above the animal's head, the dura was reflected at both skull openings and the exposed brain was covered with warm paraffin oil.

For stimulation of pyramid and cord, each cathode was a tungsten wire, 0·1 mm in diameter, etched to a taper and insulated with glass, except at the tip. The anode was a sprung silver ball which rested on the pia near the point at which the cathode penetrated the surface. Each anode/cathode pair was mounted on a Narishige micro-manipulator. The pyramidal electrode was advanced ventrally through the cerebellum to reach the left pyramid at stereotaxic co-ordinates

Downloaded from J Physiol (jp.physoc.org) at unknown institution on March 9, 2010

12·0 mm caudal and 11·5 mm ventral to the bregma (Fifkova & Marsala, 1967). The vertical position of the electrode tip was then slightly adjusted, if necessary, to maximize the short latency response (see Results) on the surface of the cerebral cortex. Electrodes at spinal levels were inserted into the right dorsal column and were similarly adjusted; the depth required to evoke maximal early cortical responses was approximately 1·7 mm which correlates well with the known location of the rat corticospinal tract in the deepest portion of the dorsal column (Dunkerley & Duncan, 1969).

Stimulation was accomplished with 0·1 ms rectangular pulses supplied from a constant current stimulator with a range of 0–1000 μA. Single stimuli or trains at frequencies up to 1000 Hz could be delivered.

Potentials evoked on the surface of the cerebral cortex were recorded differentially between a roving silver ball (0·5 mm diameter) held in a micro-manipulator and resting lightly on the cortical surface and a second ball resting on reflected dura. The animal was earthed via a silver plate in the mouth. Recording band width was 50 Hz to 5 kHz and responses were displayed on a storage oscilloscope equipped with a Polaroid camera.

Cortical single units were recorded extracellularly using glass micropipettes filled with 4 M-NaCl (impedance 5–10 MΩ at 1000 Hz) which were positioned using a hydraulic microdrive. Pulsations of the cortex were reduced by light pressure of a small Perspex plate on the pial surface and the micro-electrode was introduced into the cortex via a pore (1·5 mm diameter) in the centre of the plate. Responses were recorded differentially between the micro-electrode and a silver ball resting on the cortical surface close to the point of micro-electrode entry. Recording band width was 300 Hz to 20 kHz.

At the termination of each experiment the animal was killed by anaesthetic overdose and the lengths of cord between the different stimulating electrodes were measured *in situ*.

RESULTS

Responses to pyramidal stimulation were first characterized to establish comparability with findings of previous workers and responses to stimulation at different levels of the cord were then investigated.

Cortical responses to stimulation of the medullary pyramid

(*a*) *Responses on the cortical surface.* Responses recorded from the surface of the cerebral cortex following single shocks delivered to the ipsilateral medullary pyramid were similar in general form to those reported by previous investigators (Porter & Sanderson, 1964; McComas & Wilson, 1968; Ohta, 1968). The largest potentials were recorded within an area which extended in a wide strip between a point 4·0 mm lateral to the bregma and a point 4·0 mm posterior and 1·5 mm lateral to the bregma. This distribution appears to agree with the findings of Porter & Sanderson (1964).

As may be seen from Fig. 1*A–C* the earliest event was a surface positive deflexion with a peak at 2·0 ms ($\pm$0·16 ms S.D.; six experiments), onset at 1·3 ms ($\pm$0·1 ms S.D.) and duration approximately 1·4 ms. The latency and amplitude of this response were constant between trials and following the nomenclature of Porter & Sanderson it was denoted wave (1). It was followed by a negativity (cf. wave (3) of Porter & Sanderson) which was especially evident when later events were small in amplitude as in Fig. 1*D*. Porter & Sanderson reported that the falling phase of wave (1) was frequently notched by the presence of a second small positive wave (latency 3 ms) which was denoted wave (2). No sign of this response was observed in the present experiments with the possible exception of one case when the falling phase of wave (1) displayed a point of inflexion (see Fig. 1*C*), but a small positive wave with latency 4 ms to peak was frequently superimposed on the negative wave (3) (see Fig. 1*A–C*).

Downloaded from J Physiol (jp.physoc.org) at unknown institution on March 9, 2010

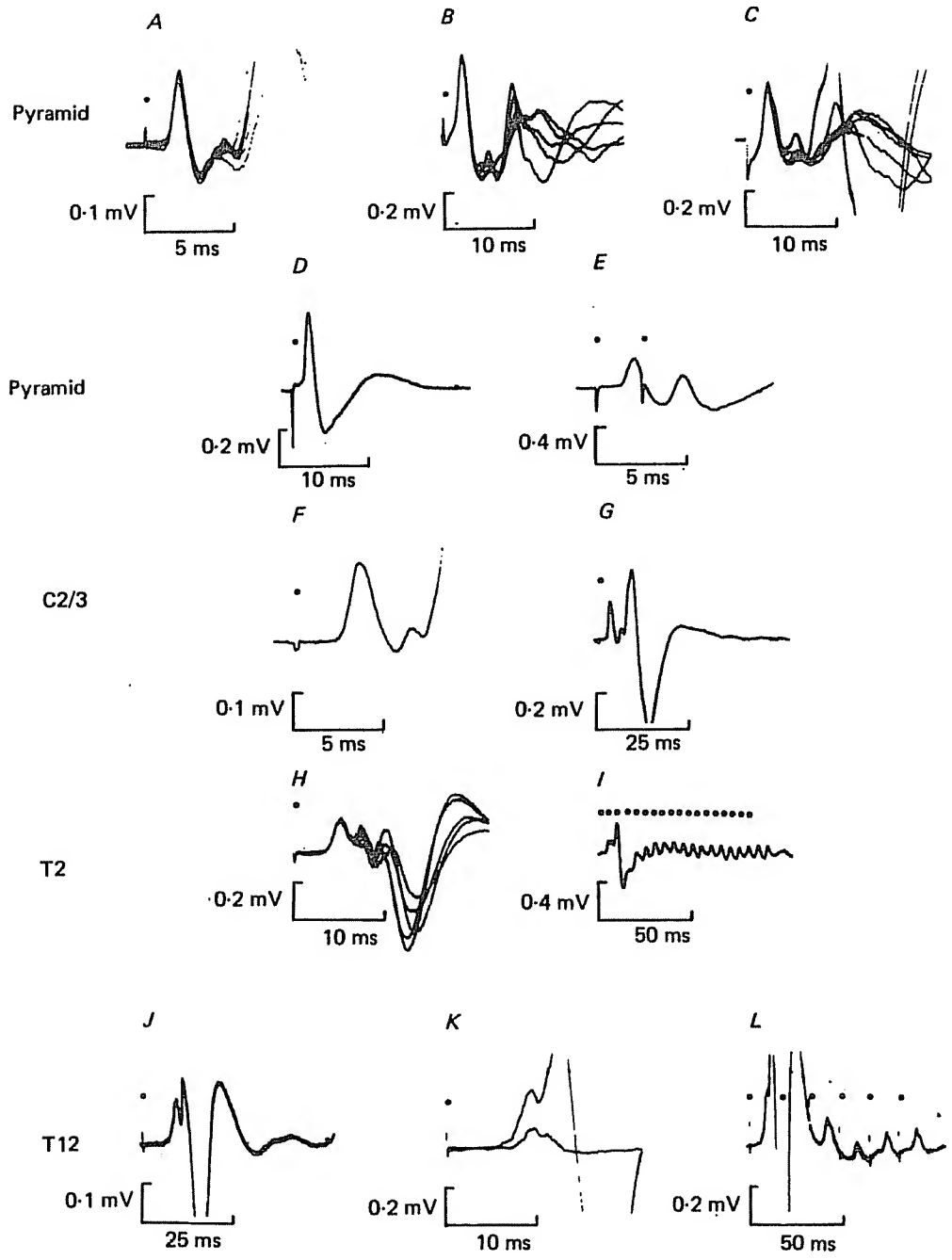

Fig. 1. Field potentials evoked on the cortical surface by supramaximal stimulation at the pyramid and at different spinal levels of the corticospinal tract. Positive up in all records. Stimuli, marked by small filled circles. *A* and *B*, five superimposed responses to single pyramidal stimuli at 1 Hz. *C*, seven superimposed responses. *A*, *B* and *C* from different animals. *D*, single response. *E*, responses to two stimuli 2·5 ms apart. *F* and *G*, single responses to stimulation at C2/3. *H*, five superimposed responses to stimulation at T2. *I*, responses to repetitive stimulation at 200 Hz. *J*, responses to one stimulus at T12. *K*, two superimposed responses to stimulation at 10 Hz; smaller response was evoked by second stimulus. *L*, stimulation with 6 pulses at 60 Hz.

Downloaded from J Physiol (jp.physoc.org) at unknown institution on March 9, 2010

It showed variations in amplitude and small variations in latency between trials and appears to correspond with wave (3P) of Porter & Sanderson. It was followed by a third positive peak with latency 7–9 ms. This large response showed very marked fluctuations in latency and amplitude (see Fig. 1*B* and *C*) and undoubtedly corresponds to wave (4P) of Porter & Sanderson. It was succeeded by a negativity which showed similar variations and this in turn was frequently followed by another wave (5P: latency to peak approximately 20 ms, not illustrated) after which the record returned to the base line.

Threshold for wave (1) ranged from 20 to 60 μA in different experiments but was constant in any one experiment. As stimulus intensity was increased the response recorded at the best point on the hemisphere reached a plateau amplitude of approximately 0·5 mV at intensities of 600–700 μA.

Fig. 1*E* shows that when two stimuli were delivered only 2·5 ms apart wave (1) was undiminished and in fact it was capable of following trains of many stimuli at 400 Hz. By contrast waves (3P), (4P) and (5P) failed completely at rates in excess of 10 Hz.

Further evidence that the different peaks were generated by different mechanisms was provided by the effect of maintenance doses of sodium pentobarbitone (5–10 mg/kg) administered to lightly anaesthetized animals; wave (1) remained constant in amplitude whilst all later events underwent a marked temporary decline which was evident within a few seconds. In addition, the potentials differed markedly in their response to anaesthetic overdose. After breathing ceased the time for the potentials to decline to zero amplitude was: wave (1), 50 sec; (3P), 25 sec; (4P), 10 sec. When, in another experiment, asphyxia was produced by tracheal occlusion the times were: wave (1), 30 sec; (3P), 15 sec; (4P), < 5 sec.

In light of this evidence there seems no doubt that as claimed by Porter & Sanderson (1964) wave (1) signals antidromic invasion of pyramidal tract neurones whilst (3P), (4P) and (5P) are generated synaptically as a result of stimulus spread to the nearby medial lemniscus and/or activation of a recurrent pathway involving axon collaterals of pyramidal tract neurones (see Discussion).

(*b*) *Single unit responses.* When micro-electrodes (see Methods) were inserted into the cortex in the region where surface potentials were largest, extracellular single unit recordings were readily obtained. The spikes were usually monophasic negative or diphasic negative–positive (see Fig. 7 for two examples) though diphasic positive–negative potentials were sometimes encountered.

Recordings were made from a total of 246 units and in respect of their responses to pyramidal stimulation they fell clearly into two groups. Units in the first group (218) yielded a single action potential which displayed a fixed threshold and a short latency which was invariant even at near threshold stimulus intensities. Such responses were invariably capable of following each of two stimuli separated by 2·5 ms. They were assumed to signal antidromic activation of pyramidal tract neurones. The frequency distribution for the latencies of the antidromic action potentials in these units is shown by the filled areas in the histogram of Fig. 2*A*.

According to Porter & Sanderson (1964) these events, occurring near synchronously in a large population of pyramidal tract neurones, give rise to wave (1). This identification was made partly on the grounds that the modal latency for single unit

Downloaded from J Physiol (jp.physoc.org) at unknown institution on March 9, 2010

responses coincided with the latency to the peak of wave (1). Fig. 2*A* shows that precisely the same finding was made in the present experiments.

A second population of twenty-eight units, encountered in the same electrode tracks, responded differently. They yielded a single action potential with variable threshold and variable (and usually longer) latency, and all failed to follow at any frequency higher than 2 Hz. These responses were presumably synaptically (i.e. orthodromically) generated. The open areas of Fig. 2*A* show the latency distribution for responses of this kind. Note that the latency range (3–9 ms) spans the period during which waves (3P) and (4P) were present on the cortical surface. When a maintenance dose of pentobarbitone was administered, synaptically driven responses rapidly (but temporarily) disappeared, a pattern of behaviour which parallels that found for waves (3P) and (4P). By contrast, like surface wave (1), antidromic single unit responses were not suppressed.

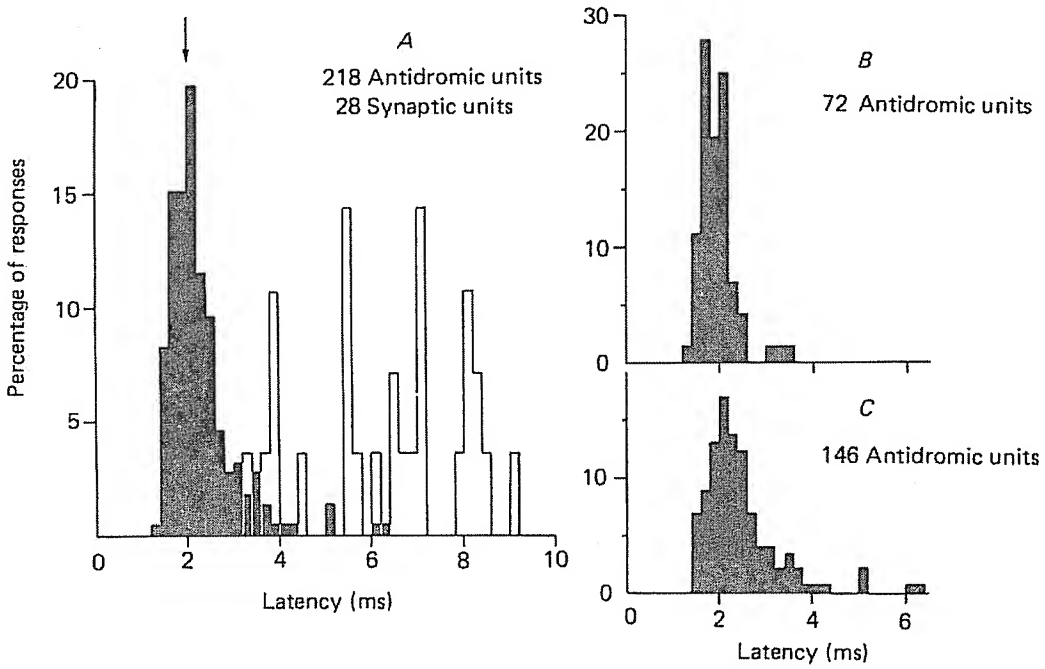

Fig. 2. Normalized latency distributions for cortical units responding to pyramidal stimulation. *A*, filled areas, antidromic responses; open areas, synaptically driven responses. Latency to peak of surface wave (1) is arrowed. *B*, latencies of antidromic responses to pyramidal stimulation for those units which were shown to project to T12. *C*, latencies of antidromic responses to pyramidal stimulation in units not tested for a projection to T12 (see text for further explanation).

Some pyramidal neurones were also tested for the presence of antidromic responses to stimulation at spinal levels (see also below) and Fig. 2*B* shows the distribution of pyramidal latencies for those units which were shown to project to T12 (i.e. cortico-lumbosacral neurones). Fig. 2*C* shows for comparison the latencies of those units recorded in experiments in which stimuli were applied at the pyramid only. This distribution presumably includes not only corticospinal axons reaching T12 but also an admixture of corticobulbar axons and corticospinal axons terminating at more rostral levels of the cord. Despite the likely presence of some cortico-lumbosacral

Downloaded from J Physiol (jp.physoc.org) at unknown institution on March 9, 2010

axons in Fig. 2*C* two differences are apparent. Firstly, the peak of the distribution in Fig. 2*B* is slightly earlier suggesting that fast axons are relatively more numerous in the cortico-lumbosacral than the 'mixed' population. Secondly, only 4% of units excitable from T12 had pyramidal latencies longer than 2·5 ms, as compared with 28% in Fig. 2*C*. This suggests that the more slowly conducting axons in the pyramid only rarely project as far caudally as T12.

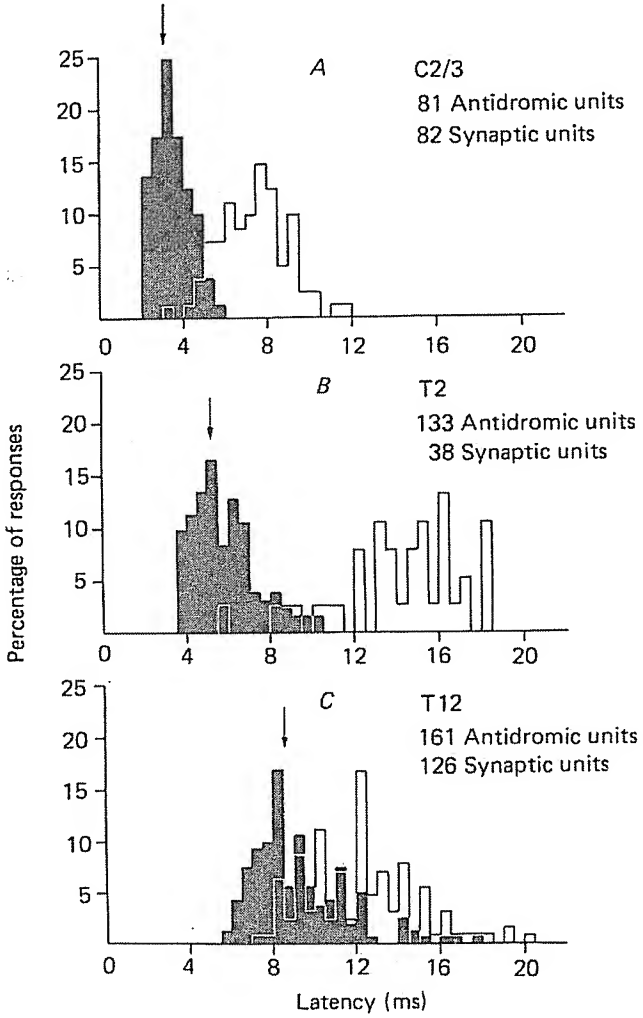

Fig. 3. Normalized latency distributions for cortical unit responses to stimulation at three spinal levels *A*, C2/3; *B*, T2; *C*, T12. Filled areas, units discharged antidromically; open areas, synaptically driven units. Latency to peak of wave (1) for each level is arrowed.

Cortical responses to stimulation in the spinal cord

(*a*) *Response latencies for surface potentials and single unit discharges.* Single shocks delivered via an electrode in the contralateral dorsal column at segmental level C2/3 evoked cortical responses very similar to those following pyramidal stimulation except that the latencies were longer (see Fig. 1*F* and *G*). From its frequency following characteristics, constant latency and amplitude, and cortical distribution

Downloaded from J Physiol (jp.physoc.org) at unknown institution on March 9, 2010

the earliest response was identifiable with wave (1). The subsequent waves, (3P) and (4P) were variable in latency and amplitude. They had latencies to peak of 6 ms and 8–10 ms respectively and failed to follow frequencies in excess of 10 Hz.

When single cortical units were recorded the results were again similar to those of pyramidal stimulation inasmuch as two distinct populations were encountered, one responding antidromically, the other driven synaptically. The frequency distribution of latencies for eighty-one antidromically driven and eighty-two synaptically driven units is shown in Fig. 3*A* by the filled and open areas respectively. Note that the mode for antidromic latencies was between 3·0 and 3·4 ms which compares well with the latency (arrowed) of the peak of wave (1) which was 3·1 ms (±0·7 ms S.D.; five experiments). Likewise the majority of synaptically driven responses occurred during the period of waves (3P) and (4P).

In many respects the results of stimulation at more caudal levels of the cord (i.e. T2 and T12) were similar to those obtained from C2/3. Fig. 1*H* shows typical responses recorded from the cortical surface following stimulation at T2 and Fig. 1*I* shows the earliest component, wave (1), following a train of stimuli at 200 Hz (it was capable of following up to 400 Hz) whilst the others are evoked only by the first stimulus. At this spinal level the latency of wave (1) was 5·2 ms (±0·7 ms S.D.; five experiments). This agrees well with the mode of the latency distribution for 133 units driven antidromically (see filled area of Fig. 3*B*), which was at 5·0–5·4 ms.

Similarly, for stimulation at T12 the latency to peak of the potential identified as wave (1) (see Fig. 1*J*) was 8·6 ms (±0·8 ms S.D.; eleven experiments) whilst the mode of the latency distribution for 161 antidromically identified units was 8·0–8·4 ms (see Fig. 3*C*). It is therefore evident that for each of the three cord levels stimulated there was a good temporal association between the peak of wave (1) and the modal latency amongst the antidromically driven cortical units. A similar association also existed between the latency to *onset* of wave (1) and the timing of the earliest antidromic responses of single units. These correlations were established by pooling the data from several experiments but they were also present in each individual experiment. This is demonstrated by Fig. 4*A* in which the latency to peak of wave (1) for each of twelve animals is plotted against the mean latency for the population of units antidromically invaded in the same experiment. The diagonal line is the regression line for this set of points and is very close to the line of equal latency.

Although the temporal correlation present at levels C2/3 and T2 between wave (1) and the antidromic unit responses was maintained at level T12 it must be emphasised that at this level the earliest response recorded from the cortical surface was not entirely attributable to antidromic invasion of corticospinal neurones. In all experiments the use of repetitive stimulation, which suppresses synaptically mediated responses, produced considerable diminution in the earliest surface potential evoked from T12. This is illustrated in Fig. 1*K* where two superimposed sweeps show the responses evoked by two trials 100 ms apart. Fig. 1*L* illustrates the further finding that the residual response was capable of following long trains of stimuli at high frequency.

The observation that the earliest response was reduced by repetitive stimulation received clarification when single unit recordings were made. As shown in the histogram of Fig. 3*C*, with T12 stimulation the latency distributions for synaptically

Downloaded from J Physiol (jp.physoc.org) at unknown institution on March 9, 2010

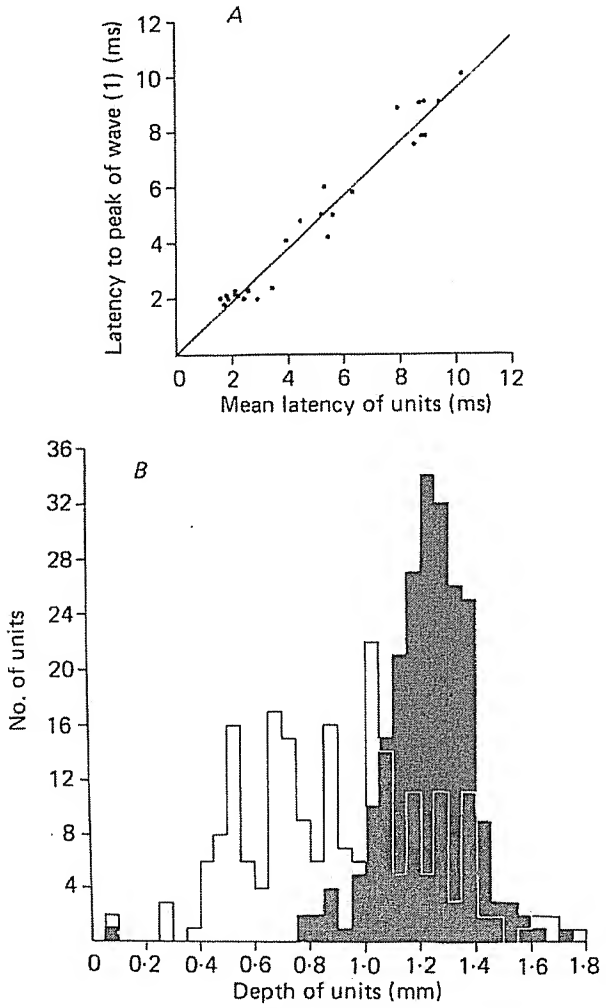

Fig. 4. *A*, temporal correlation between the latency to peak of wave (1) and the mean latency for antidromic single unit responses. Each point represents data collected during stimulation at a single site and in a single animal. Note that there is a wide range of latencies as data is represented from ten cases of pyramidal stimulation, two cases of stimulation at C2/3, six cases of stimulation at T2 and eight cases of stimulation at T12. Diagonal line is calculated regression line (gradient 0·95; vertical intercept 0·04; coefficient 0·98). *B*, depth of all cortical units responding to spinal stimulation (includes data for stimulation at C2/3, T2 and T12). Filled areas, 224 antidromic units; open areas, 215 synaptically driven units.

and antidromically mediated spikes overlap much more than for more rostral levels. Thus the first surface response is in part due to antidromic invasion of corticospinal neurones and in part to synaptically mediated events.

The most likely explanation for this change relative to the findings for more rostral stimulation is that synaptic responses to cord stimulation are mediated at least in part via an ascending path which is stimulated along with the corticospinal tract and which includes some axons with a higher conduction velocity. The dorsal column–medial lemniscal pathway is an obvious candidate and this candidature is supported by two observations. Firstly, with the cathode resting on the dorsal surface of the

Downloaded from J Physiol (jp.physoc.org) at unknown institution on March 9, 2010

cord at T12 large and variable surface potentials similar to those already described were evoked by low stimulus currents (50–100 μA) which failed to evoke wave (1). These responses completely failed at repetition rates in excess of 10 Hz. Secondly, when the electrode was advanced ventrally wave (1) first appeared at a depth of 0·7 mm. Further advance led to growth of wave (1) but to decline of the variable waves suggesting that they were evoked from structures more dorsal than those yielding wave (1).

(*b*) *Distribution and amplitude of antidromic responses on the cortical surface.* Some evidence was obtained for a topographical localisation in the origin of the corticospinal projection. When the amplitude of wave (1) was measured at many points on the cortical surface and isopotential maps were prepared (not illustrated) it was clear that large response (i.e. $> 0{\cdot}1$ mV) to stimulation at T12 were restricted to the caudomedial part of the larger area which responded to stimulation of the pyramid. This accords well with the somatotopical organization revealed by the spatial distribution of corticospinal neurones retrogradely labelled after injection of horseradish peroxidase into different segments of the spinal cord in the rat (Ullan & Artieda, 1981).

It was evident also that wave (1) is not evoked at equal amplitude from all spinal levels. The peak amplitude of the largest responses to supramaximal stimulation was approximately 0·5 mV for pyramidal stimulation but only 0·3 mV for stimulation at T2. When wave (1) was evoked from T12 and isolated for measurement by repetitive stimulation as in Fig. 1*K* and *L*, the largest responses were only 0·15 mV. This progressive reduction in amplitude for stimulation at successively more caudal levels may reflect progressive loss of axons from the corticospinal tract along the length of the cord. A further possibility is temporal dispersion of the antidromic volley with increasing conduction distance.

(*c*) *Depth distribution of cortical unitary responses.* For each unit the depth of the micro-electrode tip at which the action potential was largest in amplitude was read off from the microdrive and the frequency distribution of depths for units recruited by spinal stimulation is plotted in Fig. 4*B*. The dark area represents antidromic responses whilst synaptically driven units are represented by the open areas. It is evident that antidromic units were in the deeper layers of the cortex, only one being less than 0·75 mm below the pial surface and most being between 1·0 mm and 1·5 mm. Synaptically driven units were more widely distributed. They were quite common as little as 0·5 mm below the surface though also present in the deepest layers.

For all stimulation sites there was no correlation between the depth of an antidromically driven unit and the latency of its response (Fig. 5; ●). This is illustrated for pyramidal stimulation (Fig. 5*A*) and also for neurones stimulated at C2/3 and T12 (Figs. 5*B* and *C* respectively). A similar observation applies to the synaptically driven units (○).

Conduction velocity of corticospinal axons

The latency of wave (1) evoked from T2 was 3·6 ms to onset and 5·2 ms to peak whilst the corresponding values for the pyramid were 1·3 ms and 2·0 ms. Since the straight-line distance between the two sites was 36 mm ($\pm 1{\cdot}7$ mm S.D.; six experiments) these latency values correspond to approximate conduction velocities in the 'cervical' cord of 15·7 m/s for the fastest corticospinal fibres and 11·3 m/s for

Downloaded from J Physiol (jp.physoc.org) at unknown institution on March 9, 2010

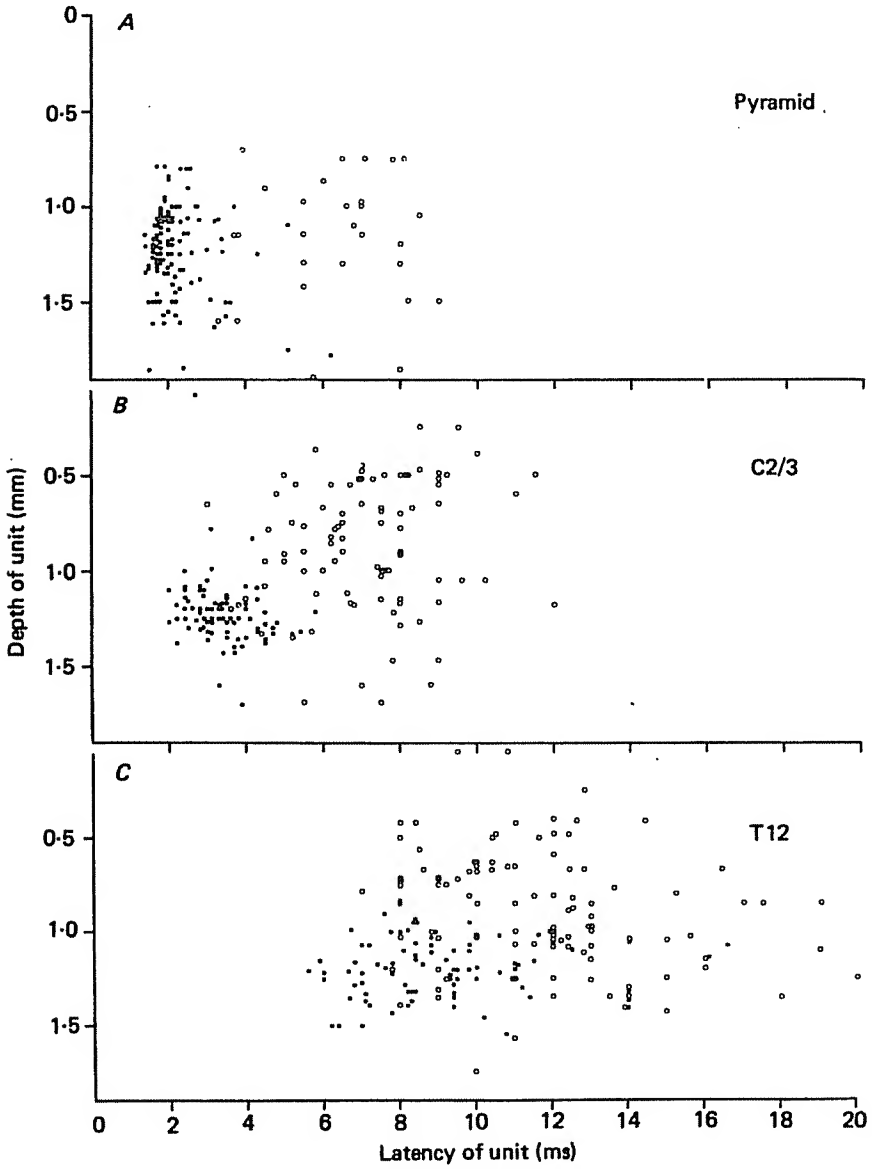

Fig. 5. Depth of cortical units plotted with respect to their latency of response. Stimulation at three sites. *A*, pyramid; *B*, C2/3; *C*, T12. ●, antidromic units; ○, synaptically driven units.

those whose activity gave rise to the peak. The corresponding values for the 'thoracic' cord (T12 to T2) were 13·7 ms and 11·0 m/s respectively.

Values for individual corticospinal axons could also be obtained when a cortical unit was antidromically activated both from the pyramid and the cord.

Care was taken in such cases to ensure that the same neurone was being activated. The spikes evoked from both sites were the same amplitude and shape and underwent parallel changes in amplitude when the position of the micro-electrode tip was changed. Sometimes the cell could be damaged with the micro-electrode and this always abolished both responses.

Fig. 6 shows frequency distributions for the conduction velocities of individual axons. Fig. 6*A* shows the values for sixty-five axons excited at both T2 and the

Downloaded from J Physiol (jp.physoc.org) at unknown institution on March 9, 2010

pyramid. The mean conduction velocity between these two sites was 11·5 m/s (±2·7 m/s S.D.). By comparison Fig. 6*B* shows the values for eighty-three axons which were excited at both T12 and T2; the mean is slightly lower at 10·5 m/s (±3·1 m/s S.D.). The over-all conduction velocity between T12 and the pyramid is shown for seventy-two axons in Fig. 6*C*; mean 11·4 m/s (±2·9 m/s S.D.). The experimental procedure employed was to begin by searching the cortex for antidromic units responding to stimulation at T12. When such a unit was encountered, and its latency determined, the latencies of its response to stimulation at T2 and the pyramid were also determined. As a result most of the values for the T2–pyramid portion of the cord (Fig. 6*A*) are for corticospinal axons which descended at least as far as T12.

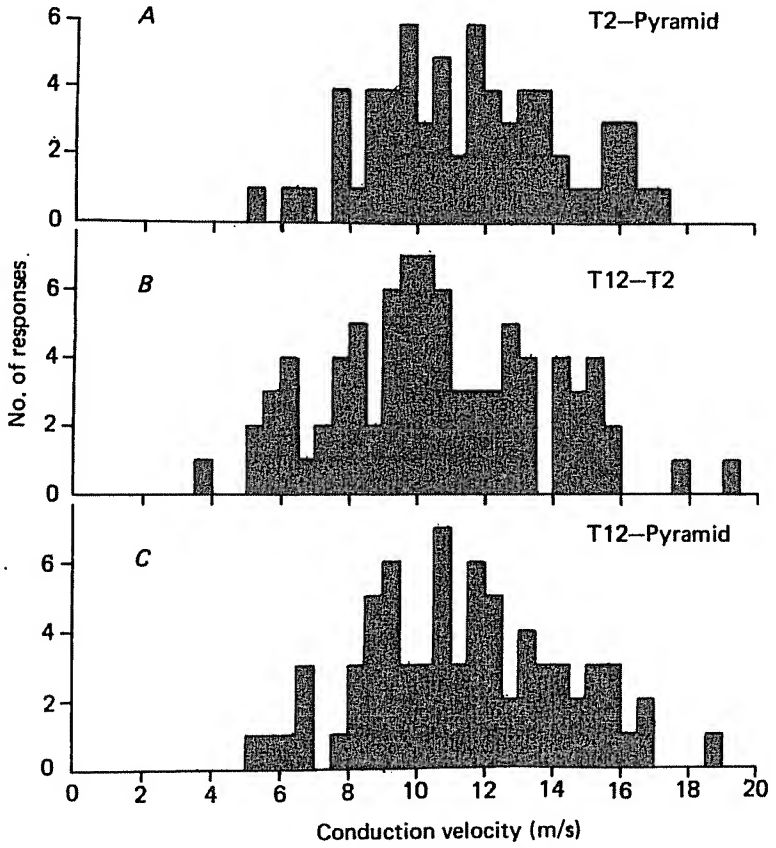

Fig. 6. Conduction velocities of single axons between *A*, T2 and the pyramid (sixty-five axons); *B*, T12 and T2 (eighty-three axons); *C*, T12 and the pyramid (seventy-two axons).

However, twelve of the sixty-five axons in Fig. 6*A* could not be recruited by stimulation at T12 and therefore probably terminated between T2 and T12. Their conduction velocities ranged from 8·4 to 17·1 m/s and therefore fell within the range for the other (i.e. cortico-lumbosacral) axons in Fig. 6*A*.

In fifty-three units excitable from T12 separate conduction velocities were calculated for the T2–pyramid and T12–T2 portions of the axon. Fig. 7*A* shows one such unit responding to a single shock delivered (in descending order) to pyramid, T2 and T12 and Fig. 7*B* shows that at each level responses could be evoked by each of 2 shocks, 2 ms apart. In this unit the conduction velocity between T12 and T2 (12·5 m/s) was almost the same as that between T2 and the pyramid (13·1 m/s).

Downloaded from J Physiol (jp.physoc.org) at unknown institution on March 9, 2010

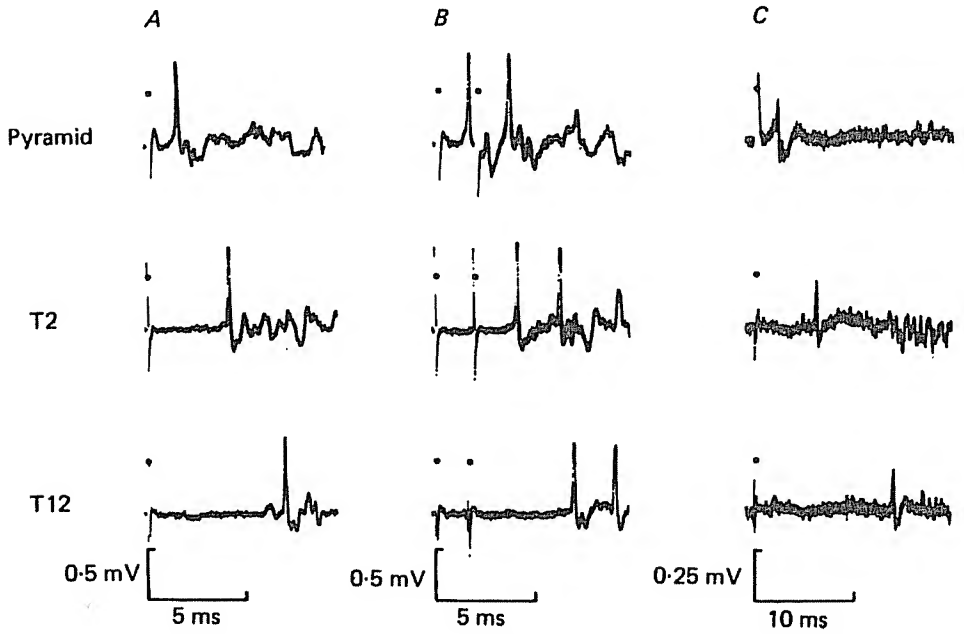

Fig. 7. *A* and *B* show responses of one antidromically driven cortical unit when stimulated at the pyramid, T2 and T12. *A*, responses to single stimuli; *B*, responses to paired stimuli with separation 2 ms. Conduction velocity calculated for the axon between T2 and the pyramid was similar to that between T12 and T2. *C*, responses of a second unit to single stimuli; conduction velocity calculated for T12–T2 was considerably slower than that for T2–pyramid (see test for further explanation). Negative up.

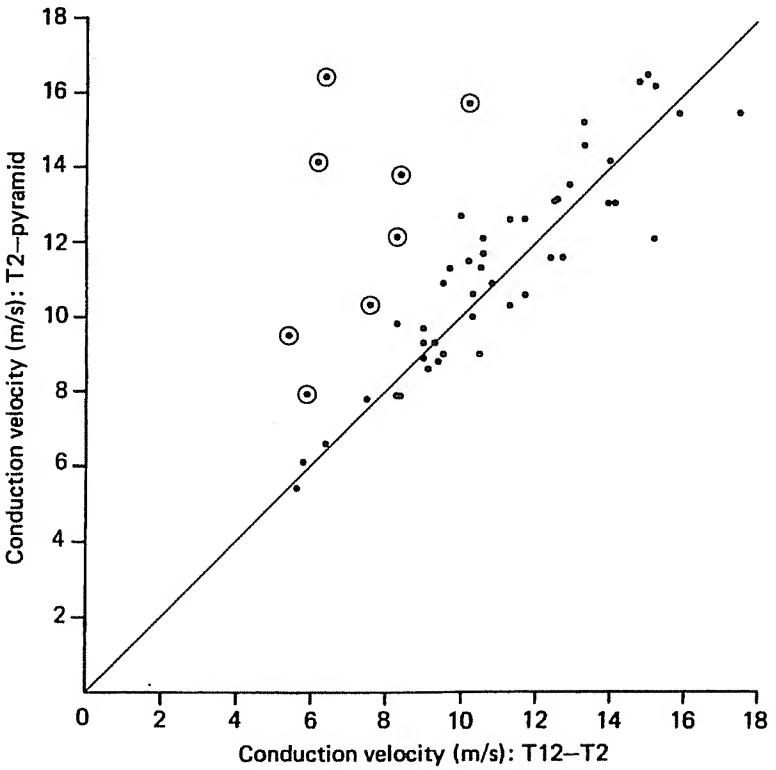

Fig. 8. Conduction velocity between T2 and pyramid plotted against conduction velocity of same axons between T12 and T2. The eight encircled points represent axons for which the conduction velocity was over 25% slower in the more caudal portion of the cord. Diagonal is line of equal velocity.

Downloaded from J Physiol (jp.physoc.org) at unknown institution on March 9, 2010

However, the different unit shown in Fig. 7*C* conducted considerably more slowly in the 'thoracic' cord (T12–T2: 5·4 m/s) than in the 'cervical' cord (T2–pyramid: 9·5 m/s).

In Fig. 8 the 'cervical' and 'thoracic' conduction velocities are compared for each of the fifty-three units and it is clear that in the majority of cases the values fall on or close to the line of equality. However, the conduction velocity for eight axons was at least 25 % slower in the 'thoracic' cord and in these cases (encircled points) it seems likely that real slowing occurred as the axons descended.

Small departures from equality are probably ascribable to the inevitable inaccuracies which attend the measurement of conduction distances. In particular no allowance was made for the deviation from a straight-line course which must occur in the pyramidal decussation. It is likely, therefore, that the calculated conduction velocities are underestimates and the degree of underestimation will be greater for the 'cervical' values. However, the errors are unlikely to be substantial because the conduction distances were considerable (means of 36 mm for T2–pyramid and 41 mm for T12–T2).

DISCUSSION

Cortical responses to pyramidal stimulation

The cortical surface response evoked from the pyramid in these experiments was very similar to that recorded by Porter & Sanderson (1964) with the small exception that little sign was seen of their wave (2). Results from single unit recordings were consistent with their hypothesis that wave (1) signals antidromic invasion occurring near-synchronously in a large number of pyramidal tract neurones. Porter & Sanderson reported wave (2) to be a small positive peak at a latency of about 3 ms which notched the downstroke of wave (1), followed repetitive stimulation at 200 Hz and coincided in latency with single unit antidromic spikes. In the experiments reported here single units with appropriate latencies were recorded (Fig. 2*A*) despite the absence of wave (2). However, both Porter & Sanderson (1964) and Ohta (1968) found that wave (2) was not invariably present and in the rabbit, Chang (1955) encountered an analogous wave only when the cerebral cortex was cooled to 20–23 °C; at physiological temperatures it was obscured by the negativity which follows wave (2).

Ohta (1968) recorded the mass antidromic response at different depths in the rat cortex and found that wave (2) reversed polarity at a depth of 1·6 mm whilst wave (1) reversed at 2·0 mm. He considered that wave (2) was caused by antidromic invasion of pyramidal tract neurones with slower axons and was situated more superficially in the cortex. A similar conclusion was reached by Towe, Patton & Kennedy (1963) who made single unit recordings in the cat and found that the shortest latency antidromic responses occurred in layer V and that longer latency responses occurred in layer III. However, in the present experiments there was no such correlation between the depth and the latency of units driven antidromically from either the pyramid (i.e. pyramidal tract neurones) or the spinal cord (i.e. corticospinal neurones). It is consistent with our observations that Ullan & Artieda (1981) have reported that rat corticospinal neurones retrogradely labelled using horseradish peroxidase were found only deep in the cortex (in layer Vb). Similarly, Deschenes Labelle & Landry (1979) have found pyramidal tract neurones are restricted to layer V in the cat.

Downloaded from J Physiol (jp.physoc.org) at unknown institution on March 9, 2010

Regarding the late and variable waves on the cortical surface, Porter & Sanderson (1964) demonstrated that they coincided with synaptically mediated discharges in cortical neurones other than pyramidal tract neurones and we have confirmed this finding. These authors also discussed the possible mechanisms which might generate such discharges. They include cortical activation via intracortical recurrent collaterals of the pyramidal axons and via pyramidal collaterals to ascending pathways. Alternatively, the medullary stimulus may spread to excite the medial lemniscus. The importance of this last possibility was later emphasised by the work of Stone (1972) who selectively diminished the late waves by sectioning the medial lemniscus in the medulla. It is also reinforced by the present experiments because apparently identical late waves could be evoked by stimulation in the dorsal part of the dorsal columns at intensities too weak to evoke a wave (1) response. By contrast, when the same stimuli were delivered deeper in the cord, where they succeeded in evoking wave (1), the late waves were smaller.

Conduction velocities in the corticospinal tract

Our most important findings relate to the conduction velocities of corticospinal axons. Stimuli applied to the medullary pyramid inevitably excite corticobulbar axons so that measurements of antidromic latency from this site allow deduction only of a limit above which corticospinal axons are unlikely to conduct. Moreover, estimates of the conduction distance from pyramid to cortex are necessarily very approximate. As a result, little evidence has previously existed concerning corticospinal velocities in the rat. The only direct measurements are of a few axons in the upper cervical cord (McComas & Wilson, 1968) and these results differ markedly from those of Elger *et al.* (1977), who deduced a velocity of 60 m/s for the fastest fibres (see below). Both from the latency of the antidromic response on the cortical surface and on the basis of single unit recordings we conclude that the fastest fibres conduct at somewhat less than 20 m/s whilst the fibres contributing to the peak of wave (1) conduct at about 11 m/s. The value for the fastest unit we encountered was 19·1 m/s.

It is evident that our results are in reasonable agreement with those of McComas & Wilson (1968) who found a range of 7·6 m/s to 10·8 m/s but conflict directly with those of Elger *et al.* (1977). It is therefore necessary to discuss the results obtained by the latter group to determine whether reconciliation is possible.

Following cortical stimulation Elger *et al.* (1977) recorded a field potential from the cord dorsum at L3/4 which had a latency of 1·7 ms to peak and which followed repetitive stimulation at 300 Hz. Conversely, when the dorsal surface of the cord was stimulated at L3/4 a cortical evoked potential was recorded with similar latency and frequency-following characteristics. In addition, Janzen, Speckmann, Caspers & Elger (1977) recorded excitatory post-synaptic potentials (e.p.s.p.s) (apparently monosynaptic) in lumbar motoneurones with latencies as short as 1·7 ms following cortical stimulation. Elger *et al.* concluded that an uninterrupted corticospinal pathway exists to the lumbar cord in which the fastest fibres conduct at about 60 m/s. However, as they noted, electron microscopy indicates that the tract consists of axons no larger than 3·7 μm in diameter (Dunkerley & Duncan, 1969) and application of the Hursh factor (6 m/s per μm; Hursh, 1939) to such fibres would yield maximum velocities of about 22 m/s. Elger *et al.* therefore suggested that the Hursh factor is

Downloaded from J Physiol (jp.physoc.org) at unknown institution on March 9, 2010

not applicable to corticospinal axons and that some much higher factor is required. However, a study in the cat by Towe & Harding (1970) has suggested that the Hursh factor errs on the high side and that a factor of 4·72 is more appropriate. It may be noted here that the Hursh factor gives a maximum conduction velocity of 22 m/s whilst the factor proposed by Towe & Harding would yield a value of 17·5 m/s. Both these values are close to the velocity for our fastest fibres. However, the mode of the fibre diameter spectrum for the rat pyramid occurs at 0·5–1·0 μm (Dunkerley & Duncan, 1969) which corresponds to approximate conduction velocities of 3–6 m/s (Hursh) or 2·4–4·7 m/s (Towe & Harding). These values are substantially lower than the mode of the velocities in the present study, but this discrepancy can be accounted for if the micro-electrode technique exhibits substantial bias towards cells with large diameter axons. This is indeed likely to be the case as the existence of a large bias has invariably been inferred in electrophysiological studies of the pyramidal tract in the cat (e.g. Towe & Harding, 1970). Since very similar values of conduction velocity were obtained in the present experiments from the latencies of the antidromic field potentials a similar bias presumably exists for this type of response.

Though the above suggests that our estimate of maximum conduction velocity is substantially correct it does not of course account for the results of Elger *et al.* (1977). It may be noted however, that these workers employed computer averaging techniques capable of resolving very small signals recorded from the brain surface. It is therefore possible that the antidromic potentials they recorded from the cortical surface were in fact generated at a distance (i.e. beneath the cortex) and signalled transmission in another pathway (e.g. rubrospinal or reticulospinal). This suggestion gains support from a recent study (Armstrong & Drew, 1980) which has shown that, in the small brain of the rat, tract waves generated in the medulla can easily be recorded from the surface of the cerebellum even without averaging.

As regards the tract waves which Elger *et al.* recorded from the cord surface following stimulation of the cortical surface, it is possible they were generated by synaptic or direct excitation of a descending pathway subcortical in origin and conducting substantially faster than the corticospinal tract. Such paths do exist, for Shapavolov & Gurevitch (1970) stimulated the medullary reticular formation and recorded a tract wave from the dorsal surface of the lumbar spinal cord with a latency of 1·3–2·1 ms to peak which followed repetitive stimulation at up to 500 Hz. This path conducted at a mean velocity of 65 m/s and evoked monosynaptic e.p.s.p.s in lumbar motoneurones with latencies short at 1·6 ms (cf. the 1·7 ms of Elger *et al.* 1977).

Eight out of fifty-three of our corticospinal axons (i.e. approximately 15 %) showed substantially slower 'thoracic' (T12–T2) than 'cervical' (T2–pyramid) conduction velocities. Such a change presumably reflects a decrease in axonal diameter and in this connexion it may be noted that in the cat, Shinoda & Yamaguchi (1978) have provided electrophysiological evidence that corticospinal axons in the cat may provide collaterals to different segmental levels and that the provision of branches can be associated with a reduction in the conduction velocity of the stem axon. Future studies should show whether the slowing we have demonstrated in some axons in the rat is due to a similar phenomenon or whether tapering can occur even in the absence of collateralization.

Downloaded from J Physiol (jp.physoc.org) at unknown institution on March 9, 2010

We wish to thank Dr D. M. Armstrong for advice during the experiments and in preparation of the manuscript, Mrs A. Lear for typing and Mr C. Makepeace for photography. We would like to acknowledge the financial support of the MRC (for N.K.M.) and the Scottish Education Department (for J.A.R.N.).

REFERENCES

ARMSTRONG, D. M. & DREW, T. (1980). Responses in the posterior lobe of the rat cerebellum to electrical stimulation of cutaneous afferents in the snout. *J. Physiol.* **309**, 357–374.

BROWN, L. T. (1971). Projections and terminations of the cortico-spinal tract in rodents. *Exp. Brain Res.* **13**, 432–451.

CHANG, H.-T. (1955). Cortical response to stimulation of medullary pyramid in the rabbit. *J. Neurophysiol.* **18**, 332–352.

DESCHENES, M., LABELLE, A. & LANDRY, P. (1979). Morphological classification of slow and fast pyramidal tract cells in the cat. *Brain Res.* **178**, 251–274.

DUNKERLEY, G. B. & DUNCAN, D. (1969). A light and electron microscopic study of the normal and the degenerating cortico-spinal tract in the rat. *J. Comp. Neurol.* **137**, 155–184.

ELGER, C. E., SPECKMANN, E.-J., CASPERS, M. & JANZEN, R. W. C. (1977). Corticospinal connections in the rat. I. Monosynaptic and polysynaptic responses of cervical motoneurons to epicortical stimulation. *Exp. Brain Res.* **28**, 385–404.

FIFKOVA, E. & MARSALA, J. (1967). Stereotaxic atlas of the rat. In *Electrophysiological methods in biological research*, ed. Bures, E. J., Petran, M., Zachar, J. & Hahn, P. London: Academic Press.

HURSH, J. B. (1939). Conduction velocity and diameter of nerve fibres. *Am. J. Physiol.* **127**, 131–139.

JANZEN, R. W. C., SPECKMAN, E.-J., CASPERS, H. & ELGER, C. E. (1977). Corticospinal connections in the rat. II. Oligosynaptic and polysynaptic responses of lumbar motoneurons to epicortical stimulation. *Exp. Brain Res.* **28**, 405–420.

MCCOMAS, A. J. & WILSON, P. (1968). An investigation of pyramidal tract cells in the somatosensory cortex of the rat. *J. Physiol.* **194**, 271–288.

OHTA, M. (1968). Cortical motor function and the antidromic cortical response to stimulation of the medullary pyramidal tract in the rat. *Jap. J. Physiol.* **18**, 100–124.

PORTER, R. & SANDERSON, J. H. (1964). Antidromic cortical response to pyramidal-tract stimulation in the rat. *J. Physiol.* **170**, 355–370.

SHAPAVOLOV, A. I. & GUREVITCH, N. R. (1970). Monosynaptic and disynaptic reticulospinal actions on lumbar motoneurons of the rat. *Brain Res.* **21**, 249–263.

SHINODA, Y. & YAMAGUCHI, T. (1978). The intraspinal branching patterns of fast and slow pyramidal tract neurons in the cat. *J. Physiol. (Paris)*, **74**, 237–238.

STONE, T. W. (1972). Cortical responses to pyramidal tract stimulation in the rat. *Expl. Neurol.* **35**, 492–502.

TOWE, A. L. & HARDING, G. W. (1970). Extracellular microelectrode sampling bias. *Expl. Neurol.* **29**, 366–381.

TOWE, A. L., PATTON, M. D. & KENNEDY, T. T. (1963). Properties of the pyramidal system in the cat. *Expl. Neurol.* **8**, 220–238.

ULLAN, J. & ARTIEDA, J. (1981). Somatotopy of the corticospinal neurons in the rat. *Neurosci. Lett.* **21**, 13–18.

Downloaded from J Physiol (jp.physoc.org) at unknown institution on March 9, 2010

Exhibit E

Brain Research, 508 (1990) 341–344
Elsevier

BRES 23952

Corticospinal responses to electrical stimulation of motor cortex in the rat

Mark Stewart, Gregory J. Quirk and Vahé E. Amassian

Department of Physiology, State University of New York, Health Science Center, Brooklyn, N.Y. 11203 (U.S.A.)

(Accepted 24 October 1989)

Key words: Pyramidal tract; D-wave; I-wave; Spinal cord; Urethane

Direct and indirect corticospinal responses to electrical stimulation of motor cortex were identified in urethane-anesthetized rats. 'Killed-end' recordings were taken from the corticospinal tract at the level of the cervical cord (C_1–C_2) and from the medullary pyramid. The identities of direct (D) and indirect (I) corticospinal responses were confirmed by: (1) removing motor cortex to eliminate I activity, and (2) pharmacologically increasing neocortical excitability, prior to any lesions, to increase I activity. Our data indicate that the conduction velocity of the fastest corticospinal fibers is approximately 18 m/s. Our identification of the components of the corticospinal response will permit the interpretation of the more complicated surface or 'non-killed-end' depth recordings which have shown particular utility in evaluating spinal cord damage.

A brief electrical stimulus applied to the motor cortex of cats and monkeys elicits a distinct sequence of corticospinal waves[11]. The first wave reflects the direct (D) activation of corticospinal neurons in response to the stimulus. The D-wave is followed by one or more indirect (I) waves which are attributable to the re-activation of these corticospinal neurons, and the novel activation of others, via excitatory synaptic inputs. Each D to I or I to I interval appears to involve one additional synaptic delay[1,12].

Recent interest in the rat central nervous system for modeling various types of spinal cord trauma emphasizes the importance of defining in these animals the pattern of corticospinal responses to electrical stimulation. Several attempts to characterize orthodromic and antidromic corticospinal responses in the rat have been previously published[5,6,10]. A controversy becomes apparent when the estimates of maximum corticospinal conduction velocity are compared; values ranging from 19 m/s[10] to nearly 70 m/s[5,6] have been reported. Part of the confusion may come from latency measurements of 'peaks' in surface or other recordings that generally have more complicated appearances than 'killed-end' recordings. Damage to axons by the recording electrode in 'killed-end' recordings prevents conduction beyond the recording location and leads to a nearly monophasic appearance of the responses[9,11]. In addition to the greatly simplified appearance of the responses, killed-end recordings can reveal significantly larger I-waves relative to the D-wave than are detected in surface recordings[1,11]. This is because of the cancellation of extracellular voltages from out-of-phase polyphasic action potentials which can limit the amplitude of population responses in surface or even depth 'non-killed-end' recordings.

Our objective was to utilize killed-end recordings to define the population D and I corticospinal responses in the rat and to describe some of the properties of these responses. In addition, measurements were made of the conduction velocity of corticospinal fibers in an effort to resolve past differences in the literature.

Three male Sprague–Dawley albino rats (330–340 g) were anesthetized with urethane (1.5 g/kg i.p., supplemented as needed) and fitted with tracheal cannulae. Animals were held in a Kopf stereotaxic frame and maintained af 37–39 °C with a shielded heating lamp. Neocortex was exposed by first removing bone with a small drill and a rongeur from 1 mm anterior to lambda to 3 mm anterior to bregma and from the midline to 6 mm laterally. Dura mater was incised and reflected laterally to expose neocortex. The cortical surface was protected from drying by a mixture of petroleum jelly and mineral oil. Cervical cord segments C_1–C_3 were exposed by laminectomy. The motor cortex (MI) was focally stimulated by applying 100-μs pulses ($\pm$ 0–5 mA) between a pair of silver ball electrodes (ball diameter $\approx$ 0.5 mm), one placed on motor cortex and the other on posterior parietal cortex. A closely spaced bipolar electrode (125 μm formvar-insulated nichrome wire) was used to stim-

Correspondence: V.E. Amassian, Department of Physiology, Box 31, SUNY Health Science Center, 450 Clarkson Avenue, Brooklyn, N.Y. 11203, U.S.A.

0006-8993/90/$03.50 © 1990 Elsevier Science Publishers B.V. (Biomedical Division)

ulate the internal capsule. Corticospinal responses were recorded with 125 μm Teflon-insulated tungsten wire that was cut square so as to produce optimal killed-end recordings from: (1) the dorsal column[2] at C_1–C_2, and (2) the medullary pyramid. A similar electrode was used to record surface responses from the cervical cord. For a given stimulation site on MI, the optimal corticospinal tract recording site was determined. Subsequently, the focal stimulating electrode was moved to locate the optimal stimulation site that corresponded to the site of recording. Recordings were amplified, passively filtered (bandpass = 0.8 Hz–10 kHz), and displayed on an analog storage oscilloscope or recorded on FM tape (bandwidth = DC to 2 kHz) for off-line display and analysis. Corticospinal latencies were measured from the start of the stimulus artifact to the earliest positivity.

Pentylenetetrazol (Metrazol, 100 mg/ml) was topically applied to the cortical surface in two rats in order to increase cortical excitability and thereby enhance the I activity. In one of these rats, gallamine triethiodide (12 mg/kg i.v.) was given to eliminate contamination of the recordings by EMG activity. In two rats, the neocortex within 2 mm of the cortical stimulating location was removed by aspiration and stimuli were applied to the underlying white matter (internal capsule). The electrode location for recording corticospinal responses within the medullary pyramid was confirmed by histological localization of an electrolytic lesion (50 μA, 10 s).

Focal electrical stimulation of motor cortex produced clear D corticospinal discharges in all rats. The evoked I activity was considerably more diffuse than the relatively discrete I-waves normally recorded from cats and monkeys[1,11]. Fig. 1 (top) shows typical corticospinal responses to focal anodal (4.0 mA) stimulation of the contralateral motor cortex. A large initial wave (latency = 1.2 ms) is followed by a smaller more complex wave (latency = 4.7 ms). The initial wave was identified as a D-wave because it persisted, without significant change in configuration, when white matter was stimulated after terminally removing motor cortex (Fig. 1, bottom). In contrast, the later wave was lost following the lesion, indicating that this later wave probably reflects transynaptic or indirect activation of corticospinal neurons. To test the possibility that the response identified as the D-wave might be contaminated by postsynaptic activity within the spinal cord or by activity in another descending pathway, corticospinal recordings were also taken from the medullary pyramid (Fig. 2). The similarity of the D-wave recorded from the medullary pyramid to that recorded from the cervical cord indicates that relatively uncontaminated killed-end corticospinal recordings can

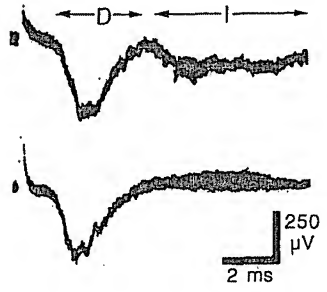

Fig. 1. The effect of neocortical aspiration on corticospinal responses to focal anodal stimulation of motor cortex. Five superimposed sweeps recorded before (top) and after (bottom) removal of motor cortex, recorded killed-end from the cervical spinal cord at C_1–C_2. The D- and I-waves are labelled. Except where specifically noted, all recordings are killed-end. Negativity is up in all figures.

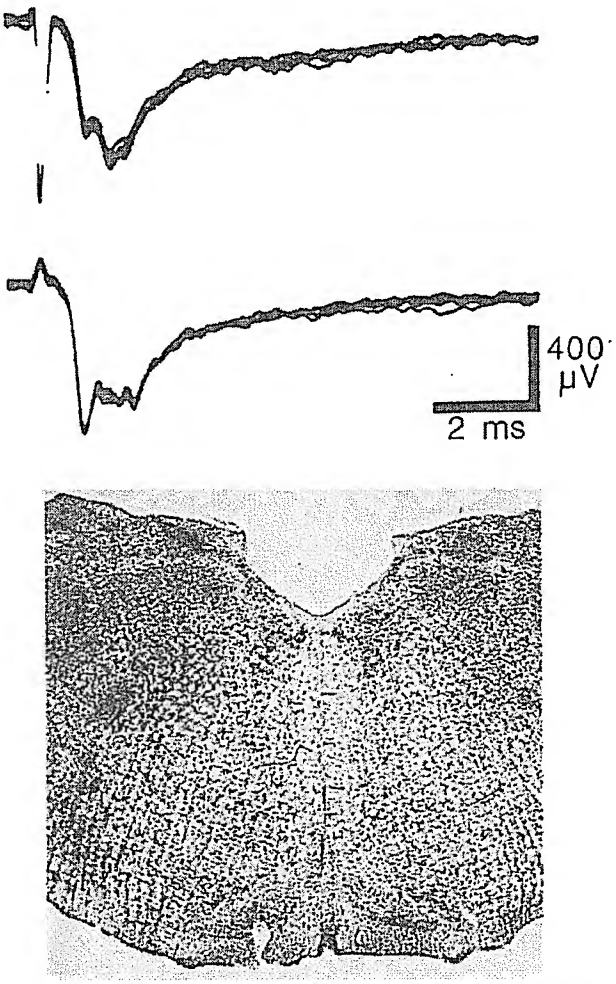

Fig. 2. The effect of motor cortical aspiration on pyramidal tract responses to focal anodal stimulation. Five superimposed responses to stimulation of the cortical surface before the lesion (top) and to stimulation of the underlying white matter after removal of motor cortex (bottom). The recording location in the pyramid on the left side is visible in the frozen section (50 μm) stained with Cresyl violet.

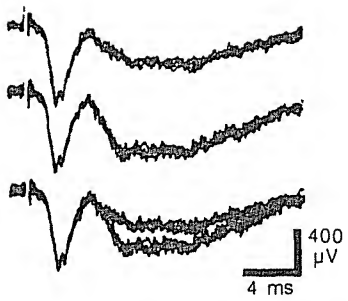

Fig. 3. The effect of a pentylenetetrazol-induced increase in neocortical excitability on I activity. Five superimposed responses before (top) and after (middle) topical application of pentylenetetrazol to the motor cortex. All traces are superimposed (bottom) to facilitate comparison.

be obtained from the dorsal columns.

Prior to any cortical lesions, I-waves were always considerably smaller than the D-waves. Indirect corticospinal activity could, however, be enhanced by topical application of pentylenetetrazol to the cortex surrounding the stimulating electrode (Fig. 3). Whereas there was no detectable change in the D-wave, even the earliest component of the indirect corticospinal response was enhanced by the drug. This is evidenced by the more rapid rising slope of the I-wave (Fig. 3, middle and bottom).

Corticospinal responses recorded from the spinal cord at C_1–C_2 for increasing intensities of focal anodal and focal cathodal stimulation are shown in Fig. 4. The threshold for the D-wave was always lower with anodal stimuli than with cathodal stimuli (anodal/cathodal: 0.9/1.3, 0.6/1.0, 0.7/1.8 mA), although these differences were somewhat larger than those observed in monkeys[1]. The largest D-wave that we recorded in response to a 2.0-mA anodal pulse was 650 μV. Although more pronounced in the higher mammals[1,11], the increased I activity with focal cathodal stimulation as compared to

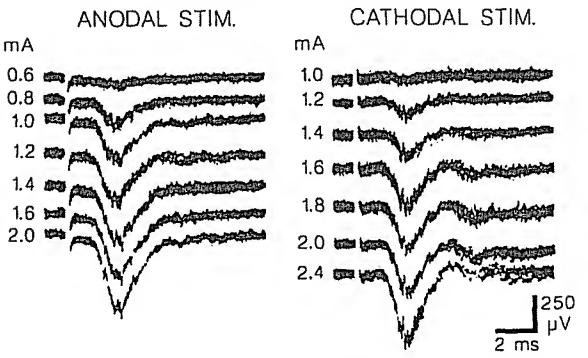

Fig. 4. Corticospinal responses to increasing anodal and cathodal stimuli applied to the surface of motor cortex. Five traces superimposed at each intensity.

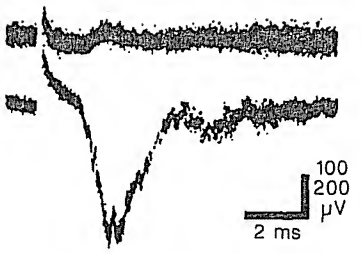

Fig. 5. Comparison of killed-end and surface recordings of corticospinal responses to focal anodal stimulation of motor cortex. Five traces superimposed.

focal anodal stimulation is also apparent in the rat.

The latency to the onset of the D-wave recorded at C_1–C_2 was 1.0–1.2 ms. Over a conduction distance of 20 mm estimated from gross measurements on the removed brain, these latencies yielded an average conduction velocity of about 18 m/s for the fastest corticospinal fibers contributing to the D-wave. The duration of the D-wave was typically as long as 3 ms. Allowing 0.5 ms for the duration of the action potential, the slowest fibers contributing to the D-wave conducted at about 5 m/s. In most of our killed-end recordings, the D-wave had one or more 'notches', presumably the result of activity in relatively discrete subgroups of corticospinal fibers (based on their conduction velocities).

The differences between a killed-end recording and the corresponding recording from the surface of the spinal cord are illustrated in Fig. 5. In the surface recording (top traces), the D-wave is diphasic (positive–negative) with a peak-to-peak amplitude of only 30 μV, i.e. less than 1/20th the amplitude of the D-wave seen in the killed-end recordings (bottom traces). Note that the polarity change in the surface recording corresponds to the rising phase of the killed-end response. Whereas the small D-wave was readily detected in individual surface responses, there was virtually no indication of any I activity in such recordings.

The pattern of corticospinal activity in the rat differs substantially from that of cats and monkeys[1,11] in several ways: (1) the D-wave is much longer in duration in the rat, (2) the I-wave in the rat lacks the periodicity seen in cats and monkeys, and (3) the D to I interval in the rat is much longer than the interval found in the higher mammals. The long duration D-wave in the rat is consistent with the broad distribution of moderate-sized fibers within the rat corticospinal tract[4]. The wide range of conduction velocities of rat corticospinal fibers could contribute to the apparent lack of periodicity in the I-wave as well. Repetitive discharges in individual corticospinal fibers would be obscured if the 'size-principle'[7] were applied to the transynaptic activation of cortico-

spinal neurons. The smaller neurons with lower conduction velocities would be indirectly activated more easily than the larger, faster units. Recordings from single corticospinal units are required to determine if this is the correct explanation for the appearance of the I-wave in the rat.

In addition to its more diffuse pattern of I activity, the rat corticospinal response differs from that of cats and monkeys by having a much longer D to I interval. Measuring about 3.5 ms from the start of the D-wave to the start of the I-wave, this interval is approximately twice that found in cats and monkeys. Since the D to I interval in cats appears from intracellular recordings to reflect a monosynaptic delay[12], possible explanations for the long D to I interval in the rat include: (1) an increased monosynaptic delay, and (2) two or more synapses between the stimulated presynaptic fiber and the corticospinal neuron. A small excitatory interneuron[3] interposed between an excited presynaptic fiber and a corticospinal neuron would lengthen the rat D to I interval, paralleling the increased delay for the inhibitory postynaptic potential (IPSP) in the cat[12]. (The increased delay for the IPSP was attributed to the difficulty of directly exciting a small inhibitory interneuron by an external electric field.) If the first I discharge were, in fact, mediated disynaptically, the additional temporal dispersion of unit responses would also contribute to the diffuse pattern of I activity seen in the rat. Although the rat brain has been widely studied, we know of no evidence for prolonged synaptic delays in the rat cortex. We favor, therefore, the notion of multiple synapses contributing to the re-excitation of corticospinal neurons, but whatever the explanation for the prolonged D to I interval in the rat, it is clear that I activity is *not* detectable at C_1–C_2 before about 4.5 ms. Consequently, we question the interpretation of Fehlings et al.[6] who identified peaks in recordings from thoracic cord, all with latencies less than 4 ms, as 'I-waves'.

Our estimate of the conduction velocity (18 m/s) of the fastest corticospinal fibers in the rat agrees well with the value reported for rats by Mediratta and Nicoll[10], but is less than 1/3 the velocity found in cats and monkeys. A similar conduction velocity (22 m/s) was derived from the Hursh factor[8] along with measurements of the largest corticospinal fiber diameters in the rat[4]. It is unclear what accounts for the three-fold higher estimates reported for the rat by others[5,6], but activity in reticulospinal fibers, which appear to conduct at high velocities[13] may account for the very early components of the 'corticospinal' responses used in their estimates of conduction velocity.

Recordings of population corticospinal responses provide a distinct advantage over electromyographic (EMG) recordings for assessing long tract damage in the spinal cord. A small reduction in the corticospinal response, resulting from a decrease in stimulus intensity or cryogenic blockade of conduction in corticospinal fibers, can completely eliminate an EMG response[1]. Thus, the number of conducting corticospinal fibers is much more closely related to the size of the population killed-end response than to an EMG response which depends upon at least one synapse between the corticospinal neuron and the α-motoneuron. Unfortunately, in a *chronic* animal preparation, the effects of experimental trauma to the spinal cord can be longitudinally studied only by recording population responses from the spinal cord surface. However, our data indicate that killed-end recordings from the spinal tract should be used *terminally* to identify the components of the surface recordings.

1 Amassian, V.E., Stewart, M., Quirk, G.J. and Rosenthal, J.L., Physiological basis of motor effects of a transient stimulus to cerebral cortex, *Neurosurgery*, 20 (1987) 74–93.

2 Brown Jr., L.T., Projections and termination of the corticospinal tract in rodents, *Exp. Brain Res.*, 13 (1971) 432–450.

3 Colonnier, M., The electron-microscopic analysis of the neuronal organization of the cerebral cortex. In F.O. Schmitt, F.G. Worden, G. Adelman and S.G. Dennis, (Eds.), *The Organization of the Cerebral Cortex*, MIT Press, Cambridge, 1981, pp. 125–152.

4 Dunkerley, G.B. and Duncan, D., A light and electron microscopic study of the normal and the degenerating corticospinal tract in the rat, *J. Comp. Neurol.*, 137 (1969) 155–184.

5 Elger, C.E., Speckmann, E.-J., Caspers, H. and Janzen, R.W.C., Cortico-spinal connections in the rat. I. Monosynaptic and polysynaptic responses of cervical motoneurons to epicortical stimulation, *Exp. Brain Res.*, 28 (1977) 385–404.

6 Fehlings, M.G., Tator, C.H., Linden, D. and Piper, I.R., Motor and somatosensory evoked potentials recorded from the rat, *EEG Clin. Neurophysiol.* 69 (1988) 65–78.

7 Henneman, E., Somjen, G. and Carpenter, D.O., Functional significance of cell size in spinal motoneurons, *J. Neurophysiol.*, 28 (1965) 560–580.

8 Hursh, J.B., Conduction velocity and diameter of nerve fibers, *Am. J. Physiol.*, 127 (1939) 131–139.

9 Lloyd, D.P.C., The spinal mechanism of the pyramidal system in cats, *J. Neurophysiol.*, 4 (1941) 525–546.

10 Mediratta, N.K. and Nicoll, J.A.R., Conduction velocities of corticospinal axons in the rat studied by recording cortical antidromic responses, *J. Physiol. (Lond.)*, 336 (1983) 545–561.

11 Patton, H.D. and Amassian, V.E., Single- and multiple-unit analysis of cortical stage of pyramidal tract activation, *J. Neurophysiol.*, 17 (1954) 345–363.

12 Rosenthal, J., Waller, H.J. and Amassian, V.E., An analysis of the activation of motor cortical neurons by surface stimulation, *J. Neurophysiol.*, 30 (1967) 844–858.

13 Shapovalov, A.I. and Gurevitch, N.R., Monosynaptic and disynaptic reticulospinal actions on lumbar motoneurons of the rat, *Brain Research*, 21 (1970) 249–263.

Exhibit F

Pergamon

0306-4522(93)E0011-E

Neuroscience Vol. 59, No. 3, pp. 699–711, 1994
Elsevier Science Ltd
Copyright © 1994 IBRO
Printed in Great Britain. All rights reserved
0306-4522/94 $6.00 + 0.00

MOTOR CORTEX AND PYRAMIDAL TRACT AXONS RESPONSIBLE FOR ELECTRICALLY EVOKED FORELIMB FLEXION: REFRACTORY PERIODS AND CONDUCTION VELOCITIES

C. A. CHAPMAN and J. S. YEOMANS*

Department of Psychology, University of Toronto, Toronto, Canada M5S 1A2

Abstract—Double-pulse methods are used here to measure the refractory periods and conduction velocities of the pyramidal tract axons which cause forelimb flexion in pentobarbital anesthetized rats. In the refractory period experiments, conditioning and test pulses were delivered to the motor cortex, the ipsilateral internal capsule, or the ipsilateral pyramid, and the maximum force exerted by the contralateral forelimb was measured at various conditioning–test intervals. The movements increased as conditioning–test interval increased from 0.5 to 1.0 ms in pyramid sites, from 0.6 to 1.5 in internal capsule sites, and from 0.6 to 2.0 ms in surface cortical sites, suggesting longer refractory periods for the substrates at more rostral sites. In cortical sites, as the conditioning–test interval increased from 4.0 to 20.0 ms, the movements decreased gradually to the single-pulse level, suggesting decreasing temporal summation at longer conditioning–test intervals.

In the collision experiments, when conditioning pulses were delivered to one site and test pulses to a second site, the movements increased at conditioning–test intervals that were longer by 0.5–1.3 ms than the refractory periods in either site. This suggests that collisions occurred between orthodromic and antidromic action potentials in the pyramidal tract axons responsible for the limb movement. The collision-like increase was greater between internal capsule and pyramid than between cortex and pyramid, or between cortex and internal capsule. The estimated conduction times were 0.9–1.5 ms between cortex and pyramid, 0.4–0.8 ms between cortex and internal capsule, and 0.5–0.8 ms between internal capsule and pyramid. The range of conduction velocities, therefore, was quite narrow between all pairs (8.8–16.8 m/s). The largest pyramidal tract axons appear to be responsible for most of the force of forelimb flexion in pentobarbital anesthetized rats.

The pyramidal tract has been the most exhaustively studied efferent pathway of the motor cortex in the rat,[3,5,10,21,24,33,44] but the relative contributions of fast and slower fibers to electrically evoked forelimb movements is not clear. The range of conduction velocities in pyramidal tract axons has been measured directly by observing the antidromic latencies of unit and population responses in motor cortex following stimulation of the pyramidal tract.[27,28] Antidromic latencies range predominantly between 0.9 and 3.6 ms.[14,20,40] These studies indicate that conduction velocities of rat pyramidal tract axons range between approximately 4 and 16 m/s, and that the large majority of axons conduct at velocities under 12 m/s.

Much higher estimates of 60 and 67 m/s for the fastest conduction velocities in rat pyramidal tract axons have been obtained by stimulating the motor cortex and measuring the latency of unit and population fiber responses in the spinal cord.[8,9] Using similar methods, however, Stewart *et al.* estimated conduction velocities which ranged between 5 and 18 m/s, and suggested that the unusually fast conduction times observed in the earlier studies may have been due to recruitment of fast reticulospinal axons.[39]

Estimates of the number of non-myelinated axons in the rat pyramidal tract range from 53,000 to 140,000, and the diameters of these fibers range between 0.05 and 1.21 μm with a central tendency near 0.15 μm.[12,13,18,22,23] The diameters of the 100,000 or so myelinated fibers in the adult can be as large as 4 or 5 μm but most are under 1 μm.[3,12,13,18,22,23]

The importance of each of these different pyramidal tract populations to the evoked behavioral response is not yet determined. Although direct corticomotoneuronal connections and fibers with the fastest conduction times likely play an important role in limb movement,[8,24] the quantitative contributions of slower conducting fibers have been more difficult to evaluate.

Double-pulse stimulation is used here to estimate the refractory periods and conduction velocities of the axons mediating forelimb flexion evoked by stimulation of rat pyramidal tract. First, conditioning and test pulses are delivered via one electrode (Fig. 1, top). The number of action potentials doubles when the conditioning–test interval increases from below to above the refractory periods of the directly stimulated axons. Any response that is sensitive to a doubling

*To whom correspondence should be addressed.
Abbreviations: EMG, electromyograph.

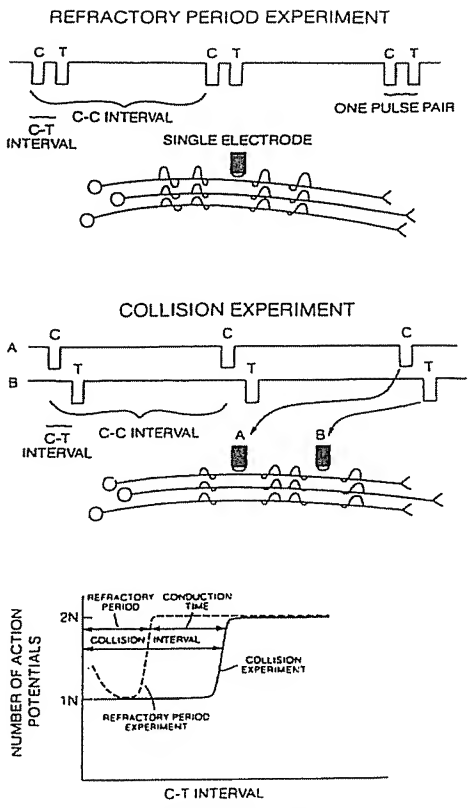

Fig. 1. Refractory period and collision models. In the refractory period experiment (top), conditioning (C) and test (T) pulses are delivered through a single electrode. In the collision experiment (middle), conditioning pulses are delivered through one electrode (A) and test pulses are delivered through the second electrode (B). The total number of action potentials evoked in a bundle of axons in each experiment is shown schematically as a function of conditioning–test interval (bottom). N = number of axons. The conduction time between the two electrodes is estimated by subtracting the refractory period from the collision interval.

in the number of action potentials will, therefore, increase as the conditioning–test interval increases from below to above the refractory periods. This method has been used to estimate the refractory periods of the axons responsible for many electrically evoked behaviors.[7,15,46,48,54,55] Since the refractory periods are estimated by the behavioral response, the importance of each refractory period group to the response is estimated.

Next, conditioning pulses are delivered via one electrode and test pulses via the second electrode (Fig. 1, middle).[37,55] If the same axons are excited by both electrodes, then antidromic action potentials from the downstream electrode will collide with orthodromic action potentials from the upstream electrode at short conditioning–test intervals. A doubling in the number of action potentials in the axons excited by both electrodes will occur when the conditioning–test interval is increased to above the collision intervals of the axons. If the response is due to continuous axons passing between the two electrodes, an increase in response intensity is observed as conditioning–test interval is increased from below to above the collision interval (Fig. 1, bottom).

In this experiment, then, the refractory periods of the substrates mediating forelimb flexion were measured in motor cortex, internal capsule and pyramid. Collision tests were also performed and the conduction times between these sites were estimated by subtracting the refractory periods from the collision intervals. The results indicate that the fastest pyramidal tract axons produce most of the forelimb flexion response. Part of this work has been presented previously.[50]

EXPERIMENTAL PROCEDURES

The monopolar stimulating electrodes were stainless steel, and insulated with Epoxylite. The hemispherical exposed tips were 60 μm in diameter in pyramid or internal capsule, and 100 μm in diameter in cortex. The ground electrode was attached to an ear bar of the stereotaxic instrument.

Male rats (Long–Evans, Charles River) weighing between 298 and 511 g were anesthetized with 60 mg/kg sodium pentobarbital i.p. and with 0.1 cc atropine sulphate. To maintain anesthesia level, a steady dose of 0.133 mg/min of sodium pentobarbital was infused i.v. via a Harvard Apparatus compact syringe pump, Model 975,[32] or in a few animals, by 10% i.p. booster doses.

The head of the animal was placed in a stereotaxic instrument and the body supported in the horizontal plane. The body temperature of the animal was monitored with an internal probe and maintained near 37°C with a heating pad. Warmed mineral oil was applied to the exposed dura. A thin wire was wrapped snugly around the wrist of the forelimb and connected via a length of 2–3 cm to a Grass Force/Displacement transducer (Model no. FT.03, isometric) placed below the wrist. The elbow was set at an angle of about 90°, so that elbow flexions would raise the transducer beam vertically. The elbow was not fixed in place, however. Although elbow flexions appeared to account for most of the force, shoulder movements also contributed to the response in many cases. These vertical wrist movements are, therefore, simply called "forelimb flexions". The transducer responses and constant current stimuli were monitored on a Tektronix 5223 digital oscilloscope. The peak displacement of the voltage signal in the 50 ms following the stimulation was measured.

The electrodes in cortex were placed near the large representation of the contralateral forelimb in motor cortex,[11,26] usually about 1.5–2.5 mm lateral to the midline at bregma. Only sites where reliable contralateral wrist displacements in the vertical direction could be evoked were studied further. After locating an effective cortical site, a second electrode was placed in the internal capsule or pyramid. Alternatively, electrodes were placed in the internal capsule and pyramid.

A Grass S88 stimulator delivered monophasic pulses of 0.2 ms duration through constant-current photoelectric stimulation-isolation units. Cathodal stimuli were applied to pyramid (40–520 μA) and internal capsule sites (110–360 μA). Epidural anodal stimuli (500–6000 μA) were applied to the motor cortex.[17]

Refractory period experiments

Stimuli were delivered as trains of four single pulses, each pulse spaced by 5 ms, or as four paired pulses (four conditioning and four test pulses) with the conditioning pulses spaced by 5 ms and the test pulses presented at a conditioning–test interval in the range from 0.3 to 2.5 ms. To begin, the vertical electrode placement and current level was set so that the single-pulse condition would evoke a

response amplitude of roughly 5 g. Then, a conditioning–test interval was chosen at random and the response was measured. A period of at least 20 s without stimulation preceded each trial. All conditioning–test intervals and at least two single-pulse trials were tested in this way to generate a complete replication ($n = 1$). Several such replications were completed in at least four different rats for each electrode orientation. In addition, in five cortical sites, only one conditioning pulse and one test pulse were delivered at conditioning–test intervals of 0.3–20 ms.

Previous refractory period studies have shown that response amplitude measures can be limited by floor and ceiling effects.[46] Floor effects occur when some action potentials are evoked in a response-relevant pathway, but no response is elicited. Ceiling effects occur when the magnitude of a strong behavioral response is not increased when the number of action potentials evoked is increased. Threshold measures, especially frequency threshold measures, are therefore theoretically preferable.[46] Single-pulse response levels of forelimb flexion were chosen so that neither floor nor ceiling effects were apparent in the range of evoked response amplitudes studied, i.e. response levels increased smoothly as the number of stimulation pulses increased from four to eight. To compare between different sites, response amplitudes were then normalized, as described in the results section.

Collision experiments

In the collision experiments, four conditioning pulses were delivered to one site and four test pulses were delivered to a second site, with conditioning–conditioning intervals of 5.0 or 10.0 ms and conditioning–test intervals that varied from 0.3–2.5 or 5.0 ms. Collision tests were performed between cortex and internal capsule, cortex and pyramid, and internal capsule and pyramid. Only collision tests between cortex and pyramid required the use of conditioning–conditioning intervals of 10.0 ms. For each combination of sites, separate collision tests were conducted in which the electrode to which conditioning and test pulses were delivered was reversed. In cortical sites epidural anodal stimulation was used for collision tests, while in internal capsule and pyramid sites cathodal stimulation was delivered. The currents were set at each site so that responses of roughly 5 g were obtained in single-pulse tests. Also, the response had to increase reliably by at least 2 g as the conditioning–test interval was increased from 0.3 to 2.0 ms before systematic testing began.

Conduction time estimates

Because the sites to which conditioning and test pulses were delivered were reversed in separate collision tests, it was possible to measure conduction times in both orthodromic and antidromic directions to test for symmetry in the collision data. When conditioning pulses are delivered to a rostral site and test pulses are delivered to a more caudal site (e.g. Fig. 1, middle), the collision interval is equal to the orthodromic conduction time between the electrodes plus the refractory period at the caudal site where the test pulses were delivered. Alternatively, when conditioning–test pulses are delivered to a caudal site the collision interval begins at conditioning–test intervals greater than the antidromic conduction time between the two electrodes plus the refractory period at the rostral site. To determine conduction times the refractory period for the site where test pulses were delivered was subtracted from the collision interval.

The difference between collision curves and refractory period curves was determined using the methods of Yeomans and Linney.[51] Since collision occurs in only some of the axons, while refractoriness occurs in all axons which fire, a problem results when attempting to compare the two curves: which part of the refractory period curve should the collision curve be compared with? Two methods were used for comparing refractory period and collision curves. First, the collision curves were matched to the initial rise in the refractory period curves by "zeroing" the collision curves (e.g. see Fig. 6). This was done by subtracting a zeroing constant from all normalized response amplitudes. The zeroing constant was the mean of all scores at conditioning–test intervals from 0.3 to 0.6 ms. Use of the zeroing method assumes that the axons producing collision are the axons with the shortest absolute refractory periods, and, indeed, short absolute refractory periods are correlated with low thresholds and fast conduction velocities.[29,41] This method, however, yields estimates of conduction velocity that are too low, since axons will not be recruited strictly in order of their refractory periods because the location of axons relative to the electrode is critical to the order of recruitment.

Second, in order to match the collision curves to the entire range of the refractory period curves, the response amplitudes for the zeroed curves were divided by the highest score at long conditioning–test intervals. Use of the "stretching" method assumes that the axons producing collision are an unbiased sample of the axonal population stimulated in refractory period tests, such that they have the same thresholds and absolute refractory periods. The axons producing collision cannot be an unbiased sample, though, because low threshold axons are more likely to be excited by both electrodes and to show collision.[51] The stretching method, therefore, yields estimates of conduction velocity which are too high. As the amount of collision which is observed increases, the estimates obtained from the zeroing and stretching methods converge. When incomplete collision is observed, however, the true range of conduction velocities must fall between the estimates obtained from the two methods, so that the average of the estimates obtained with the two methods is more accurate than either estimate alone.

The conduction times were measured at 20, 50 and 80% of the amplitude range of both zeroed and stretched collision curves to yield measures of the fastest, average, and slowest fibers, respectively.[51] For both zeroing and stretching methods, the orthodromic and antidromic conduction times were averaged at each of the three levels. The three conduction time estimates obtained using the zeroing procedure were then averaged with the three estimates obtained using the stretching procedure.

Conduction distances for the calculation of conduction velocities between sites were measured from the locations of electrodes along the length of the curved path from the motor cortex at bregma, through the internal capsule and pyramidal tract.[31]

Histology

Electrode tracts through the medulla were examined in Thionin-stained brain sections from eight rats where evidence of collision was obtained. In all eight, the behaviorally effective electrode tracks were found to pass through the pyramid (range, 9.8–11.3 mm posterior to bregma, and 0.24–0.84 mm lateral to the midline). All eight behaviorally effective electrode tracks through the diencephalon were found between 3.1 and 3.8 mm behind bregma, between 2.6 and 3.3 mm lateral to the midline and 7.8–8.6 mm ventral to the bregma-lambda line, all within the borders of the internal capsule.[31] Histological analyses of the cortical placements were not performed.

RESULTS

Pyramid stimulation

In preliminary mapping studies, startle-like bilateral movements of shoulders and limbs were evoked 2 mm dorsal to the pyramids.[6,54] Ipsilateral forelimb flexions were evoked near the pontine-medullary border immediately dorsal and lateral to the pyramid. The

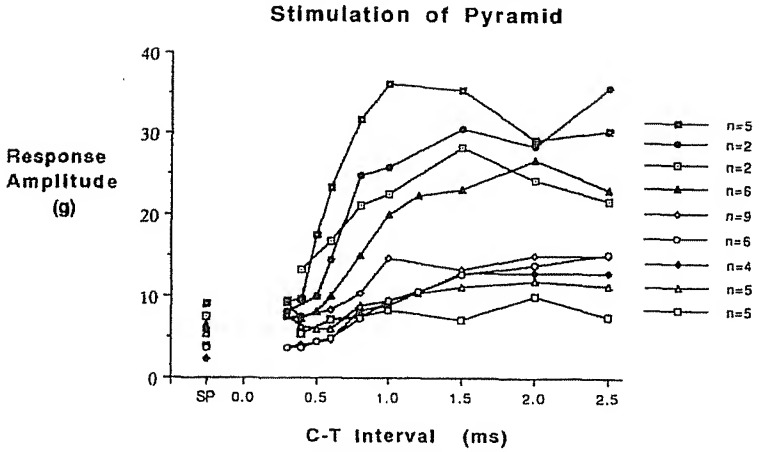

Fig. 2. The peak amplitude in grams of the forelimb flexion response following stimulation of the pyramid is shown as a function of conditioning–test (C–T) interval in the refractory period experiment. Each line represents the mean of two to nine observations at each conditioning–test interval obtained from a single stimulation site. SP indicates mean response amplitudes observed in each site in the single pulse condition where conditioning pulses were delivered without test pulses.

lowest threshold contralateral forelimb flexions were obtained in the middle of the pyramid (0.3–1.0 mm lateral) at currents of 40–100 μA.

A minimum of two or three pulses was required to evoke a contralateral response at currents below 500 μA, as reported previously by Bannister and Porter.[1] For double-pulse studies, therefore, four pulse pairs were delivered. Currents of 40–400 μA were used, with most in the 40–70 μA range.

At conditioning–test intervals of 0.3 and 0.4 ms, the observed responses were almost identical to the responses observed in single-pulse conditions. As conditioning–test interval increased from 0.5 to 1.0 ms, response amplitudes increased sharply. As conditioning–test interval increased from 1.0 to 2.5 ms, response amplitudes increased very little. This overall pattern was seen in all nine rats (Fig. 2).

The difference between single-pulse and peak double-pulse responses varied considerably in different animals. At conditioning–test intervals above 1.0 ms, the test pulses increased the response over single-pulse levels by as little as 118% in one site, and by as much as 453% in another site. For the purposes of comparing across animals, the data were normalized so that the mean single-pulse response (R_{sp}) for each replication was taken as 0 and the peak response (R_p) for that replication at any conditioning–test interval above 0.4 ms was taken as 1.0, using the formula:

$$\text{Normalized response amplitude} = \frac{R_{ct} - R_{sp}}{R_p - R_{sp}},$$

where R_{ct} is the response at a given conditioning–test interval. Setting R_p at conditioning–test intervals above 0.4 ms was done so that refractory period data would not be altered by local potential summation effects at conditioning–test intervals of 0.3 and 0.4 ms, which are site-dependent.[46] The mean normalized response amplitudes at each conditioning–test interval are shown in Figs 3–5.

Figure 3A shows the means and standard errors of normalized response amplitude at each conditioning–test interval in nine pyramid sites, one site per rat ($n = 44$ at all conditioning–test intervals except 0.3, 0.5, 1.2 ms, where $n = 24$). The normalization procedure greatly reduced the standard errors. The scores were not markedly different from the single-pulse level at conditioning–test intervals from 0.3 to 0.5 ms, rose steeply as conditioning–test intervals increased from 0.5 to 1.0 ms, and rose only slightly at longer conditioning–test intervals. The highest mean scores were always below 1.0 because R_p occurred at different conditioning–test intervals in different tests.

Internal capsule stimulation

The currents required to evoke reliable responses in internal capsule sites varied from 120 to 360 μA using four pulses at conditioning–conditioning intervals of 5 ms. A minimum of two pulses was required for a response. When test pulses were added (Fig. 3B), the normalized response amplitudes declined to close to single-pulse levels as conditioning–test intervals increased from 0.3 to 0.5 ms. At conditioning–test intervals shorter than the refractory periods, local potential summation can add action potentials.[7,48,52] That is, in neurons not quite excited by the conditioning pulses, conditioning pulses can evoke subthreshold, local potentials that decay within a few tenths of a millisecond. When test pulses are presented before the decay is complete, summation may occur, resulting in additional action potentials. In Fig. 1 (bottom) the added excitation due to local potential summation is shown as a declining dashed curve at conditioning–test intervals inside of the refractory period.

The scores increased sharply as conditioning–test intervals increased from 0.6 to 1.5 ms ($n = 35$ at all conditioning–test intervals except 1.2 ms where $n = 24$). As compared to pyramid sites, the rise in scores in internal capsule sites occurred at condition-

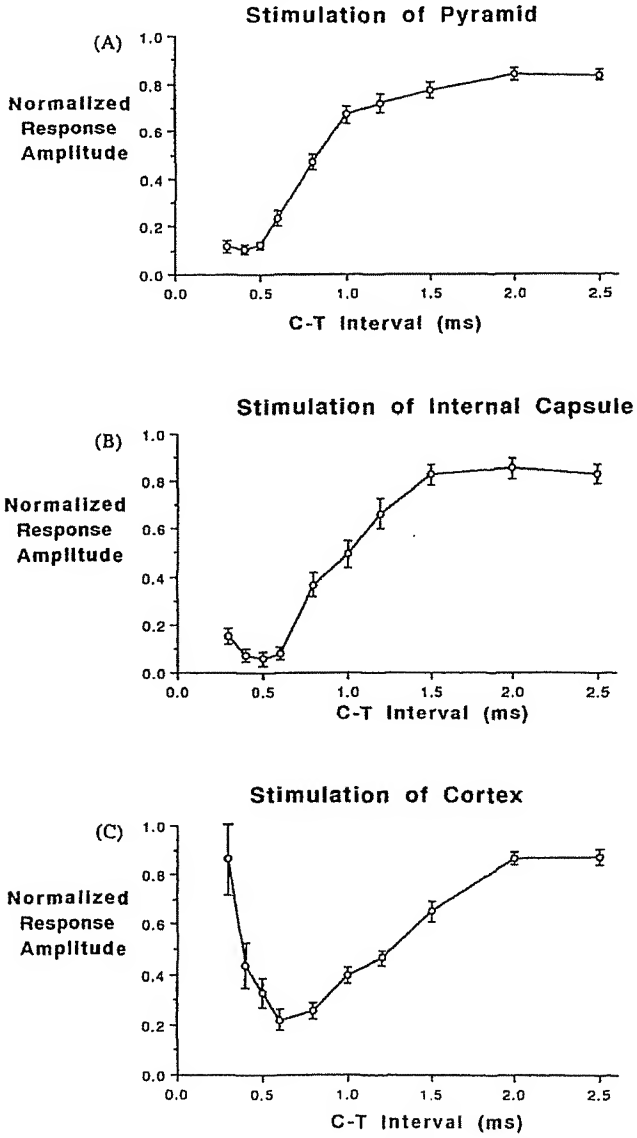

Fig. 3. Normalized response amplitudes for refractory period experiments are shown as a function of conditioning–test (C–T) interval. All responses are shown as a proportion of the maximum increase in the response above the single-pulse condition. Bars indicate standard errors of the mean. (A) In pyramid sites, the recovery from refractoriness occurred mainly at conditioning–test intervals from 0.5 to 1.0 ms. These normalized data are based on the raw data shown in Fig. 2. (B) In internal capsule sites, the recovery from refractoriness occurred at conditioning–test intervals of 0.6–1.5 ms. (C) In motor cortex sites, the recovery from refractoriness occurred at conditioning–test intervals from 0.6 to 2.0 ms.

ing–test intervals that were longer by about 0.1 ms over most of the curve.

Motor cortex stimulation

In motor cortex sites, the currents required to evoke reliable responses following a four-pulse train of epidural anodal stimulation ranged from 1080 to 2500 μA. Although only one pulse was required to produce a forelimb flexion in cortical sites, four pulse-pairs were used in most sites to be comparable to the studies of the internal capsule and pyramid. Stimulation with only one pair was used in five cortical sites primarily to test the effects of stimulating at long conditioning–test intervals.

When four pairs of pulses were delivered the normalized response amplitude declined at conditioning–test intervals from 0.3 to 0.6 ms. Normalized response amplitudes were much higher on average and much more variable in cortex sites at these short conditioning–test intervals than in either internal capsule or pyramid sites, consistent with greater local potential summation.

Response amplitudes rose at conditioning–test intervals from 0.6 to 2.0 ms when pulses were delivered to the cortex, suggesting that these substrates include populations of cells with longer refractory periods in cortex than in either of the pyramidal tract sites (Fig. 3).

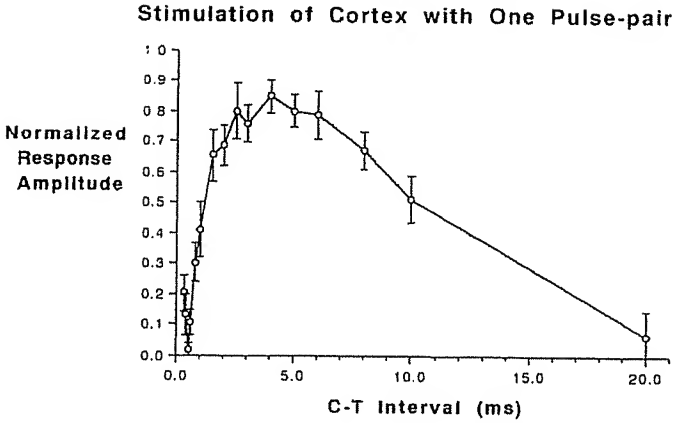

Fig. 4. Epidural stimulation of cortex sites using only one anodal pulse pair. The recovery occurred at conditioning–test (C–T) intervals from 0.5 to 4.0 ms, and the effect of the test pulses gradually declined at conditioning–test intervals longer than 4.0 ms.

When only one anodal pulse-pair was delivered to the dura surface, currents from 1220 to 6000 μA were required, with 6000 μA required in two of five sites ($n = 12$–14). At conditioning–test intervals from 0.6 to 2.5 ms, the results (Fig. 4) were similar to the four-pulse pair experiment (Fig. 3). Scores increased slightly between conditioning–test intervals of 2.5 and 4.0 ms. As conditioning–test intervals increased from 4.0 to 20 ms, normalized response amplitudes decreased steadily in a curve that is closer to linear than exponential. The test pulses were completely ineffective at a conditioning–test interval of 20 ms: Two separate movements were observed, so that the maximum response was no greater than the response to a single pulse.

Collision experiments

When the conditioning and test pulses were delivered via separate electrodes, the results were different from the single-electrode results in three ways for all six collision tests (Fig. 5). First, there were no reliable changes in normalized response amplitudes at conditioning–test intervals from 0.3 to 0.6 ms. The normalized response amplitudes at these conditioning–test intervals were reliably greater than the single-pulse level, however. Second, the rises occurred at conditioning–test intervals that were longer than in the refractory period experiment by 0.5 to 1.3 ms. Third, the normalized response amplitudes were near maximum at the longest conditioning–test intervals (which were 2.0 and 2.5 ms, except for the tests between cortex and pyramid, where the scores were near maximum at conditioning–test intervals from 2.5 to 5.0 ms). These results are all consistent with the axonal collision model of Shizgal *et al.*[37]

The greatest increase in normalized response amplitude (about 0.67) occurred when testing between internal capsule and pyramid (Fig. 5A). All scores were between 0.15 and 0.30 at conditioning–test intervals from 0.3 to 1.0 ms, and all scores were between 0.80 and 0.88 at conditioning–test intervals of 2.0 and 2.5 ms. Sharp increases occurred as conditioning–test intervals increased from 1.0 to 2.0 ms, with 0.50 of the rise occurring as conditioning–test intervals increased from 1.0 to 1.5 ms. Therefore, most of the collision effect is due to axons with a narrow range of conduction velocities. The two collision curves rose at very similar conditioning–test intervals except for small differences at conditioning–test intervals between 0.5 and 1.0 ms.

In collision tests between cortex and internal capsule (Fig. 5B), the rise in normalized response amplitude was about 0.44 at conditioning–test intervals from 0.8 to 2.0 ms. At conditioning–test intervals from 0.3 to 0.8 ms, all scores were between 0.4 and 0.5, suggesting incomplete collision. The rise occurred at slightly longer conditioning–test intervals when the conditioning pulses were presented to the internal capsule and the test pulses were presented to the cortex (1.0–2.0 ms), than when the conditioning pulses were presented to the cortex and the test pulses to the internal capsule (0.8–1.5 ms). The resulting difference in collision intervals of 0.2 to 0.35 ms was approximately equal to the difference in the refractory periods of the two sites.

When testing between cortex and pyramid, the normalized response amplitudes were between 0.20 and 0.40 at all conditioning–test intervals of 1.0 ms and shorter, but near 0.80 at all conditioning–test intervals 2.5 ms and longer (Fig. 5C). Therefore, normalized response amplitudes increased by about 0.53 on average at conditioning–test intervals of 1.0 to 3.0 ms. Recovery occurred at shorter conditioning–test intervals (1.0–2.5 ms) when the conditioning pulses were delivered via the cortical electrode, than when the conditioning pulses were presented via the pyramid electrode (1.5–3.0 ms). The approximately 0.4 ms difference in the collision intervals is similar to the difference in the refractory periods of the two sites.

Therefore, the collision effect was greater between the two pyramidal tract sites, than between the cortex and the internal capsule or between the cortex and the pyramid. Also, the collision effect was more

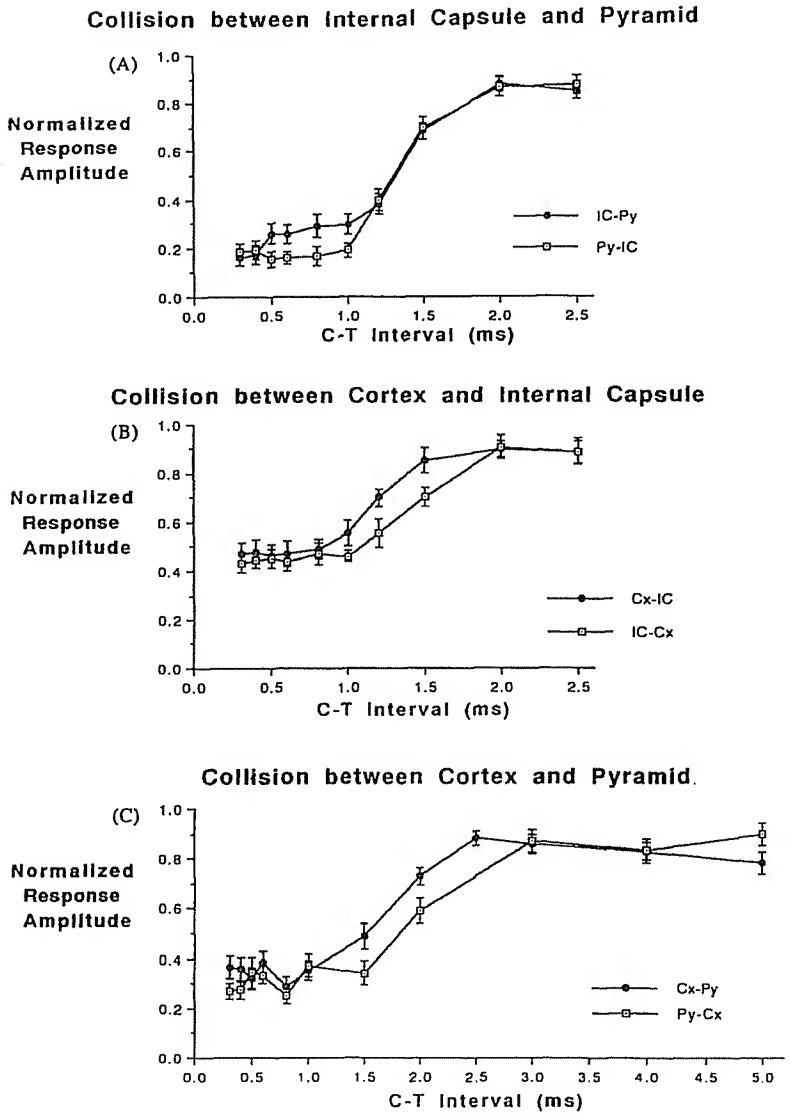

Fig. 5. Collision experiment results. Increases in normalized response amplitude occurred at longer conditioning–test (C–T) intervals (1.0–2.5 or 3.0 ms) in the collision experiments than in the refractory period experiments. (A) Collision between internal capsule and pyramid sites. "IC-Py" indicates results obtained when C pulses were delivered to the internal capsule and T pulses were delivered to the pyramid (eight sites, $n = 30$). "Py-IC" indicates the delivery of conditioning pulses to the pyramid and test pulses to the internal capsule (seven sites, $n = 23$). (B) Collision between cortex and internal capsule sites (three sites, $n = 10$ for both curves). "Cx-IC" indicates delivery of conditioning pulses to the cortex and test pulses to the internal capsule. "IC-Cx" indicates delivery of conditioning pulses to the internal capsule and the test pulses to the cortex. (C) Collision between cortex and pyramid sites. "Cx-Py" indicates that conditioning pulses were delivered to the cortex and test pulses to the pyramid (nine sites, $n = 32$ except at conditioning–test intervals 2.5 and above where $n = 22$). "Py-Cx" indicates delivery of conditioning pulses to the pyramid and test pulses to the cortex (five sites, $n = 18$). In collision tests involving stimulation of cortical sites, the collision intervals were longer when test pulses were delivered to the cortex than when they were delivered to the pyramidal tract sites.

symmetrical between internal capsule and pyramid than between the cortex and either of the pyramidal tract sites. The asymmetries in the collision effects involving the cortex were in the same direction: i.e. the collision curves rose at shorter conditioning–test intervals when the conditioning pulses were delivered to the cortex than when the conditioning pulses were delivered to a pyramidal tract site.

Conduction time estimates

The conduction times were estimated using the method of Yeomans and Linney.[51] As shown in Fig. 6, the collision curves were first "zeroed" to match the initial rise in the refractory period data, and then "stretched" to span the entire range of the stretched refractory period curves (see Experimental

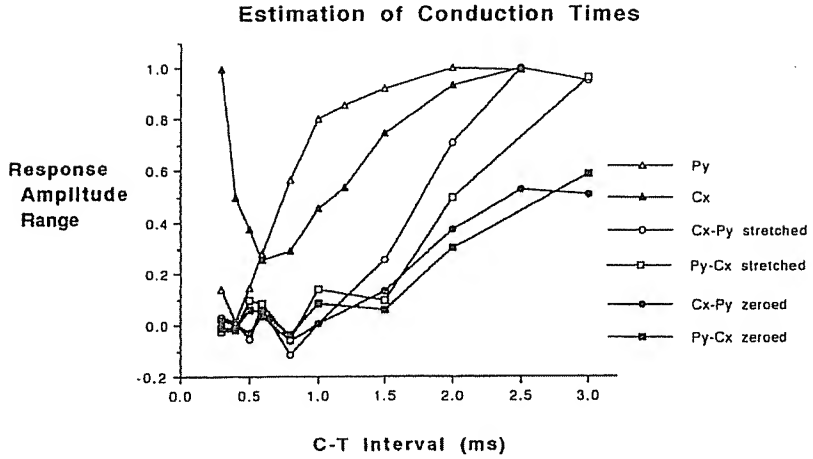

Fig. 6. An example of the procedure used for the estimation of conduction times. The collision data obtained between cortex and pyramid (see Fig. 5C) have been zeroed and stretched for comparison with the stretched refractory period data from the cortex (Cx) and the pyramid (Py). See Fig. 3, and the text for details. The labeling convention is the same as that used in Fig. 5. Conduction times were estimated according to the model in Fig. 1 by subtracting the refractory periods from both the stretched and zeroed collision intervals at 20, 50 and 80% of the response amplitude range. For each collision curve, the refractory period obtained from the site to which the test pulses were delivered was subtracted from the collision curve because it is this site which must recover from refractoriness before both conditioning and test pulses can result in behaviorally effective action potentials.

Procedures). Estimates of conduction time were taken at 20, 50 and 80% of the peak rise of both zeroed and stretched collision curves in both orthodromic and antidromic directions. Within the stretched and zeroed data, the orthodromic and antidromic conduction times were very similar, consistent with the symmetric conduction of action potentials in axons (Table 1).

For each combination of sites, the largest average of orthodromic and antidromic conduction times was always obtained from zeroed data at 80% of the response range. The shortest average conduction times were always obtained from stretched data at 20% of the response range. These averages of orthodromic and antidromic conduction times at each level form the basis of estimates of the range of conduction times between sites. Conduction time and conduction velocity estimates based on averages of the stretched and zeroed data at each level were also computed, and provide estimates of mean conduction times for the fastest, medium, and slowest fibers (Table 1).

Table 1. Conduction time and conduction velocity estimates

	Stretched			Zeroed			CV
	Ortho.	Anti.	Mean	Ortho.	Anti.	Mean	(m/s)
A. IC-Py							
80%	0.65	0.53	0.59	0.88	0.79	0.84	11.7
50%	0.61	0.55	0.58	0.73	0.62	0.68	13.2
20%	0.58	0.49	0.54	0.65	0.51	0.58	14.8
Mean	0.61	0.52		0.75	0.64		13.2
B. Cx-IC							
80%	0.36	0.17	0.27	0.72	0.88	0.80	13.2
50%	0.39	0.34	0.37	0.55	0.72	0.64	14.0
20%	0.35	0.48	0.42	0.43	0.60	0.52	14.9
Mean	0.37	0.33		0.57	0.73		14.0
C. Cx-Py							
80%	1.14	1.06	1.10	1.44	1.52	1.48	11.9
50%	1.02	0.88	0.95	1.16	1.18	1.17	14.4
20%	0.84	0.98	0.91	0.90	1.08	0.99	16.1
Mean	1.00	0.97		1.17	1.26		13.9

Conduction time and conduction velocity (CV) estimates were obtained from each of the three electrode configurations at 80, 50, and 20% of the response amplitude range for collision data that were both zeroed and stretched as in Fig. 6 (see text for details). Results are shown for electrode placements in internal capsule and pyramid (IC–Py), cortex and internal capsule (Cx–IC), and cortex and pyramid (Cx–Py). "Ortho." indicates orthodromic conduction times between the electrodes estimated from data in which C pulses were delivered to the rostral site. "Anti." indicates antidromic conduction times estimated from data in which C pulses were delivered to the caudal site.

Between internal capsule and pyramid sites, conduction times averaged between 0.54 and 0.84 ms at all levels. The conduction distances were estimated to range between 7.5 and 9 mm with an average of 8.3 mm. This results in conduction velocity estimates which range between 9.9 and 15.4 m/s. Between cortex and internal capsule, the estimated conduction times ranged between 0.42 and 0.80 ms. At an estimated conduction distance of 7.0 mm, conduction velocity estimates ranged between 8.8 and 16.7 m/s. Between cortex and pyramid, the estimated conduction times were 0.91–1.48 ms. For an estimated conduction distance of 15.3 mm, conduction velocity estimates were 10.3–16.8 m/s. The estimated conduction times bewteen the cortex and internal capsule, and between the internal capsule and pyramid sum to closely match the estimated conduction times between cortex and pyramid sites. In addition, the ranges of estimated conduction velocities obtained for each set of sites were very similar.

Comparisons of conduction times and electromyograph latencies

A more conventional way of estimating conduction times is by comparing electromyograph (EMG) latencies. We have compared these behaviorally estimated conduction times with latencies for biceps EMG activity in several animals following stimulation of the cortex, internal capsule and pyramid. This method of estimation is confounded in the rat pyramidal tract by the requirement that two stimulating pulses must be delivered to the pyramid or internal capsule, while only one pulse is required in cortex. Conduction times based on latency differences between cortex and internal capsule or pyramid were usually negative, therefore, and we did not find a useful way of relating biceps EMG latencies from cortex to those of pyramidal tract sites. EMG latency shortened with increasing current intensity, and asymptotic latencies for responses requiring more than one pulse ranged from 8.7 to 9.2 ms in pyramid and from 9.2 to 9.5 ms in internal capsule. High-threshold, bilateral, 4.3-ms latency responses could be evoked with one pulse in the pyramid at high currents, apparently due to stimulation of startle reflex pathways.[54] Differences in these latencies suggest conduction times of 0.3–0.5 ms between internal capsule and pyramid which are roughly similar to our shortest estimated conduction times using behavioral methods for these sites.

DISCUSSION

The collision model in Fig. 1 has been supported by several tests. First, single-unit recordings have shown that many directly stimulated units have refractory periods and collision intervals like the refractory periods and collision intervals estimated behaviorally using the collision model.[34,35,51,55] Second, behaviorally estimated refractory periods and collision intervals have been shown to change when the parameters of conditioning and test pulses are varied in ways predicted by the properties of axon bundles.[4,48,51,52,53] Third, refractory period estimates correlate well with conduction time estimates in systems mediating self-stimulation and electrically evoked turning,[48,55] consistent with the properties of axons.[29,41]

The forelimb movements observed here at various conditioning–test intervals changed in ways which are consistent with the axonal refractory period and collision models. The results support the idea that the refractory periods and conduction velocities of the pyramidal tract axons mediating forelimb flexion in rats can be estimated with this method.

Pyramidal tract refractory periods

The forelimb flexion responses observed here appear to result primarily from the recruitment of substrates in the pyramid. This is suggested by the low currents, contralateral responses and electrode sites in the middle of the pyramid. Since no cells or synapses are located in the pyramid, the responses must be due to recruitment of pyramidal tract axons, but not necessarily corticospinal axons.

The increase in the responses as conditioning–test intervals increased from 0.5 to 1.0 ms, suggests that the pyramid axons mediating contralateral forelimb flexion in rats have refractory periods between 0.5 and 1.0 ms. Because identical conditioning and test pulses were used, relative refractory periods may have contributed as well as absolute refractory periods.[47,51] The minimal rise at conditioning–test intervals above 1.0 ms, and the slight local potential summation at conditioning–test intervals of 0.3–0.4 ms, however, suggest that relative refractory period contributions were small. The short absolute refractory periods which are indicated suggest that moderate caliber myelinated axons mediate this response.[16,29,41]

Internal capsule refractory periods

Again, the location of electrode tips and the low currents used suggest that internal capsule axons are the substrates for the observed responses, although some cells and synapses are found within the internal capsule at this level (especially the entopeduncular and subthalamic nuclei). The range of refractory periods observed in internal capsule sites (0.6–1.5 ms) was slightly longer than in the pyramid. This suggests that the substrates mediating forelimb flexion in these sites include some axons which have smaller diameters than those at the level of the pyramid.

Cortical refractory periods

The very high currents used for epidural stimulation of the motor cortex make it difficult to localize the substrates which mediated forelimb flexion in these sites. High currents were required to evoke responses that matched those which were evoked in internal capsule or pyramid at much lower intensities. Since the primary aim of this first double-pulse study

was to obtain a maximum of collision, spatial resolution in cortex (which has been extensively studied in many previous works) was sacrificed. Consequently, striatal as well as distal cortical substrates are likely to have been stimulated by the high currents used.

The sharp decline in the refractory period data at conditioning–test intervals from 0.3 to 0.6 ms is consistent with declining local potential summation in axons[52] (Fig. 3C). The speed of this decline in the behavioral data suggests that short time-constant substrates (about 0.1 or 0.2 ms), such as axons, may be responsible for this effect. The time constants of cortical pyramidal cell bodies (3–15 ms in cats)[42] are much longer. The larger standard error bars at conditioning–test intervals of 0.3–0.5 ms are consistent with the local potential summation interpretation of the sharp decline in response amplitude at these intervals. If an electrode is not placed in the center of the substrates which mediate an electrically evoked response, then more local potential summation will result because of the larger contribution of substrates in the "subliminal fringe".[46,52] This can result in large between-animal differences in local potential summation due to the differing geometric distribution of substrates around the electrode. These factors should not contribute as strongly to variability in refractory period data, and standard error bars are much smaller in the refractory period range of conditioning–test intervals.[46]

The rise in the curves at conditioning–test intervals from 0.6 to 2.0 ms suggests that the substrates near motor cortex mediating forelimb flexion in rats have refractory periods between 0.6 and 2.0 ms (Fig. 3C). The results for one pulse-pair and four pulse-pair experiments at these conditioning–test intervals were very similar, so the rise at conditioning–test intervals between 0.6 and 2.0 ms is not frequency-dependent up to 200 Hz (i.e. the four-pulse experiment). It is more likely, then, that the fast rise from 0.6 to 2.0 ms is an axonal refractory period effect, rather than a synaptic summation effect. Relative refractory period effects, however, could contribute to a larger degree in the cortex and internal capsule than in pyramid sites.

In the one pulse-pair experiment, a slight further rise occurred as conditioning–test interval increased from 2.5 to 4.0 ms (Fig. 4). Previous authors have shown that pyramidal tract neurons are activated both directly and synaptically, or "indirectly", by cortical stimulation.[19,30,39] The late rise in the one pulse-pair experiment may reflect recovery from synaptically elicited action potentials in cortex,[19,30,49] which occur at roughly this latency in rats.[39]

The directly stimulated substrates mediating electrically evoked limb movements in cortex could be interneurons, output neurons, or both. The collision data, and in particular, the symmetric conduction times, suggest that direct activation of pyramidal tract neurons is more important for the response we observed than synaptically elicited action potentials. Therefore, the later rise in the refractory period curves in cortex than in pyramidal tract sites is likely due to longer absolute and/or relative refractory periods of these output neurons in cortex compared to their distal axons in internal capsule and pyramid. Refractory periods that are still longer have been estimated behaviorally in awake rats for medial prefrontal cortex and cingulate cortex sites mediating self-stimulation (1–8 ms),[36,38] and in anteromedial frontal cortex sites mediating circling (0.6–4 ms).[43]

The declining effect of test pulses at long conditioning–test intervals (4.0–20.0 ms) in the one pulse-pair experiment is attributable to declining temporal summation in follower cells (perhaps spinal motoneurons). The decline in temporal summation occurred more slowly, and less exponentially than in the reticulospinal pathway mediating the startle reflex in rats[54] or the monosynaptic hindlimb stretch reflex in cats.[25] This may reflect the additional contribution of extra synapses in the cortex or spinal cord.[8,26]

Fehlings *et al.*[9] have recorded evoked potentials in the sciatic nerve following two-pulse stimulation of the surface of the sensorimotor cortex of two rats. They found an electrical response to the test pulse beginning at conditioning–test intervals of 0.5 or 0.6 ms and reaching a peak at a conditioning–test interval of 2.0 ms, similar to the present data. It is not clear whether their response was due entirely to the pyramidal tract, however, since the response was decreased but not eliminated by severing the dorsal columns, and the maximum conduction velocity of the D-wave response was 67 m/s.

Collision experiments

There was no evidence of local potential summation at short conditioning–test intervals in any of the collision tests, consistent with the collision model of Fig. 1. The largest collision effects (65%) were obtained between internal capsule and pyramid sites suggesting that forelimb flexion responses are due mainly to continuous pyramidal tract axons which connect these two sites. The collision effects between motor cortex and either of the pyramidal tract sites were also large (44 and 53%), although smaller than between the two pyramidal tract sites (Fig. 5). This indicates that many, but not all, of the action potentials mediating forelimb flexion were blocked by collisions between these sites at short conditioning–test intervals. Therefore, axons which pass between cortex and internal capsule and between cortex and pyramid (most of these being the same axons) are responsible for much of the contralateral flexion evoked from either cortex or pyramidal tract sites.

The failure to obtain complete collision is seen in the non-zero normalized response amplitudes at conditioning–test intervals from 0.3 to 0.8 ms (Fig. 5). These failures could result from (i) misalignment of the electrodes relative to the same pyramidal tract axons; (ii) activation of a separate population of non-pyramidal tract axons during cortical stimulation,

possibly including striatal substrates; and/or (iii) activation of indirect as well as direct action potentials in cortex,[19,30] only one of which can be blocked by each antidromic action potential. If misalignment of electrodes is a factor it is likely to be due to cortical placements because collision effects between cortex and either pyramidal tract site were smaller than the collision effect between the two pyramidal tract sites. Since large currents were used in cortex, these misaligned substrates must be very distal from the electrodes, perhaps in the somatosensory cortex, or subcortical structures. Misalignment may contribute to incomplete collision, but cannot explain why stimulation of the cortex requires only one pulse, while stimulation of the pyramidal tract requires at least two pulses. Hypotheses ii and iii above both explain why collision effects between the two pyramidal tract sites were larger, and why cortex stimulation requires only one pulse, by suggesting that more action potentials are always evoked in cortex (either via a non-pyramidal pathway or via the same axons). Indirect action potentials should produce collisions at longer conditioning–test intervals, however, and these were not evidenced in the collision experiment between cortex and pyramid.

Conduction times

In the collision experiment between internal capsule and pyramid the majority of the rise in the collision curves occurred at almost identical conditioning–test intervals, whether conditioning pulses were delivered to the internal capsule or to the pyramid (Fig. 5A). The collision intervals were mainly from 1.0 to 2.0 ms for both tests, and these intervals were 0.5–0.8 ms longer than the refractory periods in both sites. Therefore the conduction times between these sites range from 0.5 to 0.8 ms.

In both collision experiments involving stimulation of cortex sites there was an asymmetry in the collision effects, and longer collision intervals were observed when the test pulses were delivered to the cortex. These longer collision intervals are due to the longer refractory periods of the cortical substrates relative to those observed in either pyramidial tract site. The estimates for orthodromic and antidromic conduction times agreed closely within each experiment because differences in collision intervals closely paralleled differences between the cortical and pyramidal tract refractory periods.

Conduction times between cortex and internal capsule ranged between 0.4 and 0.8 ms. The sum of the conduction times between cortex and internal capsule and between the internal capsule and the pyramids (0.5–0.8 ms) closely matched the estimated conduction time between cortex and pyramid sites (0.9–1.5 ms). In addition, the resulting estimated ranges of conduction velocities were very similar (8.8–16.8 m/s), and suggest that a population of fibers with a narrow range of conduction velocities mediate these electrically evoked forelimb movements.

Contributions to response amplitude of fibers which conduct at velocities under approximately 4–5 m/s may have been minimal since, for example, cortically evoked action potentials carried by these fibers likely reach motoneuron pools upwards of 6 ms later than the fastest conducting components of the volley. The temporal dispersion of action potentials in the evoked volley due to the distribution of conduction velocities may lead to poor summation of EPSPs evoked by the slowest fibers in producing movement. Our data suggest, however, that the slowest fibers mediating electrically evoked forelimb flexion conduct at velocities of at least 8 m/s; velocities well above those for which poor summation is expected.

Conduction velocities and fiber diameters

These behaviorally measured conduction times are consistent with conduction times for motor cortex units driven antidromically by stimulation of rat pyramid.[14,20,40] For example, of the 1667 pyramidal tract cell latencies recorded by Stone,[40] 0.5 ms was the shortest conduction time, and only about 10% had latencies shorter than 1.2 ms. Evoked potentials indicate that the fastest corticospinal axons conduct at 18 m/s.[39] If the constant relating conduction velocity to fiber diameter is taken to be 4.7,[16,45] then fibers 1.9–3.6 μm in diameter are responsible for the collision results. Less than 10% of pyramidal tract fibers are this large.[13]

Our data therefore suggest that the forelimb flexion response measured here is due primarily to some of the fastest conducting axons in the pyramidal tract which correspond to the largest myelinated fibers in the pyramids. Both refractory period and conduction velocity data suggest that a small, homogeneous part of the heterogeneous population of axons in pyramid is responsible for most of the flexion observed.

Behavioral estimates of axonal properties can be contaminated, in some systems, by downstream factors between the directly stimulated axons and the response, such as synaptic summation,[54] or possibly muscles and response measurement devices. These downstream effects, however, should be the same in the refractory period and collision experiments when the same axons are stimulated by both electrodes. Therefore, conduction time estimates should not be affected by these downstream factors, and must be due to the conduction times of the behaviorally effective axons between the two electrodes.[2,55]

While EMG latencies can be useful for estimating the conduction times of the fastest of the central axons mediating a muscular response, collision tests are preferable for determining the distribution of conduction times weighted in terms of their behavioral effect (in this case, flexion force). The collision tests described here have also shown that the electrodes were aligned with the same response-evoking axons, so that the estimates of conduction times between two sites are due to the activation of many of the same pyramidal tract axons. The rough agreement between

these two methods in the present experiment with regard to the fastest conduction times, supports the hypothesis that the same pyramidal tract axons were used, and that the force is produced in part by the biceps muscle.

CONCLUSIONS

Forelimb flexions evoked by motor cortex or pyramidal tract stimulations in pentobarbital anesthetized rats are due primarily to the fastest pyramidal tract axons. These axons were found to have conduction velocities of roughly 9–16 m/s between cortex and pyramid. The refractory periods were shortest in pyramid (0.5–1.0), and longer in internal capsule (0.6–1.5) and cortex (0.6–2.0 ms). The collision effect was greatest between pyramid and internal capsule, but still strong between motor cortex and either internal capsule or pyramid, suggesting that continuous axons between cortex and pyramids were responsible for most of the effect.

Acknowledgements—Supported by NSERCC grant A7077 to J.Y. We thank Arthur Pennington and Karen Buckenham for technical assistance on this project.

REFERENCES

1. Banister C. M. and Porter R. (1967) Effects of limited direct stimulation of the medullary pyramidal tract on spinal motoneurons in the rat. *Expl Neurol.* **17,** 265–275.
2. Bramwell J. C. and Lucas K. (1911) On the relation of the refractory period to the propagated disturbance in nerve. *J. Physiol., Lond.* **42,** 495–518.
3. Brown L. T. (1971) Projections and termination of the corticospinal tract in rodents. *Expl Brain Res.* **13,** 432–450.
4. Buckenham K. and Yeomans J. S. (1993) An uncrossed tectopontine pathway mediates ipsiversive circling. *Behav. Brain Res.* **54,** 11–22.
5. Davidoff R. A. (1990) The pyramidal tract. *Neurology* **40,** 332–339.
6. Davis M. (1984) The mammalian startle response. In *Neural Mechanisms of Startle Behavior* (ed. Eaton R. C.), pp. 287–351. Plenum, New York.
7. Deutsch J. A. (1964) Behavioral measurement of the neural refractory period and its application to intracranial self-stimulation. *J. comp. Physiol. Psychol.* **58,** 1–9.
8. Elger C. E., Speckman E.-J., Caspers H. and Janzen R. W. C. (1977) Cortico-spinal connections in the rat. I. Monosynaptic and polysynaptic responses of cervical motoneurons to epicortical stimulation. *Expl Brain Res.* **28,** 385–404.
9. Fehlings M. G., Tator C. H., Linden R. D. and Piper I. R. (1988) Motor and somatosensory evoked potentials recorded from the rat. *Electroencephal. clin. Neurophysiol.* **69,** 65–78.
10. Ferrier D. (1886) *The Functions of the Brain.* Smith Elder, London.
11. Gioanni Y. and LaMarche M. (1985) A reappraisal of rat motor cortex organization by intracortical microstimulation. *Brain Res.* **344,** 49–61.
12. Gorgels T. G. M. F. (1990) A quantitative analysis of axon outgrowth, axon loss, and myelination in the rat pyramidal tract. *Devl Brain Res.* **54,** 51–61.
13. Harding G. W. and Towe A. L. (1985) Fiber analysis of the pyramidal tract of the laboratory rat. *Expl Neurol.* **87,** 503–518.
14. Harrison T. A. and Towe A. L. (1986) Antidromic response to medullary pyramid stimulation in rats and its relation to that in cats. *Brain Behav. Evol.* **29,** 143–161.
15. Hawkins R. D., Roll P., Puerto A. and Yeomans J. S. (1983) Refractory periods of neurons mediating stimulus-elicited eating and brain stimulation reward: interval scale measurement and test of a model of integration. *Behav. Neurosci.* **97,** 416–432.
16. Hursch J. B. (1939) The properties of growing nerve fibers. *Am. J. Physiol.* **127,** 140–153.
17. Jankowska E., Padel Y. and Tanaka R. (1975) The mode of activation of pyramidal tract cells by intracortical stimuli. *J. Physiol., Lond.* **249,** 617–636.
18. Joosten E. A. J. and Gribnau A. A. M. (1988) Unmyelinated corticospinal axons in adult rat pyramidal tract. An electron microscopic tracer study. *Brain Res.* **459,** 173–177.
19. Kernell D. and Wu C.-P. (1967) Responses of the pyramidal tract to stimulation of the baboon's motor cortex. *J. Physiol., Lond.* **191,** 653–672.
20. Landry P., Wilson C. J. and Kitai S. T. (1984) Morphological and electrophysiological characteristics of pyramidal tract neurons in the rat. *Expl Brain Res.* **57,** 177–190.
21. Lassek A. M. and Rasmussen G. L. (1940) A comparative and numerical analysis of the pyramidal tract. *J. comp. Neurol.* **72,** 417–428.
22. Leenen L., Meek J. and Niewenhuys R. (1982) Unmyelinated fibers in the pyramidal tract of the rat: a new view. *Brain Res.* **246,** 297–301.
23. Leenen L. P. H., Meek J., Posthuma P. R. and Niewenhuys R. (1985) A detailed morphometric analysis of the pyramidal tract of the rat. *Brain Res.* **359,** 65–80.
24. Liang F., Moret V., Wiesendanger M. and Rouiller E. M. (1991) Corticomotoneuronal connections in the rat: evidence from double-labeling of motoneurons and corticospinal axon arborizations. *J. comp. Neurol.* **311,** 356–366.
25. Lloyd D. P. C. (1946) Facilitation and inhibition of spinal motorneurons. *J. Neurophysiol.* **9,** 421–438.
26. Neafsey E. J., Bold E. L., Haas G., Hurley-Gius K. M., Quirk G., Sievert C. F. and Terreberry R. R. (1986) The organization of the rat motor cortex: a microstimulation mapping study. *Brain Res. Rev.* **11,** 77–96.
27. McComas A. J. and Wilson P. (1968) An investigation of pyramidal tract cells in the somatosensory cortex of the rat. *J. Physiol.* **194,** 271–288.
28. Mediratta N. K. and Nicoll J. A. R. (1983) Conduction velocities of corticospinal axons in the rat studied by recording cortical antidromic responses. *J. Physiol., Lond.* **336,** 545–561.
29. Paintal A. S. (1978) Conduction properties of normal peripheral mammalian axons. In *Physiology and Pathobiology of Axons* (ed. Waxman S. G.), pp. 131–134. Raven, New York.

30. Patton H. D. and Amassian V. E. (1954) Single- and multiple-unit analysis of cortical stage of pyramidal tract activation. *J. Neurophysiol.* **17,** 345–363.
31. Paxinos G. and Watson C. (1982) *The Rat Brain in Stereotaxic Coordinates.* Academic Press, Toronto.
32. Peets J. M. and Pomeranz B. (1987) Studies in suppression of nocifensive reflexes measured with tail flick electromyograms and using intrathecal drugs in barbiturate anesthetized rats. *Brain Res.* **416,** 301–307.
33. Phillips C. G. and Porter R. (1977) *Corticospinal Neurones.* Academic Press, London.
34. Rolls E. T. (1975) The neural basis of brain stimulation reward. *Prog. Neurobiol.* **3,** 71–160.
35. Rompre P.-P. and Shizgal P. (1986) Electrophysiological characteristics of neurons in forebrain regions implicated in self-stimulation of the medial forebrain bundle in rats. *Brain Res.* **364,** 338–349.
36. Schenk S. and Shizgal P. (1982) The substrates for lateral hypothalamic and medial prefrontal cortex self-stimulation have different refractory periods and show poor spatial summation. *Physiol. Behav.* **28,** 133–138.
37. Shizgal P., Bielajew C., Corbett D., Skelton R. and Yeomans J. (1980) Behavioral methods for inferring anatomical linkage between rewarding brain stimulation sites. *J. comp. Physiol. Psychol.* **94,** 227–237.
38. Silva L. R., Vogel J. A. and Corbett D. (1982) Frontal cortex self-stimulation: evidence for independent substrates within areas 32 and 24. *Soc. Neurosci. Abstr.* **8,** 625.
39. Stewart M., Quirk G. J. and Amassian V. E. (1990) Corticospinal responses to electrical stimulation of motor cortex in the rat. *Brain Res.* **508,** 341–344.
40. Stone T. W. (1972) Cortical responses to pyramidal tract stimulation in the rat. *Expl Neurol.* **35,** 492–502.
41. Swadlow H. A. and Waxman S. G. (1978) Activity-dependent variations in the conduction properties of central axons. In *Physiology and Pathobiology of Axons* (ed. Waxman S. G.), pp. 191–202. Raven, New York.
42. Takahashi K. (1965) Slow and fast groups of pyramidal tract cells and their respective membrane properties. *J. Neurophysiol.* **28,** 908–924.
43. Tehovnik E. J. and Yeomans J. S. (1987) Circling elicited from the anteromedial cortex and medial pons: refractory periods and summation. *Brain Res.* **407,** 240–252.
44. Towe A. L. (1973) Relative numbers of pyramidal tract neurons in mammals of different sizes. *Brain Behav. Evol.* **7,** 1–17.
45. Towe A. L. and Harding G. W. (1970) Extracellular microelectrode sampling bias. *Expl Neurol.* **29,** 366–381.
46. Yeomans J. S. (1975) Quantitative measurement of neural post-stimulation excitability properties with behavioral methods. *Physiol. Behav.* **15,** 593–602.
47. Yeomans J. S. (1979) Absolute refractory periods of self-stimulation neurons. *Physiol. Behav.* **22,** 911–919.
48. Yeomans J. S. (1990) *Principles of Brain Stimulation.* Oxford, University Press.
49. Yeomans J. S. and Buckenham K. E. (1988) Electrically evoked turning: asymmetric and symmetric collision between anteromedial cortex and striatum. *Soc. Neurosci. Abstr.* **14,** 956.
50. Yeomans J. S. and Chapman C. A. (1989) Forelimb flexion evoked by motor cortex or pyramid stimulation in rats is due to the largest pyramidal tract axons. *Soc. Neurosci. Abstr.* **15,** 114.13.
51. Yeomans J. S. and Linney L. (1985) Longitudinal brainstem axons mediating circling: behavioral measurement of conduction velocity distributions. *Behav. Brain Res.* **15,** 121–135.
52. Yeomans J. S., Matthews G. G., Hawkins R. D., Bellman K. and Doppelt H. (1979) Characterization of self-stimulation neurons by their local potential summation properties. *Physiol. Behav.* **22,** 921–929.
53. Yeomans J. S., Mercouris N. and Ellard D. (1985) Behaviorally measured refractory periods are lengthened by reducing electrode tip exposure or raising current. *Behav. Neurosci.* **99,** 913–928.
54. Yeomans J. S., Rosen J. G., Barbeau J. and Davis M. (1989) Double-pulse stimulation of startle-like responses in rats: refractory periods and temporal summation. *Brain Res.* **486,** 147–158.
55. Yeomans J. S. and Tehovnik E. J. (1988) Turning responses evoked by stimulation of visuomotor pathways. *Brain Res. Rev.* **13,** 235–259.

(*Accepted* 8 *September* 1993)

Exhibit G

CALCULATIONS OF INDUCED CURRENT DISTRIBUTION IN A HUMAN MODEL FROM LOW FREQUENCY ELECTRODES

Report

By

Rungkiet Kamondetdacha and John A. Nyenhuis

Project sponsored by

RS MEDICAL

School of Electrical & Computer Engineering
Purdue University

July 26, 2005

ABSTRACT

The overall objective of this work is to calculate the current distribution in the body from electrodes placed on the skin for the purpose of inducing current in the vicinity of vertebral bodies. The human model used was the Hugo model based upon the virtual human from the National Library of Medicine. The resolution of the model is 3 mm. In the calculations, two pairs of electrodes are applied at the back of the model. Firstly, a unit current is applied at both electrode pairs and their contributions are obtained separately. Once these results are known, the interferential current from the electrodes with any current or frequency (as long as the conductivities which are frequency-dependent do not change much) can be easily obtained. The report shows a sample calculation of the interferential current and its direction in the 3mm Hugo model due to the application of 1 A at the frequency of 10 kHz and 10.1kHz at each pair of electrodes.

With the current technique, the calculations for a higher resolution model are prohibited by a very huge demand of computer resource and time. However, it is likely that this challenge may be overcame by using some interpolation technique to the results obtained from lower-resolution calculation and redoing the calculation on the smaller region of interest with higher resolution using the interpolated results obtained from the prior calculations.

Accomplishment of Specific Aims

This report is for the project *Induced Currents from Electrodes* that was funded by RS Medical. The specific aims of the work were to

1. Calculate the currents induced in an 8-mm resolution human body torso by electrodes at frequencies of the order of 10 kHz. The probable method will be finite difference time domain. Calculations at finer resolutions will be attempted and the preliminary results will be reported.

2. Plot the current intensity and direction for the entire torso and near the vertebral body. The plots will include the effects of inferential stimulation.

3. Identify the most promising technique for calculating the current in the vicinity of the vertebral body at a resolution of 1 mm and estimate the effort required to make this calculation.

The deliverable will be a detailed report describing the model, the methods and the results.

A summary of the accomplishments toward these aims are as follows:

1. By use of an impedance technique, the current density from electrodes was plotted for a 3-mm resolution human model.

2. Plots of the current intensity in the torso and the vertebral bodies are included in this report.

3. The impedance method is identified to be the most promising method for enhancement of the spatial resolution of the calculation. A sub-gridding technique will be required if the resolution is to be enhanced beyond 3 mm. In this technique, the voltage at the boundaries of a volume will be determined with a 3-mm resolution model. The calculations will be then be redone in the smaller region of interest at the finer resolution.

TABLE OF FIGURES

Figures	Page
Fig. 1. Two electrodes are applied at the back of the model.	5
Fig. 2. The circuit diagram at the voxel (i,j,k)	6
Fig. 3. Tissue distribution in coronal plane at y=0.12 m (Fig. 3a), sagittal plane at x=0.3 m (Fig. 3b), and axial plane at z=0.45 m (Fig. 3c) are shown. These are the planes of interest since they contain the spine of the model. These are the same planes that the current distributions will be shown later in the report. Colors represent tissue types.	11
Fig. 4. Relative error vs. the number of iterations. It takes 40,000 iterations to get relative error less than 1x10-4 %.	12
Fig. 5. Amplitude of current density J (A/m2) on coronal plane at y = 0.12 m (Front View) due to the electrode pair A with the amplitude of the applied current equal to 1 A.	13
Fig. 6. Amplitude of current density J (A/m2) on sagittal plane at x = 0.3 m (Right view) due to the electrode pair A with the amplitude of the applied current equal to 1 A.	14
Fig. 7. Amplitude of current density J (A/m2) on axial plane at z = 0.45 m (Top view) due to the electrode pair A with the amplitude of the applied current equal to 1 A.	15
Fig. 8. Amplitude of electric field E (V/m) on coronal plane at y = 0.12 m (Front View) due to the electrode pair A with the amplitude of the applied current equal to 1 A.	16
Fig. 9. Ex, Ey, Ez and |E| along the line x = 0.3 m, y = 0.12 m, z = 0.2-0.6 m due to electrode pair A with current 1 A	17
Fig. 10. Amplitude of electric field E (V/m) on sagittal plane at x = 0.3 m (Right view) due to the electrode pair A with the amplitude of the applied current equal to 1 A.	18
Fig. 11. Ex, Ey, Ez and |E| along the line x = 0.3 m, y = 0.06 m, z = 0.2-0.6 m due to electrode pair A with current 1 A	19
Fig. 12. Amplitude of electric field E (V/m) on axial plane at z = 0.45 m (Top view) due to the electrode pair A with the amplitude of the applied current equal to 1 A.	20
Fig. 13. Ex, Ey, Ez and |E| along the line x = 0.3 m, y = 0.02-0.27 m, z = 0.2-0.6 m due to electrode pair A	21
Fig. 14. Amplitude of current density J (A/m2) on coronal plane at y = 0.12 m (Front View) due to the electrode pair B with the amplitude of the applied current equal to 1 A.	22
Fig. 15. Amplitude of current density J (A/m2) on sagittal plane at x = 0.3 m (Right view) due to the electrode pair B with the amplitude of the applied current equal to 1 A.	23
Fig. 16. Amplitude of current density J (A/m2) on axial plane at z = 0.45 m (Top view) due to the electrode pair B with the amplitude of the applied current equal to 1 A.	24
Fig. 17. Amplitude of electric field E (V/m) on coronal plane at y = 0.12 m (Front View) due to the electrode pair B with the amplitude of the applied current equal to 1 A.	25
Fig. 18. Ex, Ey, Ez and |E| along the line x = 0.3 m, y = 0.12 m, z = 0.2-0.6 m due to electrode pair B with current 1 A	26
Fig. 19. Amplitude of electric field E (V/m) on sagittal plane at x = 0.3 m (Right view) due to the electrode pair B with the amplitude of the applied current equal to 1 A.	27
Fig. 20. Ex, Ey, Ez and |E| along the line x = 0.3 m, y = 0.06 m, z = 0.2-0.6 m due to electrode pair B with current 1 A	28
Fig. 21. Amplitude of electric field E (V/m) on axial plane at z = 0.45 m (Top view) due to the electrode pair B with the amplitude of the applied current equal to 1 A.	29
Fig. 22. Ex, Ey, Ez and |E| along the line x = 0.3 m, y = 0.02-0.27 m, z = 0.45 m due to electrode pair B with current 1 A	30
Fig. 23. The induced electric field (Ex, Ey, Ez, |E|) at the point x= 0.3 m, y =0.08 m, z = 0.47 m due to the 2 pairs of electrodes with current 1 A for each pair and frequency 1 kHz and 1.1 kHz.	31
Fig. 24. The induced electric field (Ex, Ey, Ez, |E|) at the point x= 0.3 m, y =0.06 m, z = 0.53 m due to the 2 pairs of electrodes with current 1 A for each pair and frequency 1 kHz and 1.1 kHz.	32

CALCULATIONS OF CURRENT DISTRIBUTION

The objective of the work to determine the current distribution in the body from electrodes placed on the skin. Two pairs of 7-cm-diameter copper electrodes are applied at the back of the human model as shown in Fig. 1. To calculate the total current inside the body, we firstly calculate the current injected into the body due to a unit voltage applied at each pair. (While the voltage is applied at one pair of electrodes, the other pair is removed from the body.) Then, the injected current is normalized to one and the current density in the body is scaled to be the current due to a unit injected current.

As a result, we can determine the total current density in the body due to any size of applied currents from both pair of electrodes (electrode pair A and electrode pair B) by combining the contribution from each pair of electrode:

$$\mathbf{J} = \mathbf{k}_1 I_A + \mathbf{k}_2 I_B, \tag{1}$$

where I_A and I_B are the applied current at electrode A and B, $\mathbf{k}_1$ is the current density vector when $I_A = 1$ A and $I_B = 0$ A and $\mathbf{k}_2$ is the current density vector when $I_A = 0$ A and $I_B = 1$ A, and $\mathbf{J}$ is the current density vector. Note that $\mathbf{k}_1$ and $\mathbf{k}_2$ are a function of position.

Therefore, the objective is to find $\mathbf{k}_1$ and $\mathbf{k}_2$ everywhere in the model. And the current density everywhere in the body due to any size of applied current from the electrodes can be readily determined.

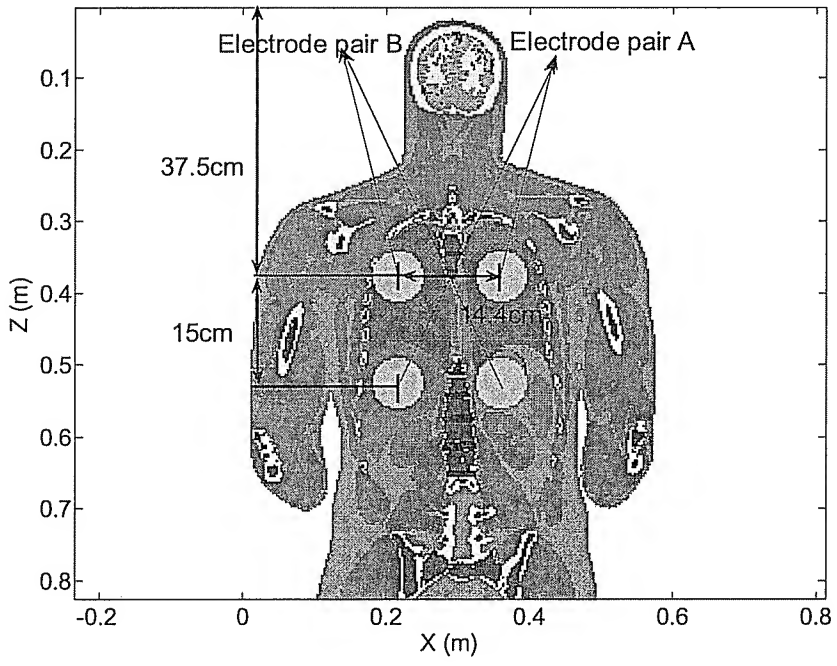

Fig. 1. Model geometry. Two pairs of 7-cm diameter electrodes are applied at the back of the model. The left and right electrodes are separated by 14.4 cm and the top and bottom electrodes are separated by 15 cm. In this diagram the colors indicate tissue types. (Front View)

The calculations were done by using Impedance method described in [1] and [2]. The domain of interest is divided into several voxels. Fig. 2 shows the 2-D representation of a voxel and its neighbors.

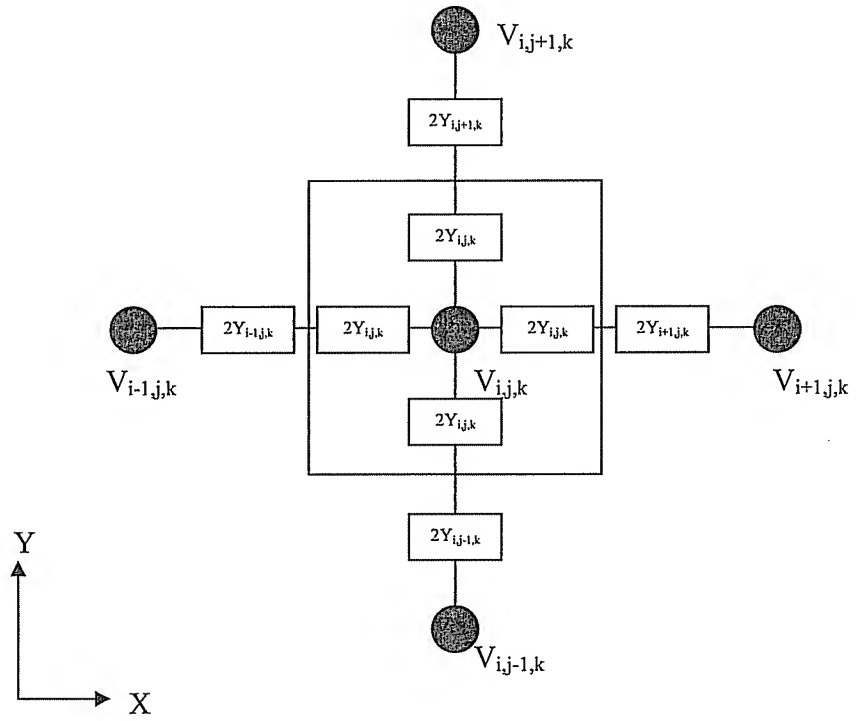

Fig. 2. The circuit diagram at the voxel (i,j,k)

Assign the electric potential at the voxel (i,j,k) as $V_{i,j,k}$. $Y_{i,j,k}$ is the admittance at the voxel (i,j,k) and it is equal to

$$Y_{i,j,k} = \Delta(\sigma + j\omega\varepsilon), \tag{2}$$

where Δ is the spatial resolution, σ and ε are conductivity and permittivity of the tissue and ω is the angular frequency of the applied voltage. In this application, the frequency of interest is in the range of 1 kHz-10 kHz. The values of σ are a lot greater than $j\omega\varepsilon$ and $Y_{i,j,k}$ can be well approximated by $\Delta\sigma$.

By application of Kirchoff's Current Law at the voxel (i, j, k), we have

$$\left\{\begin{array}{l}\left(\frac{2Y_{i+1,j,k}\cdot 2Y_{i,j,k}}{2Y_{i+1,j,k}+2Y_{i,j,k}}\right)\left(V_{i+1,j,k}-V_{i,j,k}\right)+\left(\frac{2Y_{i-1,j,k}\cdot 2Y_{i,j,k}}{2Y_{i-1,j,k}+2Y_{i,j,k}}\right)\left(V_{i-1,j,k}-V_{i,j,k}\right)+\\ \left(\frac{2Y_{i,j+1,k}\cdot 2Y_{i,j,k}}{2Y_{i,j+1,k}+2Y_{i,j,k}}\right)\left(V_{i,j+1,k}-V_{i,j,k}\right)+\left(\frac{2Y_{i,j-1,k}\cdot 2Y_{i,j,k}}{2Y_{i,j-1,k}+2Y_{i,j,k}}\right)\left(V_{i,j-1,k}-V_{i,j,k}\right)+\\ \left(\frac{2Y_{i,j,k+1}\cdot 2Y_{i,j,k}}{2Y_{i,j,k+1}+2Y_{i,j,k}}\right)\left(V_{i,j,k+1}-V_{i,j,k}\right)+\left(\frac{2Y_{i,j,k-1}\cdot 2Y_{i,j,k}}{2Y_{i,j,k-1}+2Y_{i,j,k}}\right)\left(V_{i,j,k-1}-V_{i,j,k}\right)\end{array}\right\}=0 \qquad (3)$$

After some algebra, $V_{i,j,k}$ can be obtained as

$$\frac{\left\{\begin{array}{l}\left(\frac{Y_{i+1,j,k}\cdot Y_{i,j,k}}{Y_{i+1,j,k}+Y_{i,j,k}}\right)V_{i+1,j,k}+\left(\frac{Y_{i-1,j,k}\cdot Y_{i,j,k}}{Y_{i-1,j,k}+Y_{i,j,k}}\right)V_{i-1,j,k}+\\ \left(\frac{Y_{i,j+1,k}\cdot Y_{i,j,k}}{Y_{i,j+1,k}+Y_{i,j,k}}\right)V_{i,j+1,k}+\left(\frac{Y_{i,j-1,k}\cdot Y_{i,j,k}}{Y_{i,j-1,k}+Y_{i,j,k}}\right)V_{i,j-1,k}+\\ \left(\frac{Y_{i,j,k+1}\cdot Y_{i,j,k}}{Y_{i,j,k+1}+Y_{i,j,k}}\right)V_{i,j,k+1}+\left(\frac{Y_{i,j,k-1}\cdot Y_{i,j,k}}{Y_{i,j,k-1}+Y_{i,j,k}}\right)V_{i,j,k-1}\end{array}\right\}}{\left\{\begin{array}{l}\left(\frac{Y_{i+1,j,k}\cdot Y_{i,j,k}}{Y_{i+1,j,k}+Y_{i,j,k}}\right)+\left(\frac{Y_{i-1,j,k}\cdot Y_{i,j,k}}{Y_{i-1,j,k}+Y_{i,j,k}}\right)+\\ \left(\frac{Y_{i,j+1,k}\cdot Y_{i,j,k}}{Y_{i,j+1,k}+Y_{i,j,k}}\right)+\left(\frac{Y_{i,j-1,k}\cdot Y_{i,j,k}}{Y_{i,j-1,k}+Y_{i,j,k}}\right)+\\ \left(\frac{Y_{i,j,k+1}\cdot Y_{i,j,k}}{Y_{i,j,k+1}+Y_{i,j,k}}\right)+\left(\frac{Y_{i,j,k-1}\cdot Y_{i,j,k}}{Y_{i,j,k-1}+Y_{i,j,k}}\right)\end{array}\right\}}=V_{i,j,k} \qquad (4)$$

Eq. (4) provides a relationship between the electric potential of the node of interest and its neighbors. Every node in the problem domain must satisfy Eq. (4).

By application of Eq. (4) at all voxels in the problem domain except at the electrodes, we will have a set of linear equations with the number of variables and number of equations equal to the number of voxels with unknown electric potential (the number of total voxels in the problem domain minus the number of voxels contained in the electrodes).

Due to the very large number of voxels in the problem domain, these linear equations can not be solved by using the traditional inverse of a matrix. We solved Eq. (4) by using Jacobi's iterative method [3].

Since the conductivities of tissues that we have for our Hugo model are the ones at radio frequency (64 MHz), we need to replace these by the ones at 5 kHz. After doing some

surveys in the literatures [4-11], we decided to use the values in the last column of Table 1 as the best guess of conductivities for the calculations.

Table. 1. The conductivities of tissues in the literatures and the ones used in the calculations

	Conductivity (S/m)						
Model	Hugo [4]	E. Carter [5]	M. Stuchly [6]	Gandi [7]	M. Stuchly [8]	C. Gabriel [9,10,11]	Used
Frequency	**64MHz**	**64kHz**	**1kHz**	**60Hz**	**60Hz**	**5kHz**	**10kHz**
tissue							
fat	0.066	0.033	0.4	0.2	0.4		0.4
bone	0.06	0.01	0.04	0.02	0.04	0.02	0.02
nervous white	0.292	0.34		0.0675	0.06		0.1
nervous gray	0.511	0.34		0.0675	0.1	0.1	0.1
skin	0.436		0.1	0.036	0.1	2.00E-03	0.05
eye	0.883			0.2608	0.4		0.4
skeleton muscel	0.688	0.47	0.35	0.2418	0.35	0.4	0.4
blood	1.207		0.7	0.7	0.7	0.7	0.7
neuron tissue	0.312						0.312
lens	0.286					0.2	0.2
optic nerve	0.312						0.312
cartilage	0.452			0.17	0.18		0.2
mucous membrane	0.65						0.4
lungs	0.5	0.048	0.08	0.07	0.08	0.05	0.05
intestine	0.5			0.089	0.5		0.1
kidneys	0.5		0.1	0.094	0.1	0.1	0.1
liver	0.5		0.07	0.037	0.07	0.05	0.05
gland	0.5			0.52	0.45		0.5
spleen	0.5		0.1	0.094	0.1	0.1	0.1
stomach	0.5	0.52	0.5	0.5217	0.5		0.5
pancrease	0.5			0.094	0.22		0.1
unrinary bladder	0.5			0.205	0.2	<0.2	0.2
gallbalder	0.5				1.4		0.5
intestine content	0.5				0.5		0.5
right ventricle	0.5	0.22	0.1		0.1	0.1	0.1
left ventricle	0.5	0.22	0.1		0.1	0.1	0.1
right atrium	0.5	0.22	0.1		0.1	0.1	0.1
left atrium	0.5	0.22	0.1		0.1	0.1	0.1
blood venous	0.5						0.5
blood arterial	0.5						0.5
bone marrow	0.154		0.05		0.05		0.05
spinal cord			0.1	0.0675	0.1		
electrode (copper)	5.80E+07						5.80E+07
air	1.00E-14						1.00E-14

Firstly, we tried to calculate the current distribution in the whole body Hugo model with 8 mm resolution. The results suggested that, by putting the electrodes at the back of the model as shown in Fig. 1, the legs of the model may be cut since there is low current in them. This smaller model allows us to calculate the current distribution in the model at the resolution as high as 3mm. To avoid any confusion, the viewing direction of coronal, sagittal, and axial plane are shown in Fig. 3. Fig. 1 shows the location of the two pairs of 7-cm diameter electrodes which are applied at the back of the model. The center of left and right electrodes are separated by 14.4 cm and the center of top and bottom electrodes are separated by 15 cm. The center of the tops electrodes are at 37.5 cm from the tip of the head. To calculate the current distribution due to electrode pair A, electrode pair B is removed. And electrode pair B is removed to calculate the current due to electrode pair A.

For the calculation of each case, 40000 iterations were done to get relative error about $1\text{x}10^{-4}$ % as shown in Fig. 4. Fig. 5-Fig. 7 shows the current density of the model in coronal, sagittal, and axial cross section when 1 A current is applied at electrode pair A and electrode pair B is removed. Fig. 14-Fig. 16 show those cross sections when 1 A current is applied at electrode pair A and electrode pair B is removed. In other words, they show $\mathbf{k}_1$ and $\mathbf{k}_2$ defined in Eq. (1). Therefore if $I_A \cos(2\pi ft)$ and $I_B \cos(2\pi ft)$ are applied at the electrodes A and B, the total instantaneous current density $\mathbf{J}$ will be

$$\mathbf{J} = \mathbf{k}_1 I_A \cos(2\pi f_A t) + \mathbf{k}_2 I_B \cos(2\pi f_B t + \phi) . \qquad (5)$$

Fig. 8-Fig. 13 and Fig. 17-Fig. 22 show the electric field due to electrode pair A and B with current 1 A.

From Fig. 9, Fig. 11, Fig. 13, Fig. 18, Fig. 20, and Fig. 22, the electric field induced in the tissue near the spine of the model due to a 1A electrode in can be as high as 100 – 400 V/m. Therefore, if 2 pairs of 1A electrodes are applied, the induced electric field can be as high as 200-800 V/m. Therefore, in order to obtain 6 V/m in the tissue, the 8-30 mA should be applied at each pair of electrodes.

Fig. 23-Fig. 24 show the induced electric fields (Ex, Ey, Ez, |E|) at two different locations close to the spine due to the 2 pairs of electrodes with current 1 A for each pair and frequency 1 kHz and 1.1 kHz. One is at x= 0.3 m, y =0.08 m, z = 0.47 m and the other one is at x= 0.3 m, y =0.06 m, z = 0.53 m. The Figs. show that at 2 different points near the spine, the amplitude of induced electric field can be greatly different (the electric field at the first location is about 140 V/m and the one at the second location is about 600 V/m).

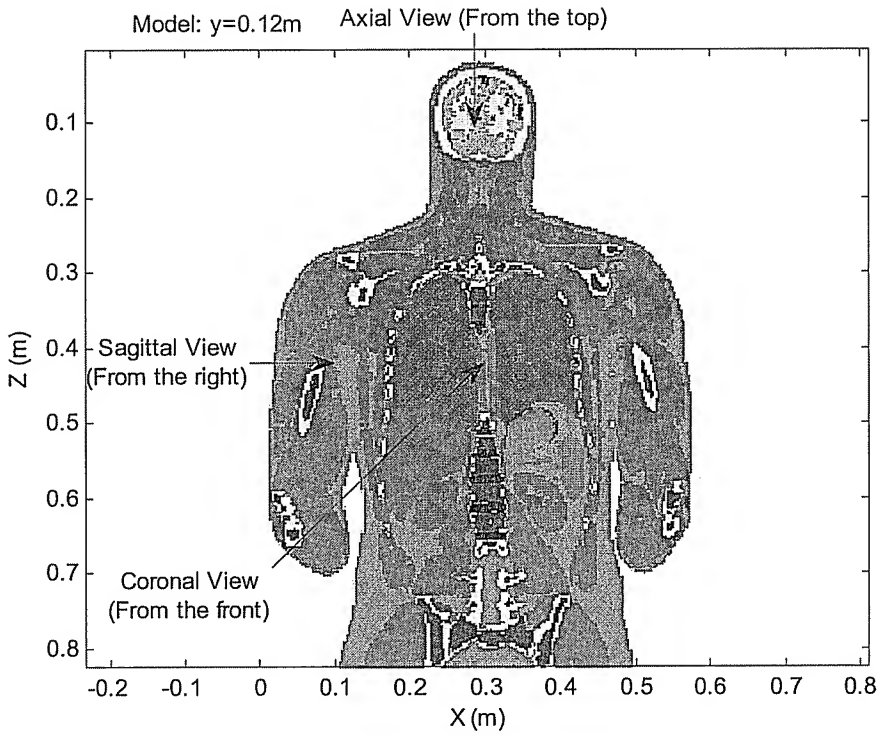
Model: y=0.12m
Axial View (From the top)
Sagittal View
(From the right)
Coronal View
(From the front)
Z (m)
X (m)
0.1
0.2
0.3
0.4
0.5
0.6
0.7
0.8
-0.2
-0.1
0
0.1
0.2
0.3
0.4
0.5
0.6
0.7
0.8

Fig. 3 (a)

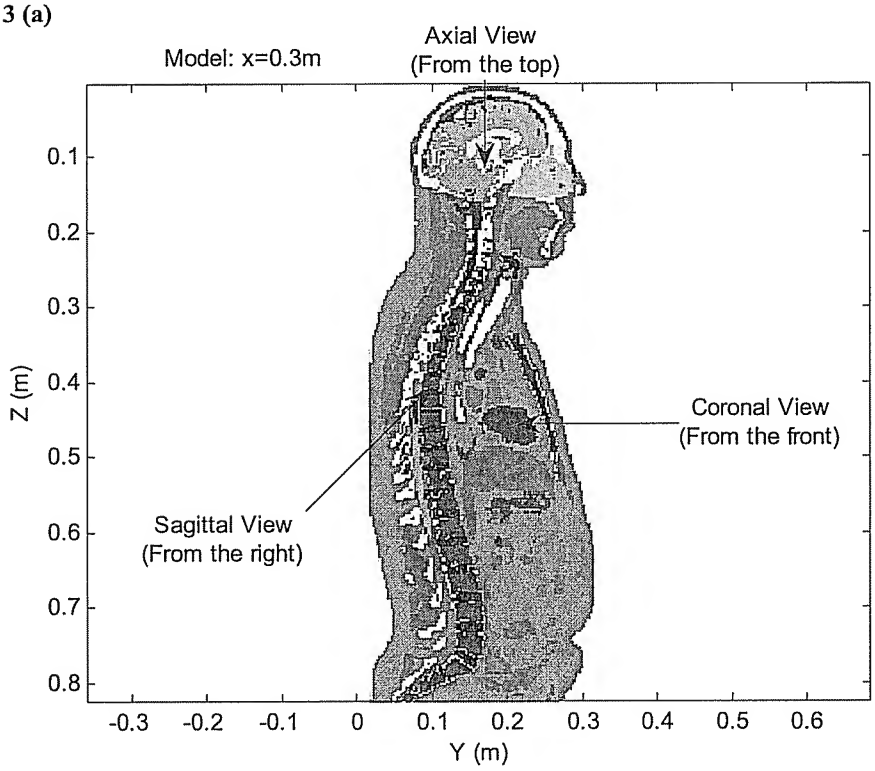
Model: x=0.3m
Axial View
(From the top)
Coronal View
(From the front)
Sagittal View
(From the right)
Z (m)
Y (m)
0.1
0.2
0.3
0.4
0.5
0.6
0.7
0.8
-0.3
-0.2
-0.1
0
0.1
0.2
0.3
0.4
0.5
0.6

Fig. 3 (b)

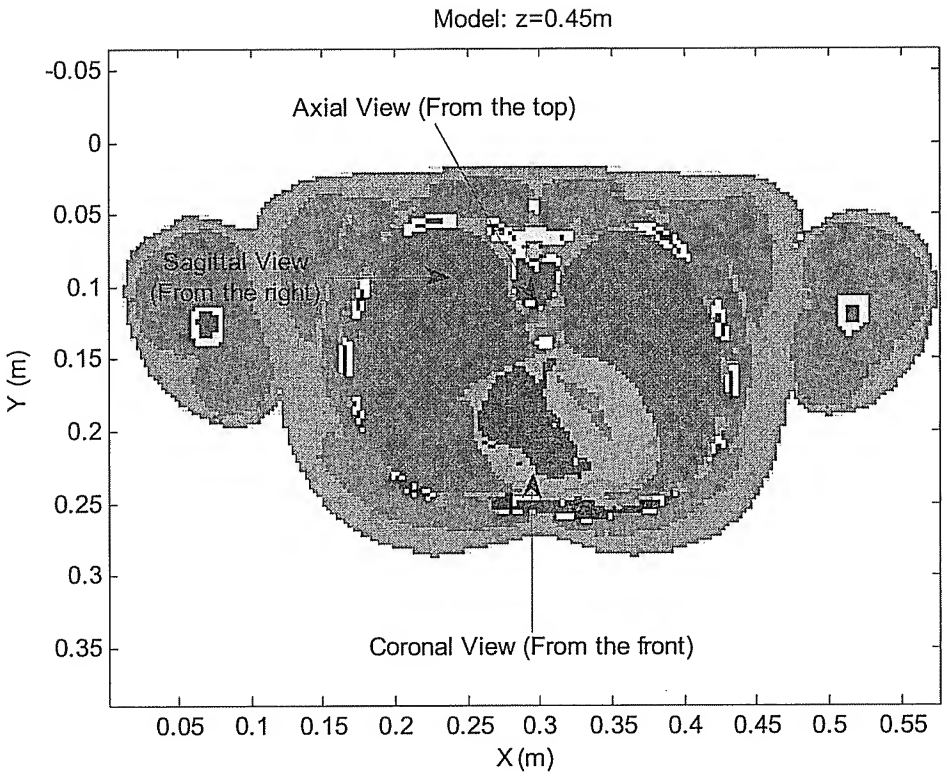

Fig. 3 (c)

Fig. 3. Tissue distribution in coronal plane at y=0.12 m (Fig. 3a), sagittal plane at x=0.3 m (Fig. 3b), and axial plane at z=0.45 m (Fig. 3c) are shown. These are the planes of interest since they contain the spine of the model. These are the same planes that the current distributions will be shown later in the report. Colors represent tissue types.

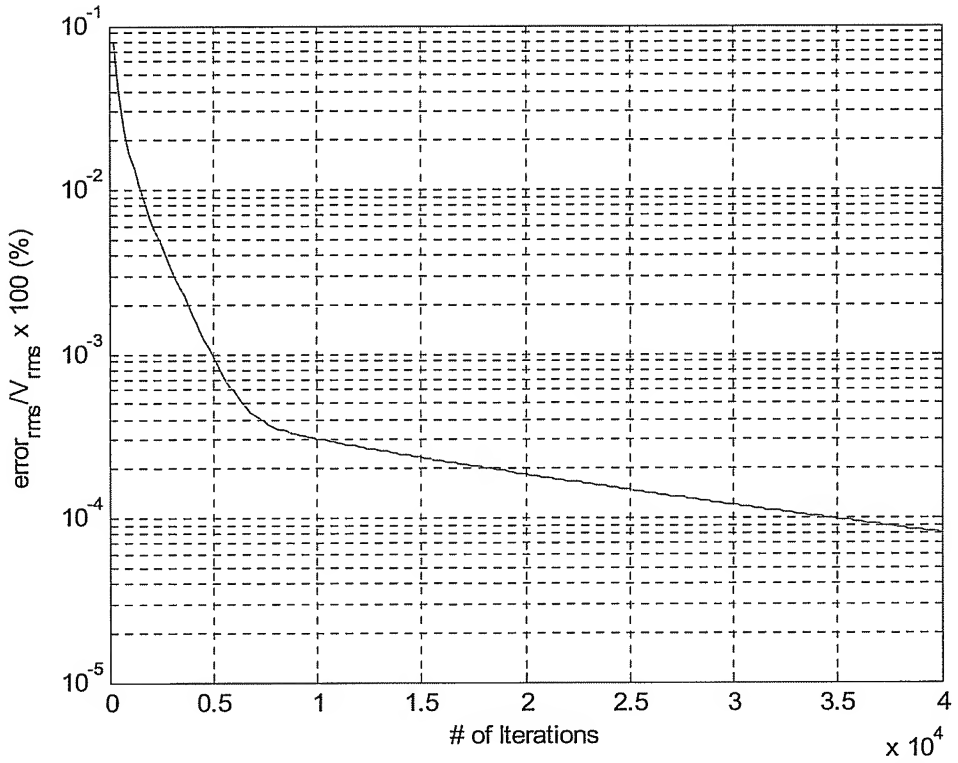

Fig. 4. Relative error vs. the number of iterations. It takes 40,000 iterations to get relative error less than $1x10^{-4}$ %.

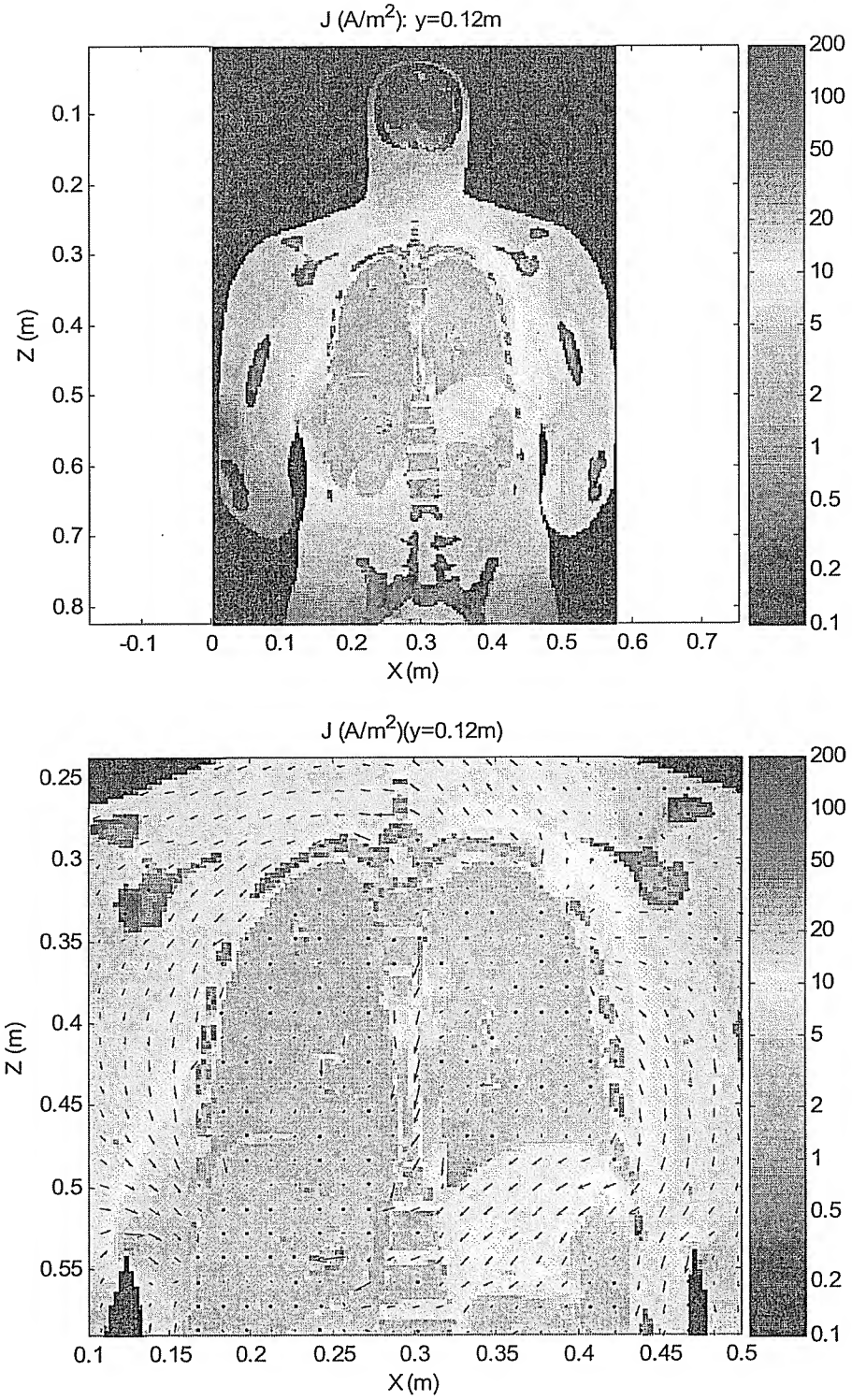

Fig. 5. Amplitude of current density J (A/m^2) on coronal plane at y = 0.12 m (Front View) due to the electrode pair A with the amplitude of the applied current equal to 1 A.

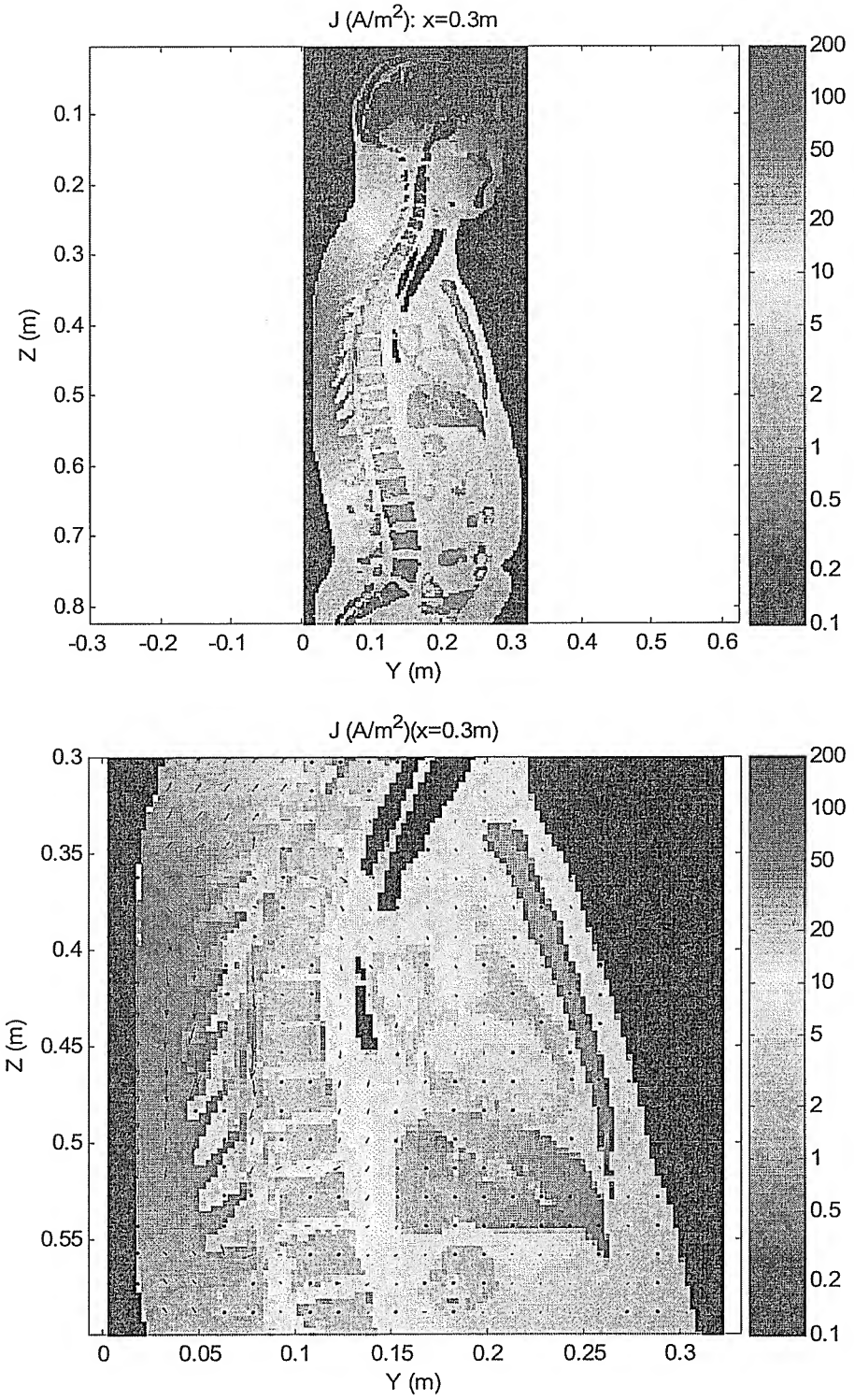

Fig. 6. Amplitude of current density J (A/m^2) on sagittal plane at x = 0.3 m (Right view) due to the electrode pair A with the amplitude of the applied current equal to 1 A.

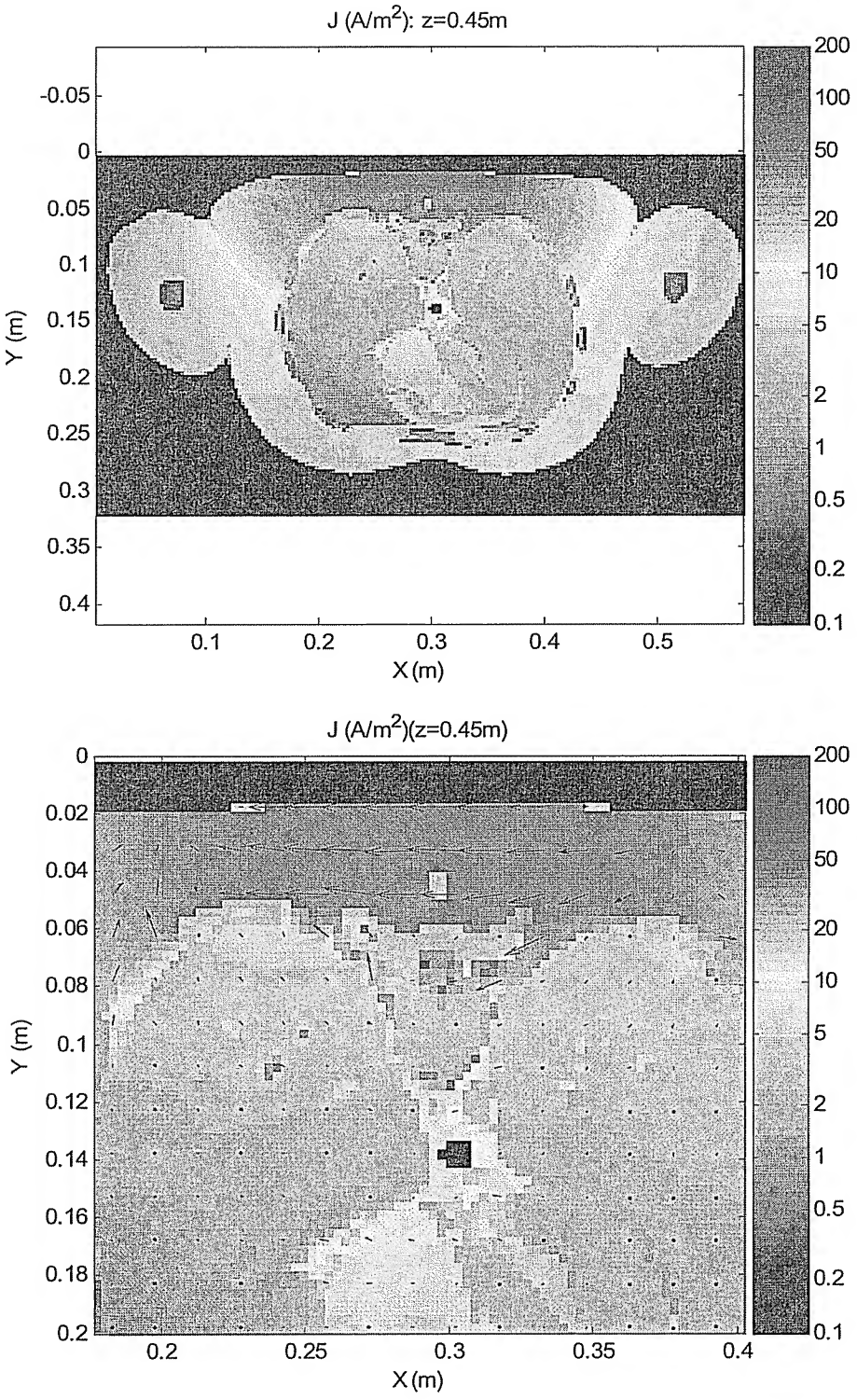

Fig. 7. Amplitude of current density J (A/m^2) on axial plane at z = 0.45 m (Top view) due to the electrode pair A with the amplitude of the applied current equal to 1 A.

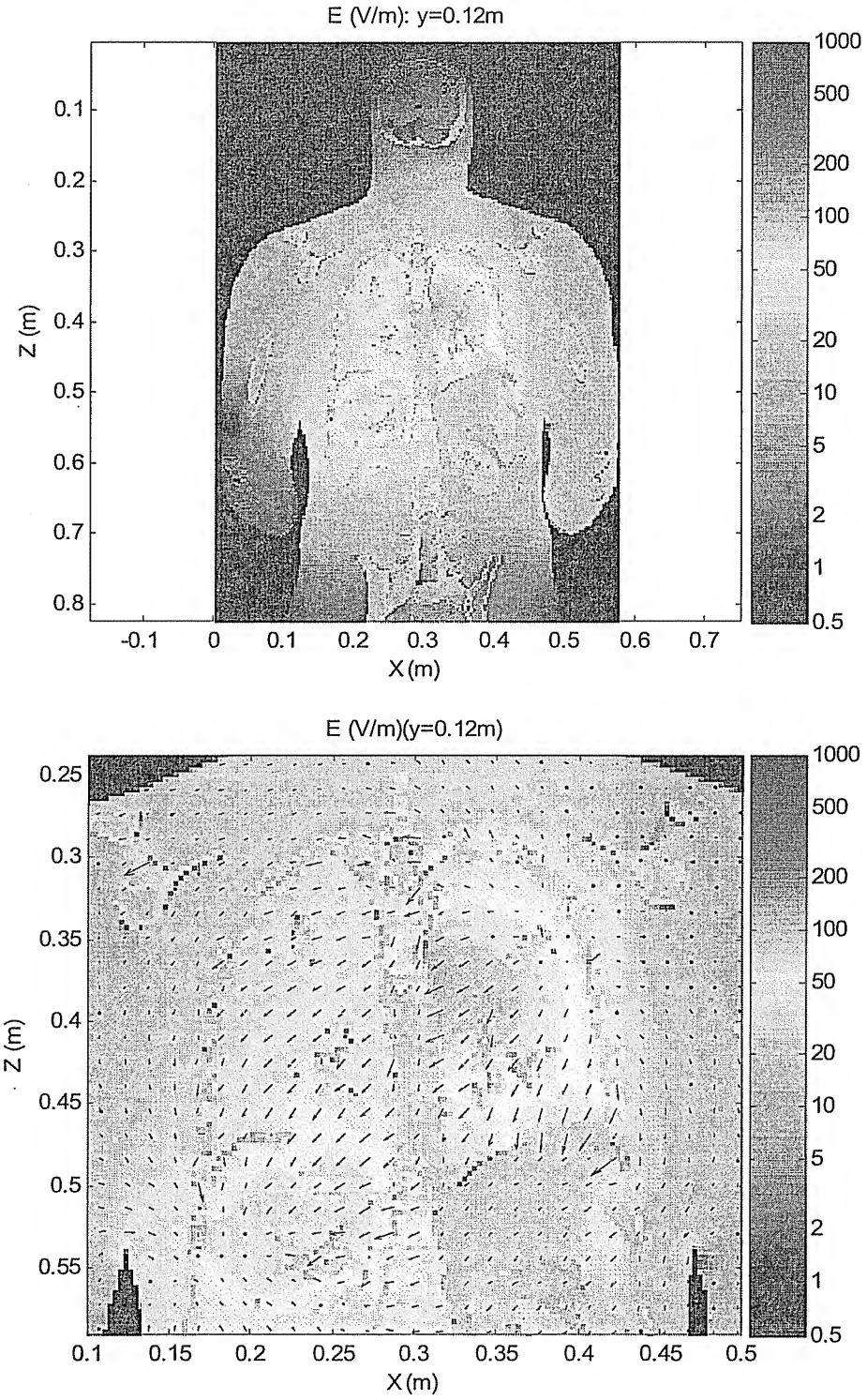

Fig. 8. Amplitude of electric field E (V/m) on coronal plane at y = 0.12 m (Front View) due to the electrode pair A with the amplitude of the applied current equal to 1 A.

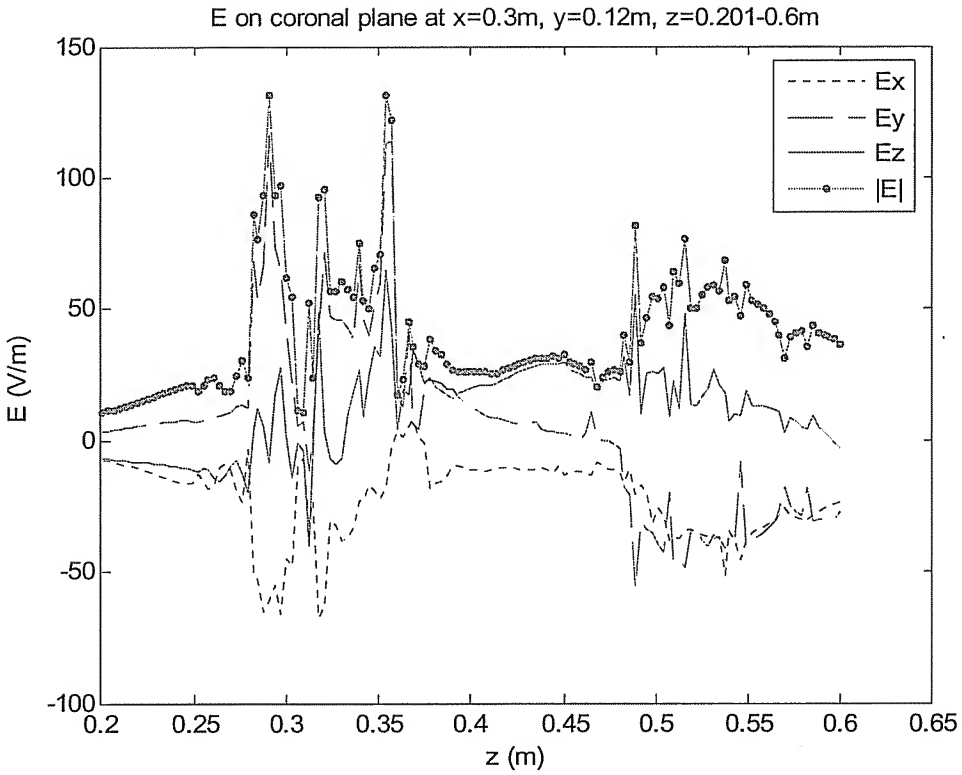

Fig. 9. Ex, Ey, Ez and |E| along the line x = 0.3 m, y = 0.12 m, z = 0.2-0.6 m due to electrode pair A with current 1 A

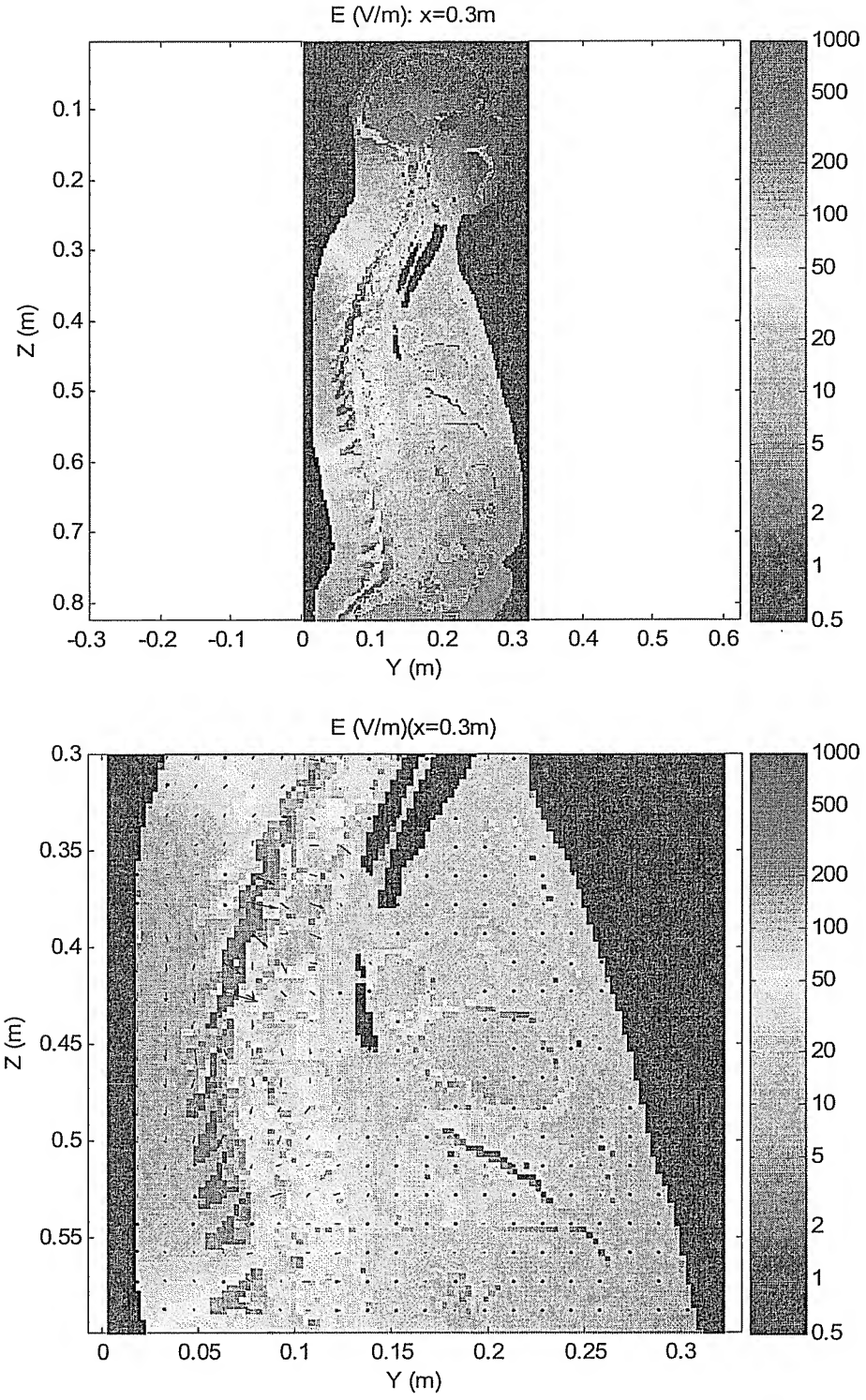

Fig. 10. Amplitude of electric field E (V/m) on sagittal plane at x = 0.3 m (Right view) due to the electrode pair A with the amplitude of the applied current equal to 1 A.

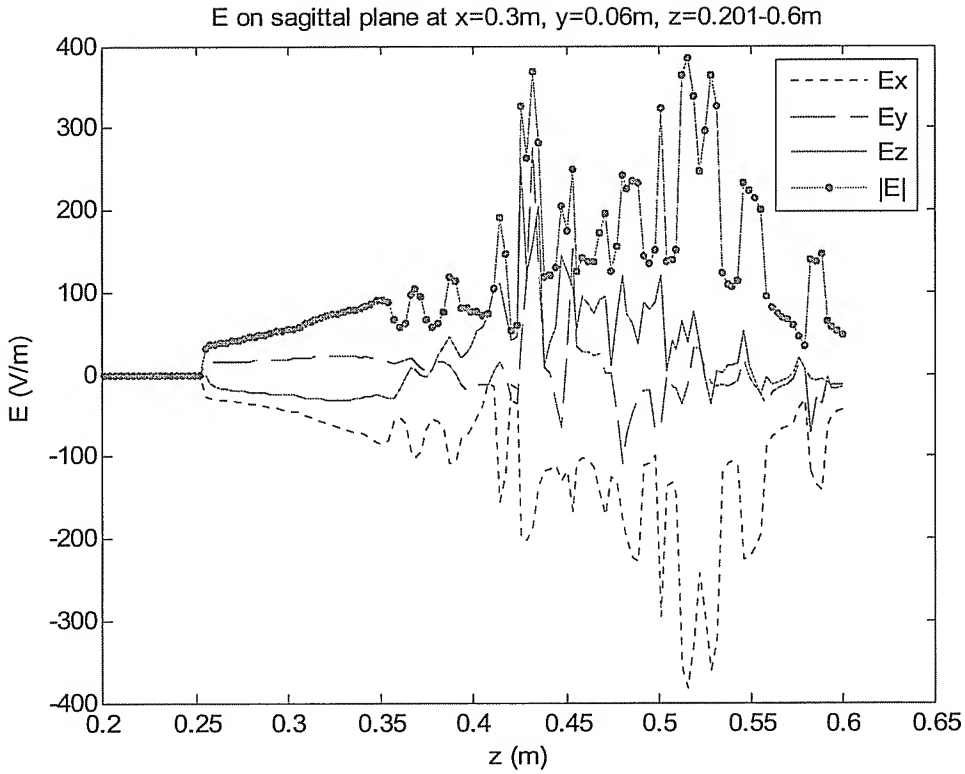

Fig. 11. Ex, Ey, Ez and |E| along the line x = 0.3 m, y = 0.06 m, z = 0.2-0.6 m due to electrode pair A with current 1 A

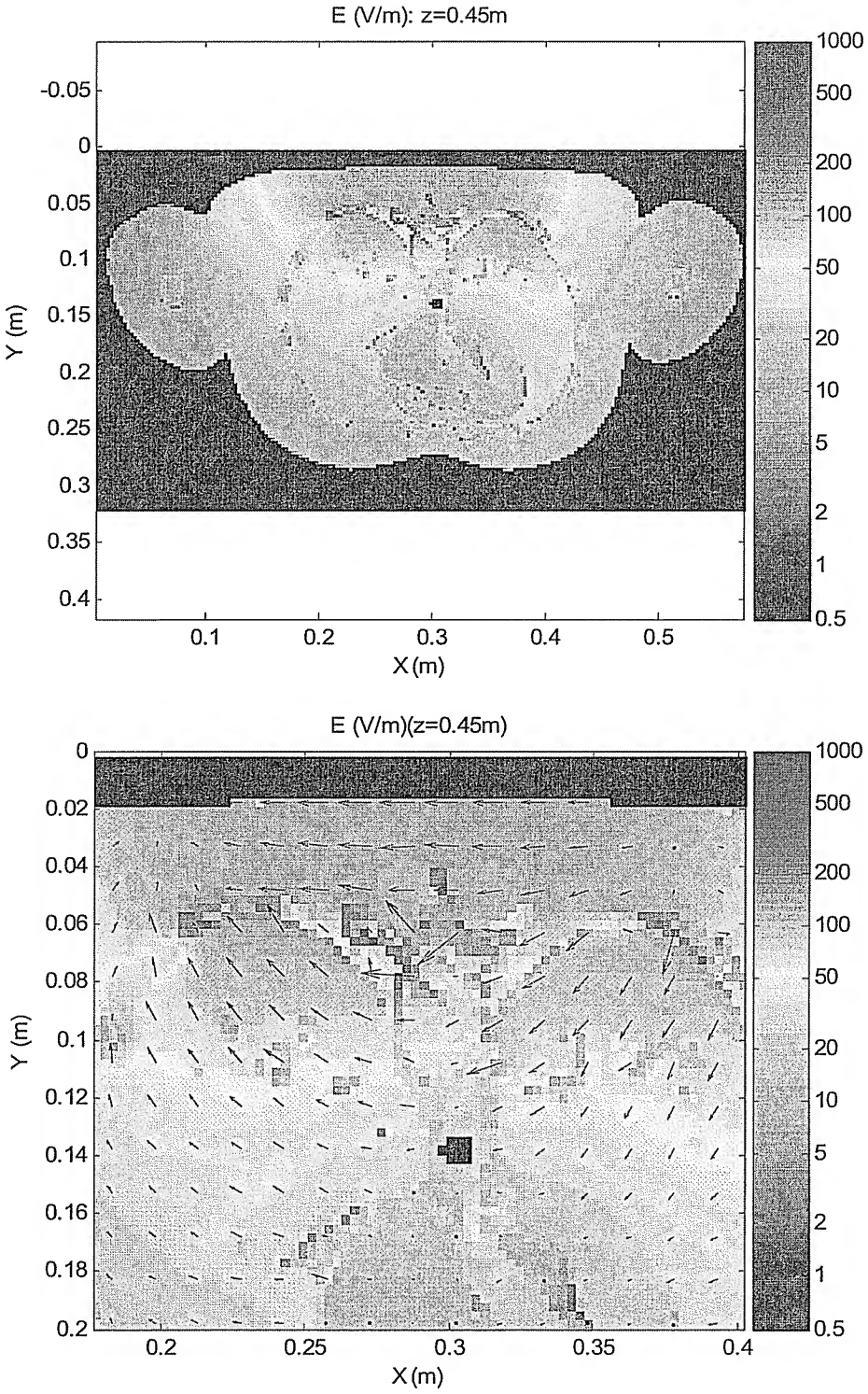

Fig. 12. Amplitude of electric field E (V/m) on axial plane at z = 0.45 m (Top view) due to the electrode pair A with the amplitude of the applied current equal to 1 A.

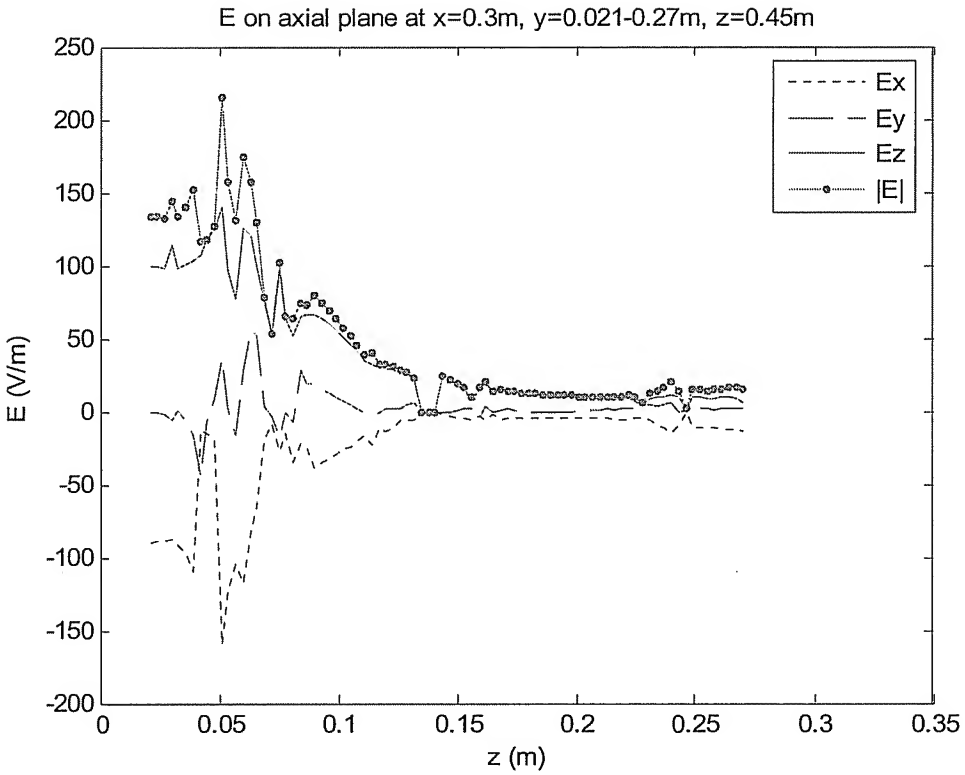

Fig. 13. Ex, Ey, Ez and |E| along the line x = 0.3 m, y = 0.02-0.27 m, z = 0.2-0.6 m due to electrode pair A

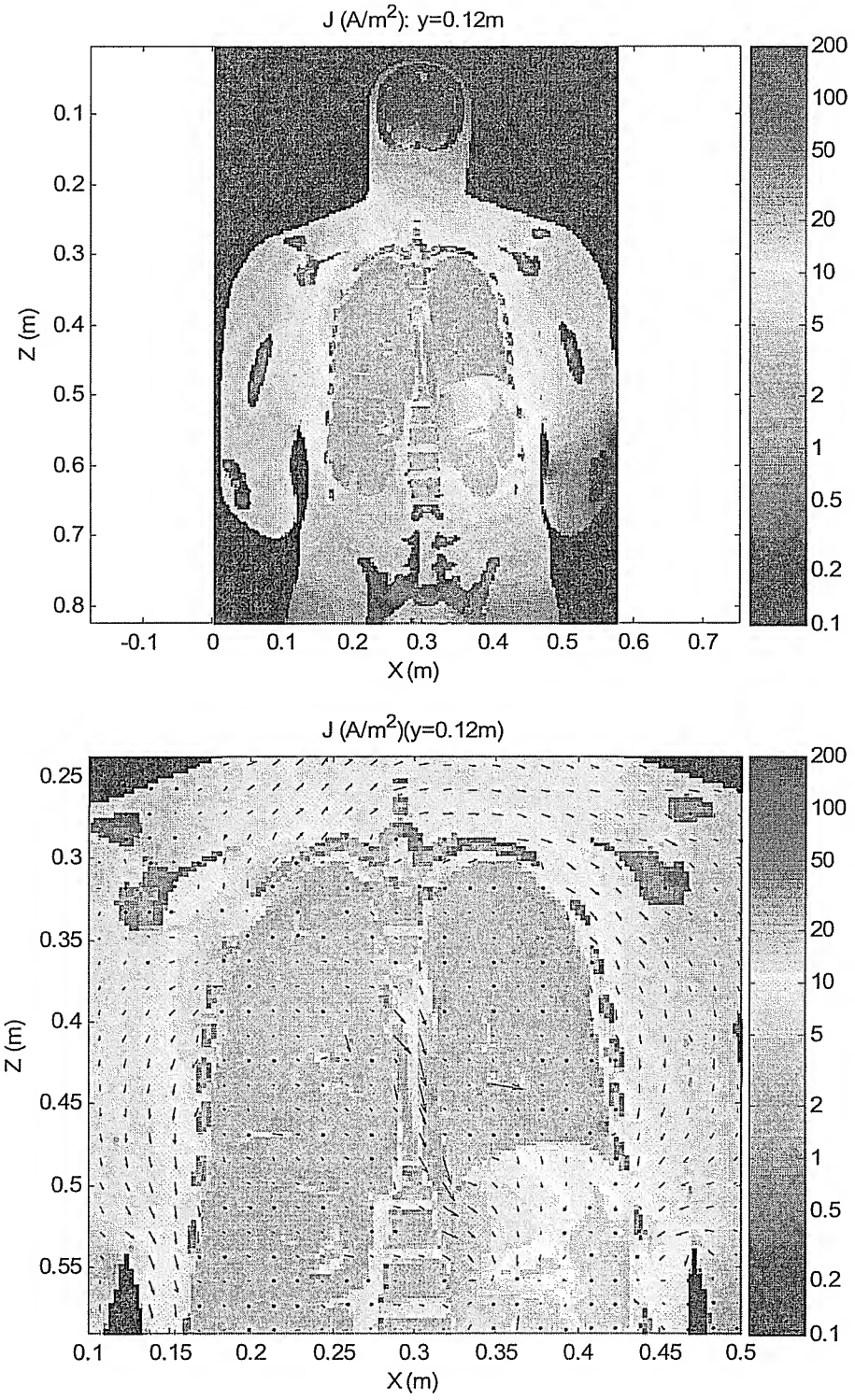

Fig. 14. Amplitude of current density J (A/m^2) on coronal plane at y = 0.12 m (Front View) due to the electrode pair B with the amplitude of the applied current equal to 1 A.

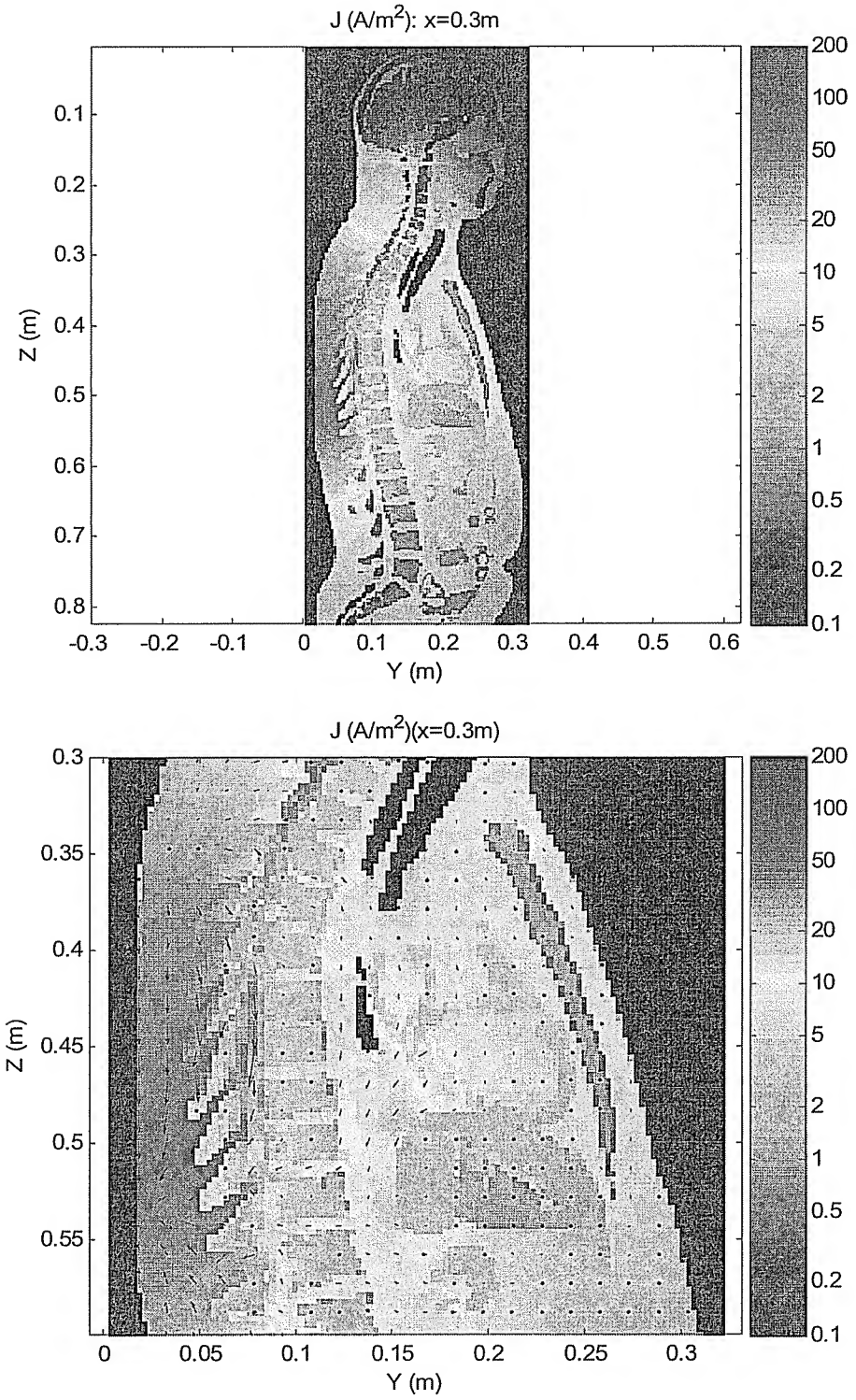

Fig. 15. Amplitude of current density J (A/m^2) on sagittal plane at x = 0.3 m (Right view) due to the electrode pair B with the amplitude of the applied current equal to 1 A.

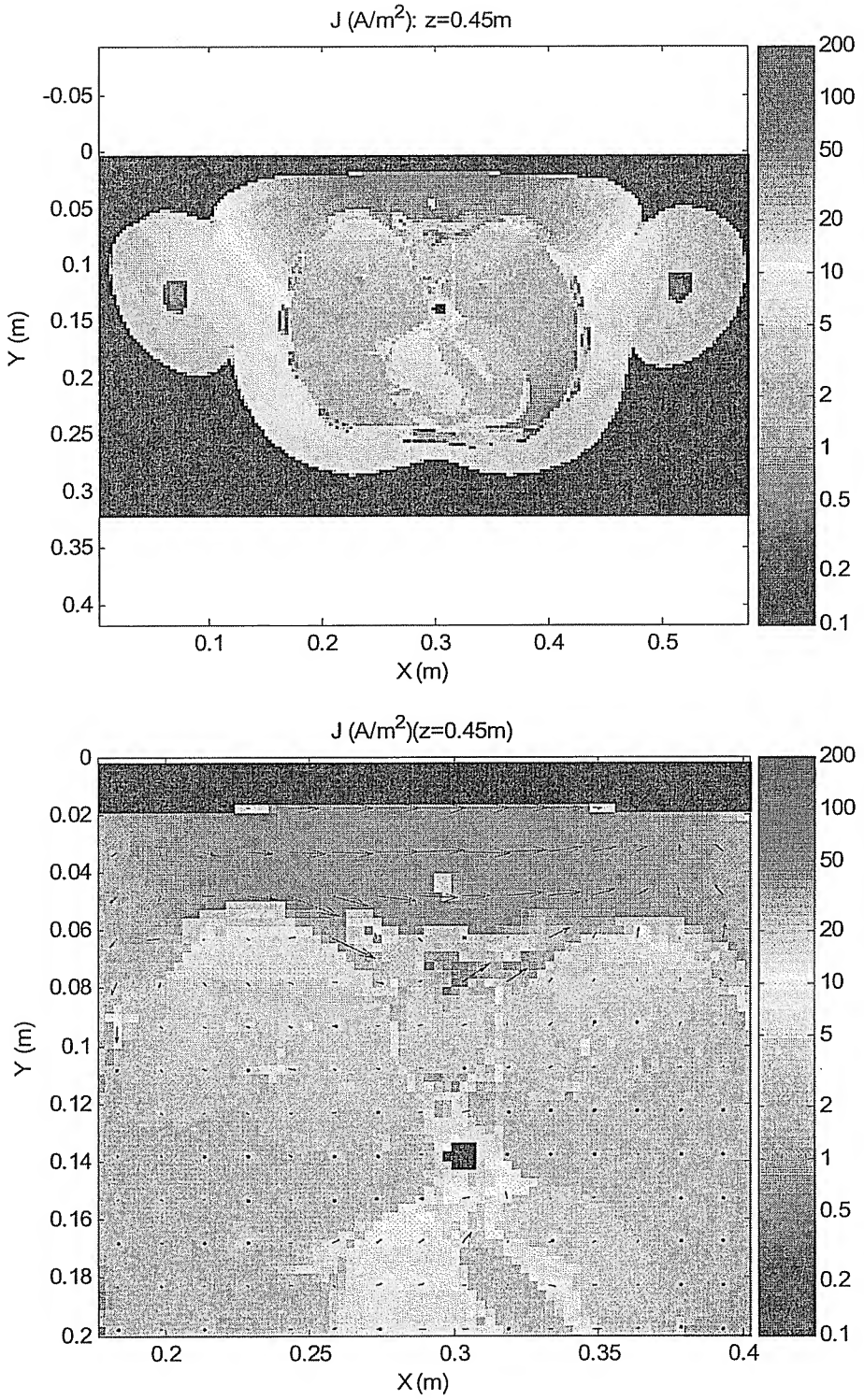

Fig. 16. Amplitude of current density J (A/m^2) on axial plane at z = 0.45 m (Top view) due to the electrode pair B with the amplitude of the applied current equal to 1 A.

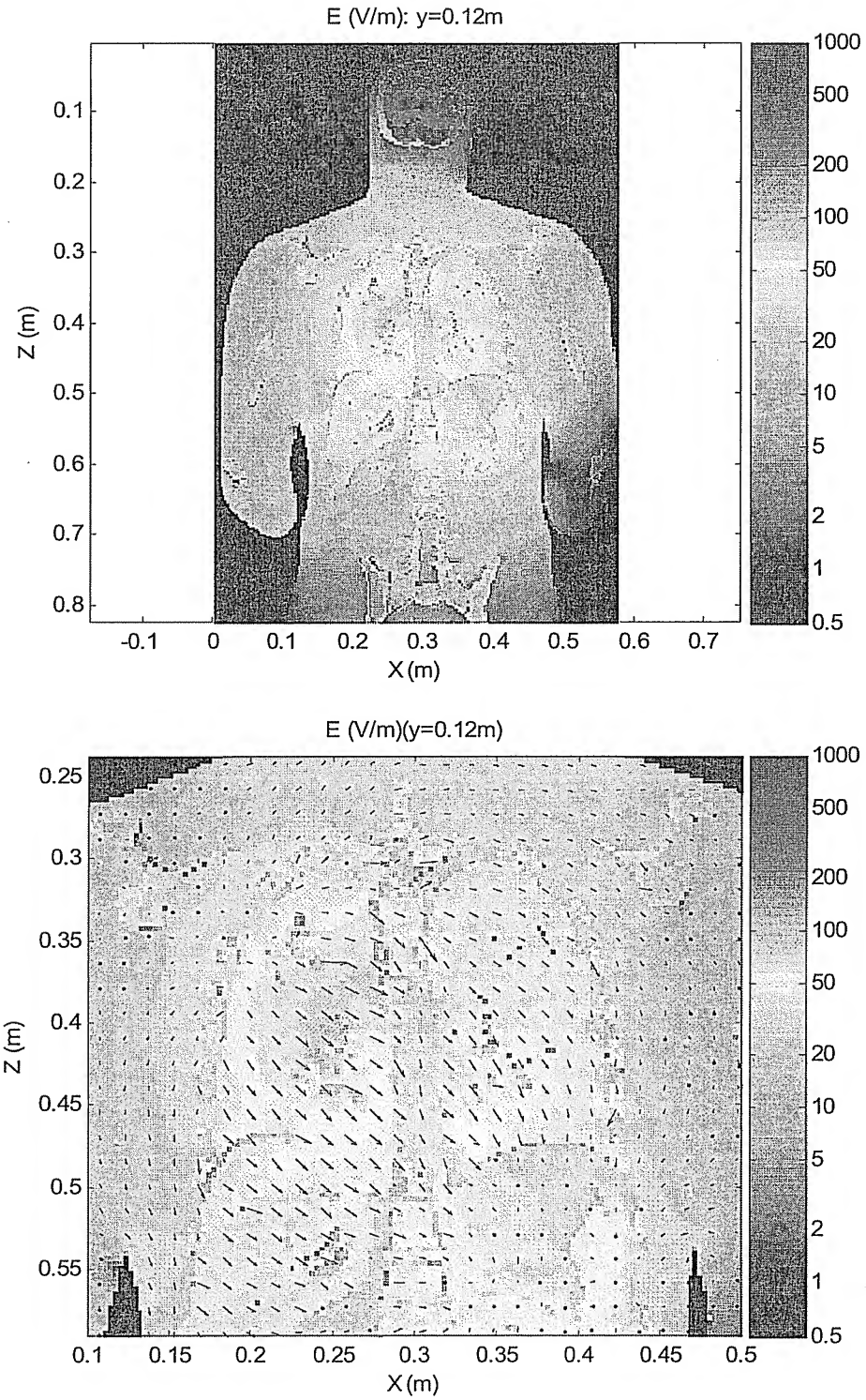

Fig. 17. Amplitude of electric field E (V/m) on coronal plane at y = 0.12 m (Front View) due to the electrode pair B with the amplitude of the applied current equal to 1 A.

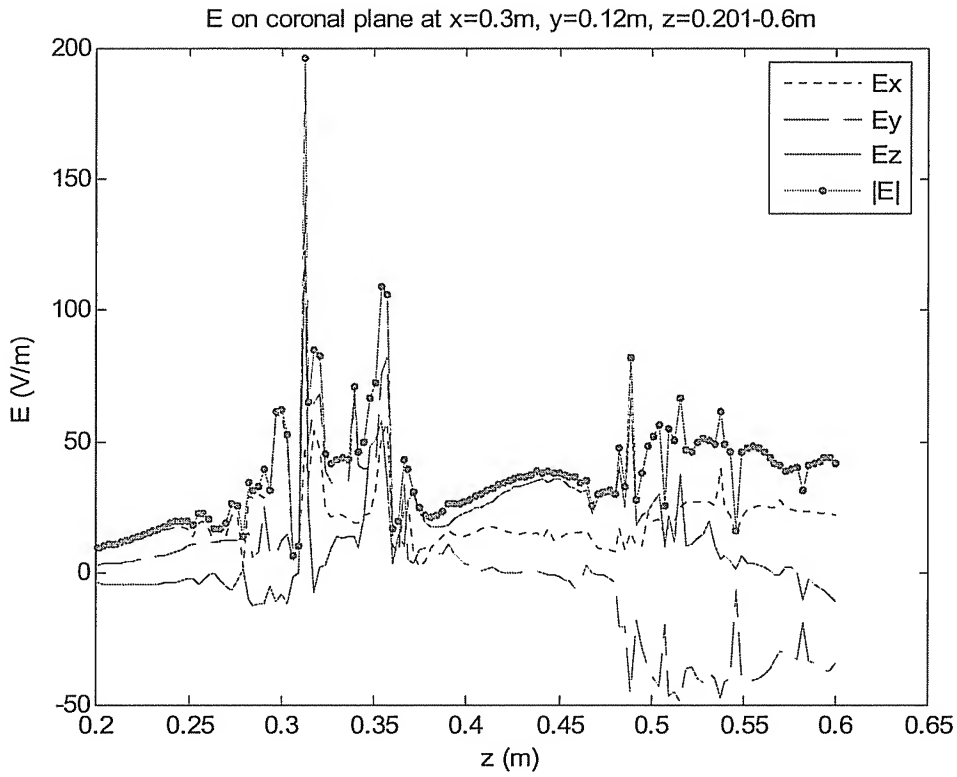

Fig. 18. Ex, Ey, Ez and |E| along the line x = 0.3 m, y = 0.12 m, z = 0.2-0.6 m due to electrode pair B with current 1 A

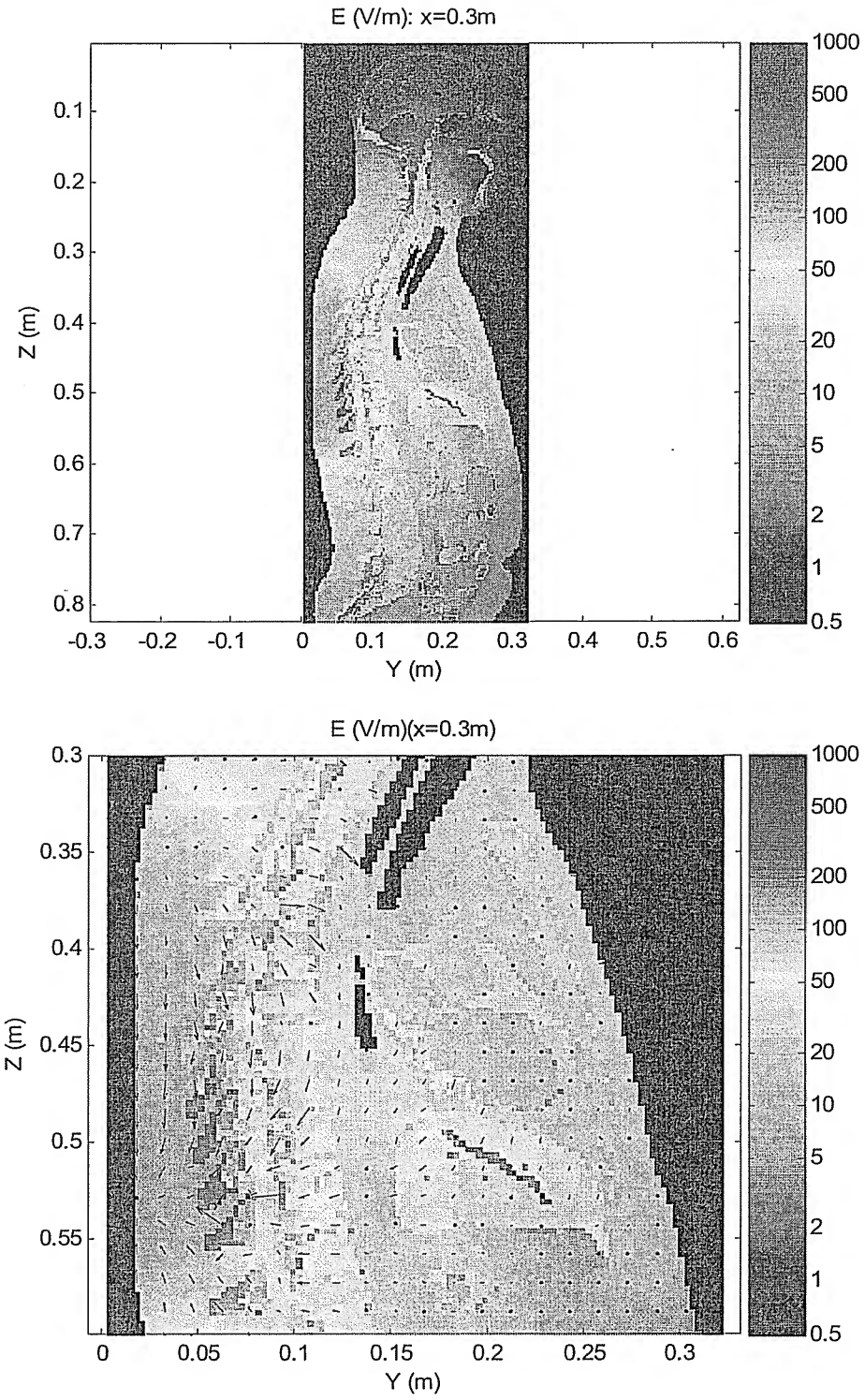

Fig. 19. Amplitude of electric field E (V/m) on sagittal plane at x = 0.3 m (Right view) due to the electrode pair B with the amplitude of the applied current equal to 1 A.

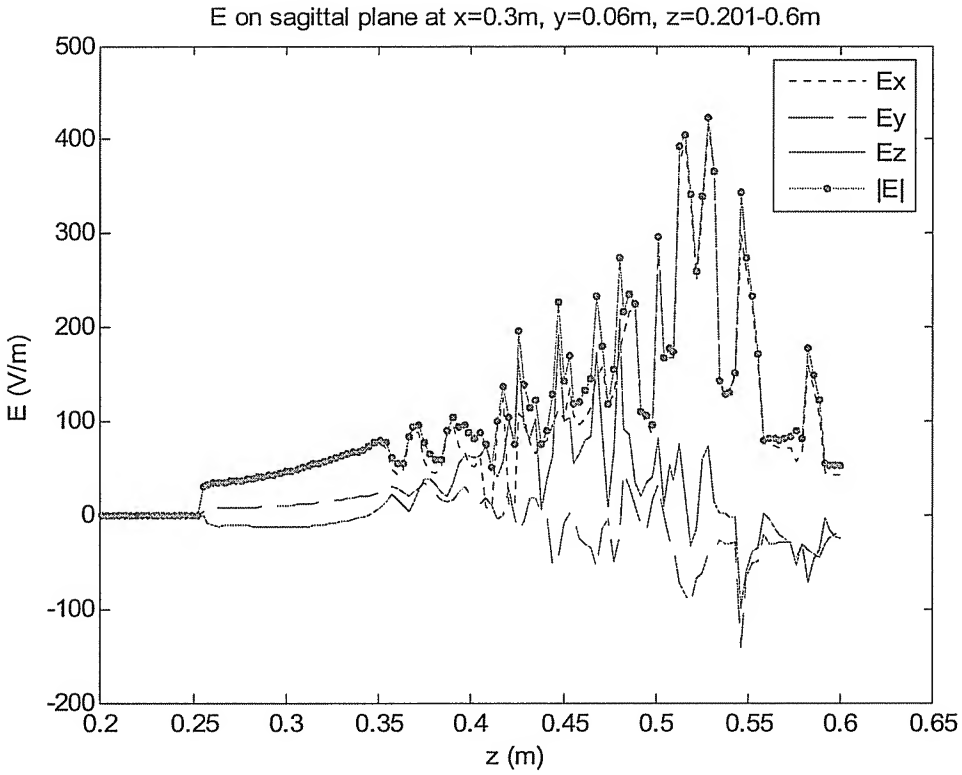

Fig. 20. Ex, Ey, Ez and |E| along the line x = 0.3 m, y = 0.06 m, z = 0.2-0.6 m due to electrode pair B with current 1 A

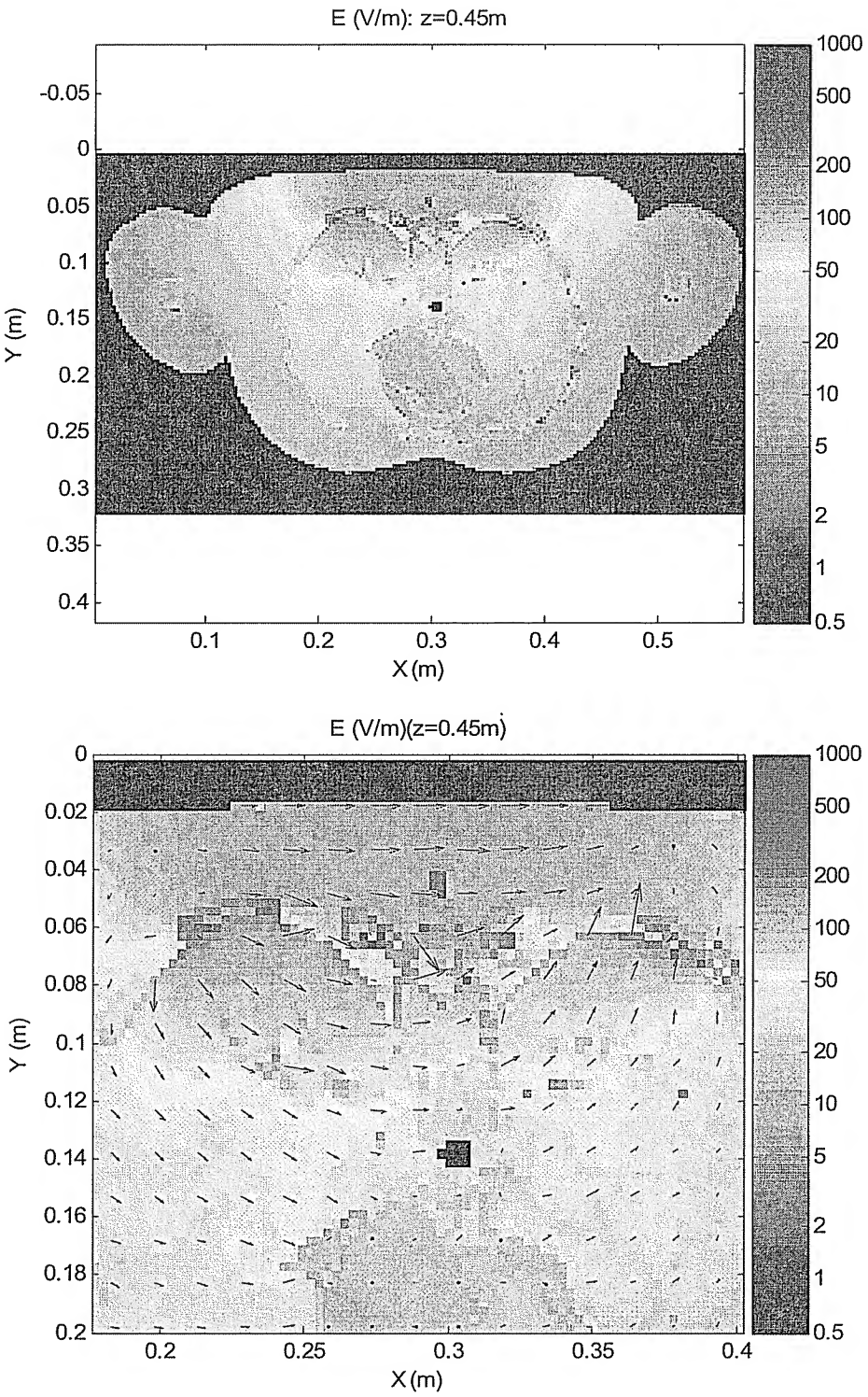

Fig. 21. Amplitude of electric field E (V/m) on axial plane at z = 0.45 m (Top view) due to the electrode pair B with the amplitude of the applied current equal to 1 A.

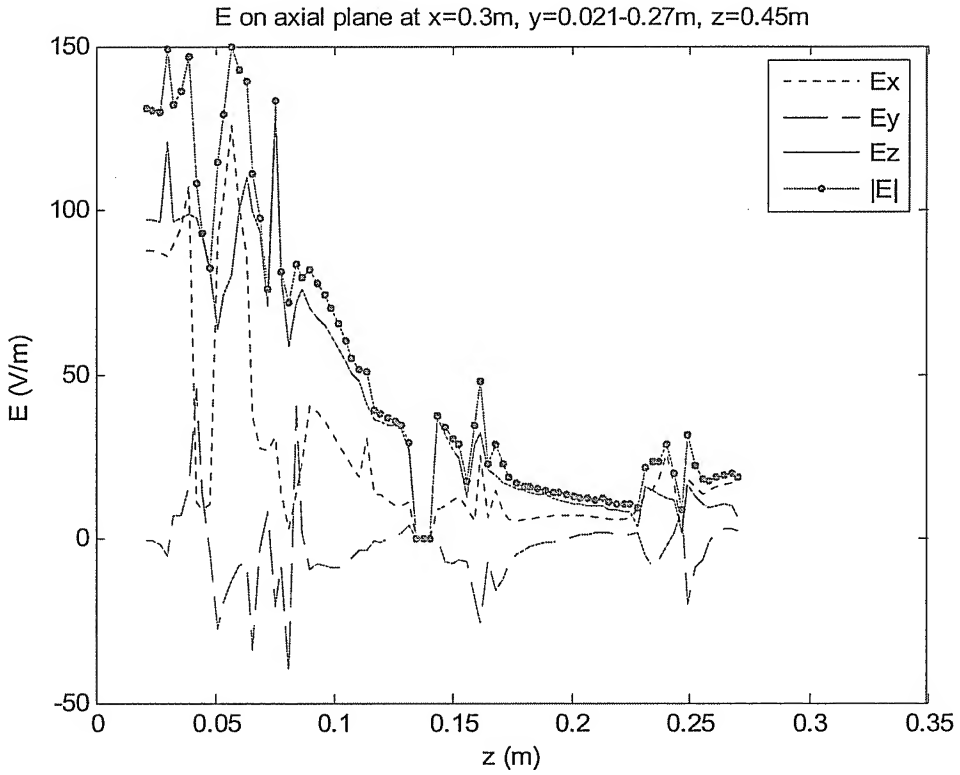

Fig. 22. Ex, Ey, Ez and |E| along the line x = 0.3 m, y = 0.02-0.27 m, z = 0.45 m due to electrode pair B with current 1 A

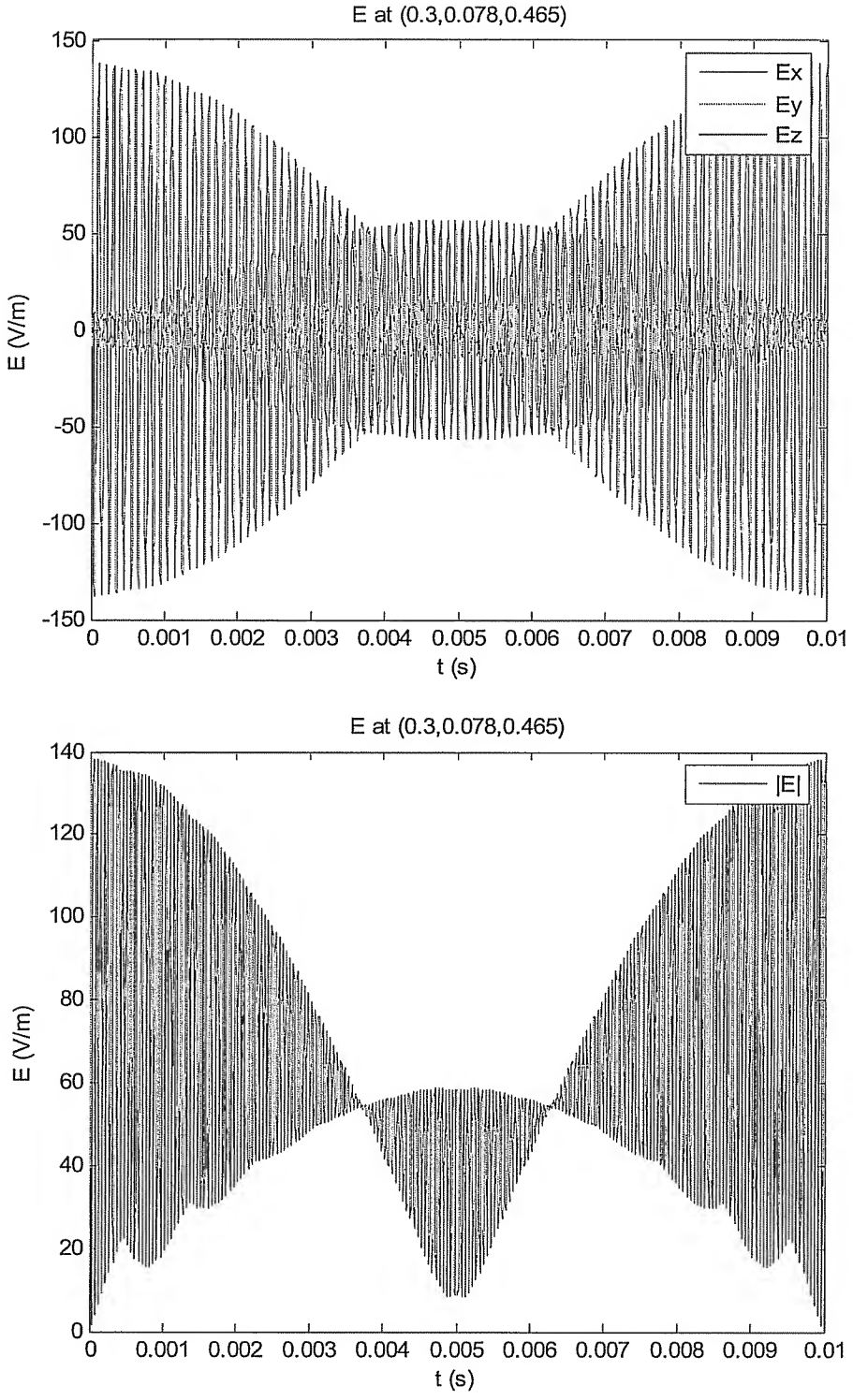

Fig. 23. The induced electric field (Ex, Ey, Ez, |E|) at the point x= 0.3 m, y =0.08 m, z = 0.47 m due to the 2 pairs of electrodes with current 1 A for each pair and frequency 1 kHz and 1.1 kHz.

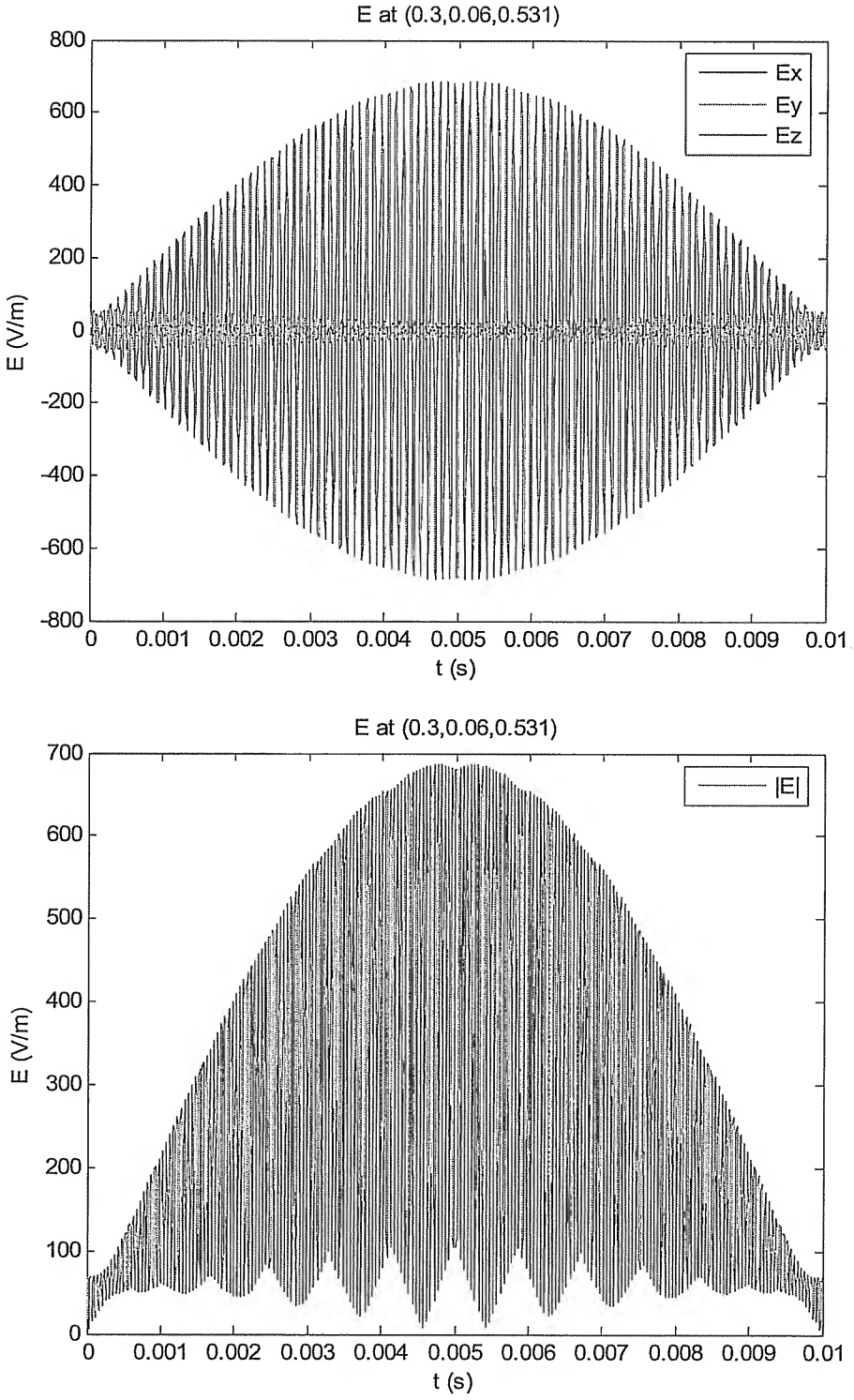

Fig. 24. The induced electric field (Ex, Ey, Ez, |E|) at the point x= 0.3 m, y =0.06 m, z = 0.53 m due to the 2 pairs of electrodes with current 1 A for each pair and frequency 1 kHz and 1.1 kHz.

REFERENCES

1. D. W. Armitage, H. H. Le Veen and R. Pethig, "Radiofrequency-induced hyperthermia: computer simulation of specific absorbtion rate distributions using realistic anatomical models", *Phys. Med Biol.* 1983, Vol. 28, No.1, pp. 31-42.

2. N. Orcutt, and O. P. Gandhi, "A 3-D impedance method to calculate power deposition in biological bodies subjected to time varying magnetic fields", *IEEE Trans. Biomed. Eng.* , Vol. 35 No. 8, Aug. 1998, pp. 577-583.

3. M. Sadiku, "Numerical Techniques in Electromagnetics", CRC Press, Inc., 1992, pp. 653-654.

4. Hugo Model, http://www.nlm.nih.gov/research/visible/visible_human.html

5. E. L. Carter, Jr., S.R. Pollack, and C.T. Brighton, "Theoretical Determination of the Current Density Distributions in Human Vertebral Bodies During Electrical Stimulation", *IEEE Trans. Biomed. Eng.*, vol. 37, No. 6, June 1990, pp. 606-614.

6. P. P.M. So., M. A. Stuchly, J. A. Nyenhuis, "Peripheral Nerve Stimulation by Gradient Switching Fields in Magnetics Resonance Imaging", ", *IEEE Trans. Biomedical Engineering*, vol. 51, No. 11, Nov. 2004, pp. 1907-1914.

7. O. P. Gandhi, G. Kang, D. Wu, G. Lazzi, "Currents Induced in Anatomic Models of the Human for Uniform and Nonuniform Power Frequency Magnetic Fields", *Bioelectromagnetics* **22**, 2001, pp. 112-121.

8. T. W. Dawson, M. A. Stuchly, "High-Resoultion Organ Dosimetry for Human Exposure to Low-Frequency Magnetic Fields", *IEEE Trans. Magn.*, Vol 34, No. 3, May 1998, pp. 708-718.

9. C. Gabriel, S. Gabriel, E. Corthout, "The dielectric properties of biological tissues: I. Literature survey", *Phys. Med Biol.* **41**, 1996, pp. 2231-2249.

10. S. Gabriel, R. W. Lau, C. Gabriel, "The dielectric properties of biological tissues: II. Measurements in the frequency range 10 Hz to 20 GHz", *Phys. Med Biol.* **41**, 1996, pp. 2251-2269.

11. S. Gabriel, R. W. Lau, C. Gabriel, "The dielectric properties of biological tissues: III. Parametric models for the dielectric spectrum of tissues", *Phys. Med Biol.* **41**, 1996, pp. 2271-2293.